Jimma University

School of Graduate Studies

Jimma Institute of Technology

Faculty of Civil and Environmental Engineering

Geotechnical Engineering Stream

Numerical Modeling for Prediction of Compression Index from Soil Index Properties in Jimma Town

A Research Submitted to the School of Graduate Studies of Jimma University in Partial Fulfillment of the Requirements for the Degree of Master of Science in Civil Engineering (Geotechnical Engineering)

By: **Yerosan Feyissa Keneni**

June 2021
Jimma, Ethiopia

Jimma University

School of Graduate Studies

Jimma Institute of Technology

Faculty of Civil and Environmental Engineering

Geotechnical Engineering Stream

Numerical Modeling for Prediction of Compression Index from Soil Index Properties in Jimma Town

A Research Submitted to the School of Graduate Studies of Jimma University in Partial Fulfillment of the Requirements for the Degree of Master of Science in Civil Engineering (Geotechnical Engineering)

By:

Yerosan Feyissa Keneni

Advisor: Dr.-Ing. Fekadu Fufa (Assoc. Professor)

Co-Advisor: Eng. Worku Firomsa (MSc)

June 2021

Jimma, Ethiopia

Jimma University

School of Graduate Studies

Jimma Institute of Technology

Faculty of Civil and Environmental Engineering

Numerical Modeling for Prediction of Compression Index from Soil Index Properties in Jimma Town

By:

Yerosan Feyissa Keneni

Approved by Board of Examiners

Dr.-Ing.Fekadu Fufa (Assoc.Professor)		
(Advisor)	Signature	Date
Dr. Endalu Tadele (Assist. Professor)		04/06/2021
(External Examiner**)**	Signature	Date
Eng. Ruhama Beyene (MSc)		
(Internal Examiner)	Signature	Date
Eng. Mohammed Yasin (MSc)		
(Chairman)	Signature	Date

DECLARATION

I, certify that the work in this thesis entitled "Numerical Modeling for Prediction of Compression Index from Soil index properties in Jimma Town" has been performed by me in Faculty of Civil and Environmental Engineering, Department of Civil Engineering, under the supervision of main-advisor: **Dr.-Ing**. **Fekadu Fufa** and Co-advisor, Engineer **Worku Fromsa**. This thesis is my original work and has not been presented by another person on award of degree at any university. Moreover, all Materials used from other sources has been greatly acknowledged and cited.

Name: Yerosan Feyissa Keneni Signature: ____________ Date: ____________

As Master's Research Advisors, we hereby certify that we have read and evaluated this MSc Final Thesis prepared under our guidance by Yerosan Feyissa entitled: "Numerical Modeling for Prediction of Compression Index from Soil index properties in Jimma Town".

We recommend that it can be submitted as fulfilling the MSc Final Thesis requirements.

Dr.-Ing.Fekadu Fufa (Assoc.Professor)	____________	__________
Main Advisor	Signature	Date
Eng. Worku Fromsa (MSc)	____________	__________
Co-Advisor	Signature	Date

ACKNOWLEDGMENT

First, I would like gratefully thank the Almighty God for His protection.

My deepest gratitude goes to my advisor Dr. Ing. Fekadu Fufa (PhD) and my co-advisor Mr. Worku Firomsa (MSc) for all their limitless efforts in guiding me through my work and for providing me useful reference materials.

Secondly, my deep hearted gratitude to Ethiopian Road Authority (ERA) and Jimma University, School of Graduate Studies, Jimma Institute of Technology, Civil Engineering Department and Geotechnical Engineering Stream for giving me the opportunity to avail the scholarship program in pursuing my master's degree in civil engineering.

Finally, I would like to say thanks a lot to all my friends who are always been there in times of difficulties and giving me moral support to complete career.

ABSTRACT

The compression index is one the compressibility characteristics concept to make estimates of soil responses, when one cannot conduct sufficient soil tests completely characterize a soil at a site. In this study, correlations are developed to predict compression index (Cc) from index tests so that one can be able to model Jimma soils with compression index using simple laboratory tests. The objective of the study is to predict the compression index from soil index properties in Jimma town. Undisturbed and disturbed soil samples from fifteen different locations of Jimma, where different clay soil is found, are collected.

Laboratory tests like specific gravity, grain size analysis, Atterberg limit and one-dimensional consolidation test for thirty test samples (at 1.5 m to 3.0 m depths per each of fifteen test pits) are conducted. From this test, compressibility soil parameters compression index (Cc) and swell index (Cs) are determined. From the results of limited tests, an indicative good correlation is observed between compression index and liquid limit, plastic limit, and plasticity index. However, a poor correlation has developed between compression index (Cc) and plastic limit (PL) when related to the other parameters. The developed correlations will be important inputs in modeling Jimma clay soils with regression analysis and artificial neural network model using simple index tests. The proposed model that obtained from the correlation between Cc and LL, PI is given as Cc = 0.0018(LL) + 0.0004(PI) +0.1231, R^2 = 0.847 with 0.012 of standard error through multilinear regression analysis. In addition, the results of this study can serve as a basis for further study of such correlations on different clay soils in the country.

The compression index of soils was mean 0.274, at least 0.227 and at most 0.33 and depended on clay soil class. The results showed that the correlation coefficient (R^2 = 0.912 and R^2= 0.841) was determined by neural network and regression method respectively. By comparing the values of R-value and error square mean (MSE) by two using methods, it was revealed that artificial neural network has the least error and the most accuracy. As a result, for estimating the compression coefficient in the study area, this method should be used.

Keywords: *ANN model, Regression model, index properties, compressibility parameter, compression index*

TABLE OF CONTENTS

Contents **page**

LIST OF TABLES

LIST OF FIGURES

ACROMYS

AASHTO	American Association State Highway and transportation official
ASTM	American Standard Test Manual
ANN	Artificial Neural network
C_c	Compression index
CH	High plasticity inorganic clays
CL	Low plasticity inorganic clay
C_s	Swelling index
C_v	Consolidation coefficient
e	Void ratio
G_s	Specific gravity
LI	Liquid Index
LL	Liquid Limit
LR	Linear regression
MH	High plasticity inorganic silts
ML	Low plasticity inorganic silts
MLP	Multilayer perception
MSE	Mean squared error
OH	with silts/clays of high plasticity
OL	with silts/clays of low plasticity
P_c	Preconsolidation
PI	Plastic Index
PL	Plastic Limit
R^2	Correlation coefficient
USCS	Unified Soil Classification system
γ_d	Dry density
w_n	Moisture content
σ	Effective stress

CHAPTER ONE

1 INTRODUCTION

1.1 Background

Settlement can occur because of construction foundation built on a compressible soil layer. Compression index (Cc) is the compressibility characteristics, which are obtained from an oedometer test to estimate the magnitude of soil compression. The process of consolidation test proceeds for longer durations. Therefore, it constructive if the value of the compression index can be interrelated with index properties, such as liquid limit, plastic limit and plasticity index. The correlations between the engineering and index properties will reduce the workload of a soil investigation program, in case of urgency.

The nature of the soil has always been an important part of civil engineering. Soil properties, including plasticity, capability of existing, or soil strength, always influence the design of the structure [1]. Failure to understand soil characteristics can result in significant construction errors. Soil applicability for a specific application must be determined by its engineering characteristics, not only by visual inspection or obvious similarities with other soil [2].

Several attempts were made in the previous to predict the compression index based on the properties of the soil index, which is rather convenient to decide and requires much less time in the laboratory. Atterberg limit values and moisture content are physical soil properties, which are used to determine the soil compression index (Cc). The objective of the research was to determine the relationship between the compression index (Cc) and the index properties of the soil. According to [3], the oedometer test is complex, time-consuming and expensive in contrast to the other soil tests. The compression tendencies of expansive soils are, quantified by the compressibility parameters. Determination of compressibility of expansive soils, namely, recompression index and compression index (Cc), is important for the design of foundations. The swell percent or volume change of soil compression is the percentage of soil load for a particular load with additional surcharge load. The external pressure that is applied to the expanded soil to prevent an increase in volume is called soil pressure [4]. Selected samples were checked for both soil index and engineering properties.

Patil and Panse [5], suggested that the results and significance of relationship have been presented as the main result of this study.

Numerical modeling is an approach or method that is used to estimate, correlation, models and analysis the relationships between dependent and independent variables. This study focuses on the correlation between compression index and Atterberg limit (i.e. liquid limit, plasticity index) by using numerical modeling (Regression analysis and ANN approaches).

Hence, many researchers have used this approach to determine the value of Cc from basic soil properties. Ann and regression analysis is used to predict the compression index from soil index properties, (i.e. LL, w and e) which are given as input data to propose the best regression models for different soil as suggested by [6, 7].

1.2 Statement of the problem

A major concern of the foundation engineer is to predict the behaviour of changes in the volume of soil stress when exposed to changes in a stressful environment. Geotechnical engineers practicing in such areas are involved in better understanding of relationships between physical and chemical properties of active clay. The soil is mostly selected fine grained and clayey or silt inherited with compressibility. Selected samples were checked for both soil index and engineering properties. The soil of Jimma is mainly red, black and gray. The black and gray soils, which cover the majority of the area, are found on flat topography with low elevation and poor drainage condition. For this reason, the foundation may be vulnerable to structural damage due to excessive processing of settlement. Expansive soil poses a serious treat due to seasonal when water content changes due to its light construction in terms of civil engineering, especially in terms of its ability to swell or shrink, [8].

Settlement can cause damage to huge structures as well as domestic utilities, which include gas pipelines, electric cables, sanitary fittings and water pipelines. Thus, it is very important to calculate the consolidation settlement of the normally consolidated and over consolidated saturated fine -grained soils.

In Jimma town, expansive soil exists and it might cause significant damage to the structures built upon it all through urban development. To determine the C_c of these soils for design purpose, time-consuming laboratory tests and complex procedures are required. To reduce cost, time and complex procedures, it is better to use simple index tests and correlate with compression characteristics.

Determining the compression index requires sample collection. The C_c from soil index of Jimma town can be predicted satisfactorily, in particular for preliminary design purposes. This has been achieved by investigating the index properties of clay soil to developing equations to predict C_c from soil index tests. However, the prediction of compression index from index properties of the soil in Jimma town has not yet been studied. This research has therefore directed to the study of the prediction of compression index from index properties of soils in Jimma town.

1.3 Objective

1.3.1 General objective

The general objective of the study is to predict the compression index from index properties of soils from Jimma town through numerical modeling.

1.3.2 Specific objective

The specific objectives of the study are

1. to determine the relation between index properties and the compressibility characteristics of the soil;
2. to evaluate the compressibility characteristics of the soils; and
3. to develop correlation between compression index (C_c) and index properties of the soil

1.4 Research questions

The research questions of the study are

1. How can index properties of soil correlate to compressibility parameters of the soil?
2. Is there a real relationship between the Jimma compressibility characteristics and the underlying basic soil properties?
3. Is there any strong relationship between compression index (C_c) and soil index properties in predicting the C_c value?

1.5 Significant of the study

This study is to develop the compression index from soil index properties on selected soil sample in Jimma town. It is proper to determine simpler and faster methods of testing; using the data of which the compression index of soils can be predicted satisfactorily in particular for preliminary design purposes. The study will provide lessons that were help the concerned body to consider appropriate measures to address problems resulting from the unavailability of the consolidation test. In addition, the research helps to simplify the lab work of huge projects in phrases of wastage of energy, cost, time. Moreover, minimize the settlement for laboratory engineering property test of compression index by predicting it from the specific study area. Furthermore, this works to use as a reference for researchers who desire to undergo further study on related titles.

1.6 Scope and Limitations of the study

The study covered prediction of compression index from soil index properties of selected soil sample in Jimma town. It has been supported by different source of literatures and a series of laboratory experiments. The relevant laboratory tests have been done by researcher was; natural moisture content, specific gravity, grain size distribution (gradation), one-dimensional consolidation, free swell, and Atterberg limit test. All the above tests have done according to American Society for Testing Materials (ASTM) standard. Thirty samples of soil were collected, excavated to a maximum depth of three meters from fifteen test pits.

This study was additionally addressing the objectives cited by conducting detail laboratory tests on disturbed and undisturbed soil samples of the selected area. The laboratory tests that carried out are consolidation test, Atterberg test. After conducting all critical laboratory test; new correlations of compression coefficient (C_c) with index properties is developed by Artificial neural networks (ANN) or statistical analysis using regression analysis model. Further, efforts have been made to determine whether models developed an early stage in other area can be envisioned by using different researchers' usage of soil compression index in chosen study region or not. However, the finding of the research was limited to investigating the index properties and consolidation characteristic of soil in Jimma town. The major faced the researcher was no excess oedometer apparatus in the geotechnical laboratory to accomplish it in time since the consolidation test was laborious, expensive and time consuming.

CHAPTER TWO

2 LITERATURE RIEVIEW

2.1 General

The goal of this chapter is to encompass and synthesize the arguments and ideas provided by previous researchers on the compression index value of fine- grained soil. To recognize those soil properties in engineering design purpose, understanding of the major factors and parameters affecting it are required. ANN will used to predict the compression index of the soil based on liquid limit and plasticity index as an input parameter. Accordingly, this literature review may have a momentous spotlight on soft clays.

It is necessary to decide the determination of the degree and rate of settlement, which used to safe and economic engineering design purposes. Through oedometer tests the compressibility parameters are conducted to determine settlement of compressible layer of soil according to Terzaghi's consolidation theory. These parameters can be act upon the quality of samples used in the tests. The compression index and other consolidation parameters are calculated from oedometer test for establish undisturbed samples conventional oedometer test comprises major disadvantages including costliness, awkward and time-consuming. Furthermore, the other major drawback of estimating the compressibility characteristics is that the graphical method directly related to personal experience. Due to these factors, numerous investigators have attempted to establish practical and fast solutions. Numerical modeling that divided into two approaches was discussed in Chapter three *sections 3.10.*

Regression analysis was referred with how 'Y' variables depend on 'X' variables. Y, which recognize as predicted value was dependent variable or response and X, which is used in predicting the value of dependent variable, is called independent or regressor variable. A regression model that contains more than one regressor variable is called multiple regression models. Alternatively, regression model containing one independent variable or regressor is termed as simple regression model. Fitting a regression model need various premises. Determination of parameter model needs various premises, which the residuals (observed value small estimated values) corresponding to different observations are uncorrelated random variables with zero mean and constant variance. In addition, one assumes that the order of the model is correct; that is, if one fits a simple linear regression model, one is assuming that the phenomenon actually behaves in a linear or first order manner [9]. During regression analysis, a regression model with higher value of R2 (coefficient of determination), which quantifies the proportion of the variance of one variable by the other, is usually accepted.

The presence of relationships between the compressibility parameters and the soil index properties has been investigated from past to present. Prediction of compression index (C_c) of different soil, correlations related to multiple linear regression analysis have been proposed by [10, 11, 12, 13, 14].

Compression index is determined from soil index properties such as the initial void ratio (e_o), natural water content (w_n), liquid limit (LL), and plasticity index (PI). Research; show that physical soil parameters significantly influence soil compressibility parameters. Fully disturbed samples are known to lose their memory due to soil structure or stress history, which used to obtain intrinsic properties. A number of previous researchers have reported that the compressibility of remolded clay has a specific relationship with the intrinsic variable of the clay [15]. According to [16], the consolidated clay soil formed by the evaluation of environmental deposition that affects the compression index of the erroneous intrinsic variables performed.

Table 2.1: The primary compression index for several kinds of soil [16]

Kind of soil	Compression index (Cc)
Dense Sand	0.0005 – 0.01
Loose Sand	0.025 – 0.05
Firm Clay	0.03 – 0.06
Stiff Clay	0.06 – 0.15
Medium – Soft Clay	0.15 – 1.0
Organic Soil	1.0 – 4.5

Artificial neural networks are computational methods that carry out multi factorial analyses. Inspired by networks of biological neurons, artificial neural network models incorporate layers of simple computing nodes that perform as nonlinear summing devices [17]. ANNs method is used to give a more efficient and accurate results, due to determine regression analysis equation.

According to, [6, 7, 18] various geotechnical engineering problems (i.e. slope stability, settlement behavior, bearing capacity) have been done using ANN methods for different foundation. Investigators suggested that the compressibility parameters (Cc, Cr) are determined by using the computing method in a short time [19, 20, 21, 22, 23].

In this research, consolidation characteristics of fine-grained soil were determined by using ANN method. Thus, it was aimed to get much better results than the empirical formulas based on the regression analysis obtained in the previous studies. The other investigation relating to estimate the compression or recompression index by using ANN models have checked carefully. It absolutely was seen that these studies most popular single output models despite employing a range of various input parameters. In the presented study, the compression index was tried to predict by using an output combined ANN model based on natural water content (w_n), initial void ratio (e_o), G_s, LL, PL and PI.

Two or more output models provided time saving and reduced the workload and these models have obtained successful results. Thirty laboratory Oedometer and index tests results of fine-grained soils obtained by the various geotechnical investigations in Jimma were used in this work to fit the ANN models. The performance of the proposed ANN model was evaluated based on the correlation coefficient (R) and mean squared error (MSE). The summary equation of the literature has given below in the Table 2.2

Table 2.2: Literature Summary [14]

Equation	Author
Cc'=0.0021WL+0.0587	Amith Nath and S.S Dedalal
Cc'=0.0888 e0+0.0525	Amith Nath and S.S Dedalal
Cc'=0.0025 IP+0.0866	Amith Nath and S.S Dedalal
Cc = 0.0046(LL –1.39)	Arpan Laskar and Sujit Kumar Pal
Cc=0.0058(PI-13.76)	Arpan laskar and Sujit Kumar Pal
Cc =0.5217(eo -0.20)	Slamet Widodo and Abdelazim Ibrahim
Cc=0.5217(Wn+11.57)	Slamet Widodo and Abdelazim Ibrahim
Cc =0.5217(WL-1.30)	Slamet Widodo and Abdelazim Ibrahim
Cc = 0.002 wL + 0.0025Ip - 0.005	Amardeep Singh

2.2 Compressibility and Consolidation test

Compressibility was a magnitude that the soil will change extent below load. For example, a structure located on a highly compressible soil is possibly to go through suffer settlement damage because the soil volume decreases beneathneath the application of static load. Compressibility also can be the lower in extent of a soil mass due to either artificial or natural method. This volume change is often because of a change with inside the extent of the voids and to a lesser extent due to a change in the volume of solids [24].

According to [25], test results for compression index property of red soil shows medium to high degree of compressibility, when Cc value in the range of 0.15 to 0.3 considered having high compressibility, Cc in the range of 0.075 to 0.15 are considered to have medium compressibility and the less than 0.075 considered to have low degree of compressibility.

Consideration of compressibility is important in two ways: (i) the usage soil to make a structure, and (ii) the location of a structure made from other materials on a soil basis. Soil compressibility divided into compaction and consolidation

Compaction is an artificial densification of soil through decreasing the volume of voids achieved through vibrating or loading and unloading the soil mass, and is performed as soil particles become reoriented to a configuration that contains fewer voids. This reduction in voids may also encompass fracturing of grains and bending or distortion of individual particles. Consolidation is one form of compressibility that take place beneath-neath static load, and is the process of deriving water in soil mass. Consolidation is a critical essential phenomenon, which need to be understood through all and sundry who attempts to advantage an understanding of soil behavior in engineering problems. It needs to be taking into consideration critically whilst a structure is based on soil. If it is not taken into consideration, it could lead to settlement that can damage the structure being based at the soil. In any case, consolidation will produce a few degrees of settlement that can range over site. The static load applied naturally can in no way be uniform everywhere. This might also additionally lead differential settlement. This differential settlement may also or might not pose a problem to the structure. Two elements are of top significance in thinking about consolidation. The overall consolidation expected - that amount of vertical displacement or settlement, which happens among begin and the end of consolidation. The nature of soil in preference to the size of the load (overburden is crucial to the amount of consolidation). For instance, over-consolidated clay will show less consolidation than a same thickness of normally consolidated clay. The amount of time required for consolidation to occur - Increases in load will now no longer boost up the time of consolidation, however the time of consolidation relies upon the nature of the soil. For instance, greater time may be required for consolidation of a thick soil mass in comparison to a skinny one.

A consolidation test has used to decide soil consolidation settlement when the soil was bounded horizontally and vertically. Test results combined with theory have used to estimate settlement condition. When a saturated soil mass is subjected to a load increment, the load is usually carried initially through the water with inside the pores due to the fact the water is incompressible in evaluation with the soil structure. The pressure, which results in the water due to the overburden increment, has named hydrostatic excess pressure due to the fact it is in excess of that stress because the weight of water. When the load is changed to the soil strata the water is driving from soil pores.

Consolidation test affords a convenient possibility for a direct measurement of permeability by the variable head or the constant head method. The fundamental motive of consolidation tests, however, is to achieve soil data, which is the compression magnitude of engineering projects built on soils, in particularly clays. Although some of the settlement of a structure on clay has because of shear pressure, most of it is far usually due to volume change, especially if the clay stratum is a thick on.

The two most important soil properties supplied with a consolidation test are: (i) the compression index (Cc), which indicates the compressibility of the specimen; and (ii) the coefficient of consolidation (Cv), which suggests the rate of compression beneathneath a load increment. A soil with larger magnitude of compression index indicates that soil has high degree of deformation when an external load acts against the soil mass [26]. The data from oedometer test make it viable to plot a stress-volume pressure curve, which frequently offer beneficial data approximately the pressure records of the soil. In order to be expecting the settlements of structures with inside the field, a technique of extrapolating laboratory test take a look at effects for settlement analysis was needed.

2.3 Factors affecting compressibility of soft soil

2.3.1 The soil type and its structure

Compression of granular soil is small when the pressure is loaded upon. Granular soil has high permeability as compare with cohesive soil, which has low permeability.

2.3.2 The effective stress

The cohesive soil has relatively smaller bearing capacity than coarse-grained soils. Therefore, they have a greater degree of compressibility. Highly plastic soils exhibit significant volume change on application of vertical stress. There will be removing of water pore causing a time dependent decrease in volume. Odometer tests are conducted to establish relationship between effective stress and void ratio. When the concentration of cation in the pore fluid is low, the *e*–log *p* relationship is linear. A direct function of void ratio, regardless of the type clay is called compression index. The void ratio decreases with increase in vertical stress.

2.3.3 The effect of pore fluid

The compressibility of clay is influenced by pore fluid [27]. Water pore is influencing the highly plastic soil to change in volume. There may be a probability the water could are available in contact of various ion organic fluids and liquid solutions. Generally, compressibility decreases with increasing pore aqueous solution concentration as presented by Budhu, [28]

2.4 One Dimensional Consolidation characteristics of Soils

2.4.1 General

When soil layers covering a large area are loaded vertically, the compression can be assumed to one-dimensional. To simulate one-dimensional compression in laboratory we compress the soil in a device called an oedometer drainage, compression, and pressure transfer are all part of the consolidation process. In geotechnical engineering, it refers to adjustment of soil to an applied loading. It may require a long time for a soil formation to come to equilibrium under load. The soil has said to consolidate, when it reaches an equilibrium condition. A process of consolidation is described as “reducing saturated soil content without replacing the water with air,” according to [29].

2.4.2 Consolidation

A consolidation test is a measurement of how soils compress, when was saturated with water and exposed to varying magnitude of load, or varying weights of the soil. Saturated conditions exist when water is added until no more can be absorbed by the soil particle.

A portion of the applied pressure has been transferred to the soil skeleton, causing the excess pore pressure to decrease. Consolidation is a process that involves gradual compression and a gradual transfer of applied pressure from the pore water to the mineral skeleton. The process opposite to consolidation has called swelling, which involves an increase in the water content due to an increase in the volume of the voids. Among the compressibility properties, compression index is by far the most important engineering property to estimate settlement of foundations. It is defined as the slope of void ratio versus logarithm of the applied load curve in one dimensional consolidation test graph [28]

2.4.3 Theories of compression and consolidation

The consolidation characteristics of the soil are dependent largely on permeability, compressibility of soil mass. Consolidation characteristics affected by size, shape and arrangement of soil particles. Settlement occurred because of construction foundation built on a compressible soil layer. Therefore; the vertical compression of the soil mass consists of the following components at elevated pressure: Deformation of the soil grains, compression of pore water or pore air, and decreasing the void ratio or porosity. A volume change of the soil mass below applied stress was be caused by water and air leaks. According to, [30]**, t**he volume change in a soil deposit can be divided into three stages.

Initial consolidation

A reduction in volume was observed when a load was applied to a partially saturated soil due to air release and void compression. Soil compression is occurred because of the gradually decreasing of the solid particles volume. Initial consolidation is occurred when volume reduction of soil immediately takes place after applying the load. Compressed solids mainly cause initial consolidation in saturated soils.

Primary consolidation

After the initial compression, the volume has further reduced due to leakage of water from the voids. When pressure is applied to saturated soil, water driving out and change in volume occurred due to the developing of hydraulic gradient. Primary consolidation is the process, when volume reduction has occurred due to soil permeability and weather. Primary consolidation for a long time occurs in fine- grained soil, whereas in coarse -grained soils primary consolidation occurs very quickly, because of high permeability.

Secondary consolidation

When the excess hydrostatic pressure was generated and at the end of primary compression the secondary consolidation occurs. After primary settlement, some secondary compression occurs in the soil, which is normally time-dependent. It has been linked to the current stress mechanism due to the plastic readjustment of solid particles and adsorbed water. It is usually minimal in most inorganic soil.

2.4.4 Factors Affecting Consolidation characteristics of Clay soils

Stress history and permeability are the major significant factors to consolidation behavior of clay soil in its natural state. The effects of these factors were explained below.

2.4.4.1 Stress history

The maximum stress to which the soil is subjected in the past influence the compression parameter of the soil in its insitu condition. In remolded soils, has lost its structural characteristics as compared with its structure in its natural condition. It was inferred that a remolded soil is unsuitable for evaluating its stress history. The insitu soil has grouped in to two categories based on stress history.

Normally consolidated soils

As defined by [31], clay has said to be normally consolidated if existing effective stress P_O is the maximum pressure to which the layer has ever been subjected in its history. Normally consolidated soil is happened, when the past pressure history is minimum to the current effective pressure. In other words, the normally consolidated soil is one whose pre-consolidation pressure is equal to its present effective overburden pressure.

Over-consolidated clay soil

According to, [31] a clay layer is said to be over consolidated, if the layer was subjected at one time in its history to a greater effective overburden pressure, p_C, than the present pressure, P_o. Over consolidated clay is one which has been completely, consolidated under a large overburden pressure in the past that is larger than the present overburden pressure. The response of over consolidated clays to applied loads, in such a way the soil shows a relatively small decrease in the void ratio along with the load at the maximum effective stress outlined by the past soil. If the effective stress on the soil specimen is increased, further the decrease of void ratio with stress level will be larger.

2.4.4.2 Permeability

The removal of pore water from a saturated clay soil by an externally applied load in the consolidation process, and the exchange in extent related with such a technique are in fact a hydraulic problem. Therefore, consolidation degree depends on the permeability of the soil. According to [8], the permeability of the soil by itself depend on the soil type, size and shape of the soil particles (rounded, angular, or flaky), and so it depends on the size and geometry of voids. In addition, the resistances also depend on the temperature of water (viscosity and surface tension effect).

Permeability is a most important engineering property of soils. Knowledge of permeability is most crucial in a number of soil engineering problems, such as settlement of buildings, yield of wells, seepage through and beneathneath the earth structures.

2.4.5 The standard one-dimensional consolidation test

The consolidation test on soil samples is, to get the important data of the compressibility properties of a saturated soil used to find out the structure settlement condition. The following test procedure was applied to any type of soil in the standard consolidation test. Moreover, the 1-D consolidation test can be obtaining a compressibility parameter (i.e. Cc, Cv), for the settlement magnitude and rate estimate. The pre-consolidation pressure p_c and thus the OCR can also be determined from this test.

The experiment was carried out on undisturbed soil sample that was put in a consolidation ring with a diameter of 45 to 115 mm. According to, [32] the sample height is between 20 and 30 mm, but 20 mm is the most thickness to reduce test time.

These properties are determined from the standard consolidation test, i.e., incremental loading test (ASTM D2435-11) or constant rate of strain test (ASTM D4186-12). The incremental loading test is the predominantly test method used [33].

2.4.6 Terzaghi's theory of one-dimensional consolidation

Theory of one-dimensional consolidation first proposed, by Terzaghi based upon the following assumptions, the mathematical implications to given in parentheses: 1) The soil is homogeneous and isotropic, 2) The soil is fully saturated, 3) The soil grains and water are virtually incompressible (γw is constant and volume change of soil is only due to change in void ratio), 4) Darcy's law is valid throughout the consolidation process, and 5) Soil is laterally confined and the consolidation takes place only in the axial direction.

In real field conditions, Terzaghi's assumptions are not entirely fulfilled. However, considering complexity of the problem, the theory gives reasonably accurate estimate the degree of settlement of a structure built on the soil. According to [34], the standard one-dimensional consolidation test is usually, carried out on saturated specimen using an Odometer.

In this test, a small-undisturbed soil is carefully trimmed and fitted into a rigid metal ring. The soil sample mounted on a porous stone base and a similar stone placed on top to permit water, which is squeezing out of the sample to escape freely at the top and bottom. Prior to loading, the height of the sample has accurately measured. In addition, a micrometer dial has mounted in such a manner that the vertical strain in the sample to measure as loads are applied. The consolidation test apparatus designed to permit the sample submerged in water during the test to simulate the position below a water table of the prototype soil sample from which the test sample taken. Loads were applied in steps in such a way that the successive load intensity P is twice the preceding one. The load intensities are commonly used being ¼, ½, 1, 2, 4,8,16 kg/cm^2. Each load allowed to standing until primary consolidation has practically ceased. The dial readings have taken at elapsed time of 0, 0.25, 0.50, 1, 2, 4, 8, 15, 30, 60 minutes...24 hours. After the greatest load required for the test has applied to the soil sample, the load is removed in decrements to provide data for plotting the soil's expansion curve to determine its elastic properties and the extent of plastic or permanent deformation. The following data has also obtained: (a) Moisture content and weight of the soil sample before the commencement of the test, (b) Moisture content and weight of the sample after completion of the test, (c) The specific gravity of the solids and (d) The temperature of the room where the test is conducted.

The consolidation characteristics (or parameters) of a soil can be determined from the test. Settlement is occurred due to change in volume of the compressible soil layer. According to [27], the coefficient of consolidation relates to how long it will take for an amount of consolidation to take place. Odometer test results can usually display in e-P, e-log P format and as a graph to read the time.

2.4.7 Compression index (Cc)

The oedometer test used to determine the engineering properties for soil compressibility characteristics. The compression index has a good relationship with liquid limit, plasticity index, and shrinkage index [10]. Settlement occurs when a structure founded on compressible soil layers. Degree of settlement is associated to the C_c. Settlement can cause damage to huge structures as well as domestic utilities, which include gas pipelines, electric cables, and water pipelines. Therefore, it is very important to estimate the consolidation settlement of the normally consolidated and over consolidated saturated fine-grained soils. Compression index (Cc) plays an important role in secondary consolidation settlement under expected stresses. The slope of the linear portion of the e-log p curve has designated as the following equation [32]. Thus

$$C_c = \frac{\Delta e}{\log\left(\frac{Po+\Delta P}{Po}\right)} \text{--Eq. (2.1)}$$

Where C_c is compression index, Po is initial effective stress Δe is change of void ratio and ΔP is the change of effective stress. The compression index can be used to calculate the field settlement.

2.4.8 Consolidation coefficient

The time rate of consolidation settlement in the field depends on the rate of dissipation of excess pore pressure induced by the imposed loading, which in turn, is defined by the soil permeability (k) and coefficient of consolidation (C_v) [27].

$$C_v = \frac{(1+e)k}{a_v.\gamma_w} = \frac{k}{m_v.\gamma_w} \text{— —Eq. (2.2)}$$

Where: C_v is the coefficient of consolidation, γ_w is the unit water, k is the coefficient of permeability, $a_{v,}$ is the coefficient of compressibility and mv is the coefficient of volume compressibility.

For the case of a soil layer loaded very quickly with drainage allowed on both sides, the time–settlement curve can be calculated, if the ultimate settlement Su, and the coefficient of consolidation Cv, are known. The ultimate settlement has calculated from the reconstructed field consolidation curve. The coefficient of consolidation for use in field analyses has also usually estimated from laboratory consolidation tests. According to [35], in the laboratory there is instantaneous initial settlement, which may be caused by elastic compression of the experimental apparatus, seating of the porous stones against improperly trimmed faces of the soil specimen, or compression of gas bubbles in the soil. This rapid settlement, termed initial compression obviously cannot to take into account by the theory. Thus, an adjustment must make to the laboratory curve to remove the effects of initial compression.

There are two procedures in common use for estimating the appropriate values of S_0 and S_{100}. These are designated Taylor's method and Casagrande's method. From t_{50} and t_{90} it may be noted that Taylor [36], recommended use of the U = 90% point. The coefficient of consolidation has then calculated as:

$$Cv = \frac{0.848H^2d}{t_{90}} \left(\frac{\text{cm2}}{\text{s}}\right) ------------------------- \text{Eq.}\,(2.3)$$

$$Cv = \frac{0.197H^2d}{t_{50}} \left(\frac{\text{cm2}}{\text{s}}\right) ------------------------- \text{Eq.}\,(2.4)$$

Where: H_d is the average drainage distance during the consolidation period (half the average total thickness for double drainage) and t_{50} and t_{90} is the time corresponding to U = 50% and U = 90 respectively.

2.4.9 Preconsolidation pressure

A soil may have been preconsolidated during the geologic past by the weight of an ice which has melted away, or by other geologic overburden or and structural loads which no longer exist. For example, thick layers of overburden soil are eroded and excavated away or heavy structures may be torn down. In addition, capillary pressures, which may have acted on the clay layers in the past, have removed for one reason or another. According to, [31] the ratio P_c to P_o is called the over consolidation ratio (OCR). The relative amount of preconsolidation is usually reported as the over consolidation ratio (OCR) defined as:

$$OCR = \frac{\boldsymbol{P_c}}{\boldsymbol{p_o}} ------------------------------ \text{Eq.}\;(2.5)$$

Where: P_c is the effective overburden pressure and P_o is the present overburden pressure

2.4.10 Correlation for compression index (C_c)

Labor and computation-intensive laboratory consolidation tests take a long time. Because of these factors, substantial efforts were attempt to correlate the compression indexes, and to some more easily determined soil index properties [1, 31].

Table 2.3: Previously suggested equations between Atterberg limits and Cc

Equation	R^2	Types of soil	Reference
Cc = 0.007PI + 0.01	0.580		[1]
Cc = 0.004LL - 0.03	0.784		
Cc = 0.0082 PI + 0.0475	0.898	Undisturbed	[2]
Cc=(0.007*LL) - 0.043	0.592	Remoulded	[7]
Cc=0.01706*(LL -1.30)	0.591	Undisturbed	[16]
Cc=0.015*(LL -20)	0.717	--------------	[15]
Cc=(0.014*LL) - 0.168	0.776	Undisturbed	[21]
Cc = 0.009(LL-10)	Normally consolidated clays		[29]
Cc=(0.0067*LL) - 0.0364	0.970	Remoulded	[37]
$Cc = 0.0054*LL^{0.7102}$	0.385	Undisturbed	[38]
Cc = (0.0024*PL) +0.042	0.249		
$Cc = 0.0196*PI^{0.4343}$	0.357		

Note: R^2 is Coefficient of determination

CHAPTER THREE

3 MATERIALS AND METHOD

3.1 Study Area

The study was conducted in Jimma town, which is located in southwest Ethiopia at distance of 335 km of capital AA (Finfinne). It is one of the towns of the Oromiya National Regional State and located in Jimma Zone. It is located at a latitude and longitude of $7^0$40'24.4"N and 36^0 50'03.9"E, respectively. As the 1986 master plan indicated, the Jimma city had an area of 46.23 km^2. It has a sub- tropical climate with an altitude of 1704-2000 m above mean sea level and a temperature range of 7.3^{o}C to 31^{o}C. Rainfall amounts vary between 1450 and 1800 mm. (JCASP, 2006)

According to [26], the soils of Jimma are mainly red, black and gray. The red colored soils are found on rolling terrain with higher elevation and good drainage condition. The black and gray soils, which cover the majority of the area, are found on flat topography with low elevation and poor drainage condition**.**

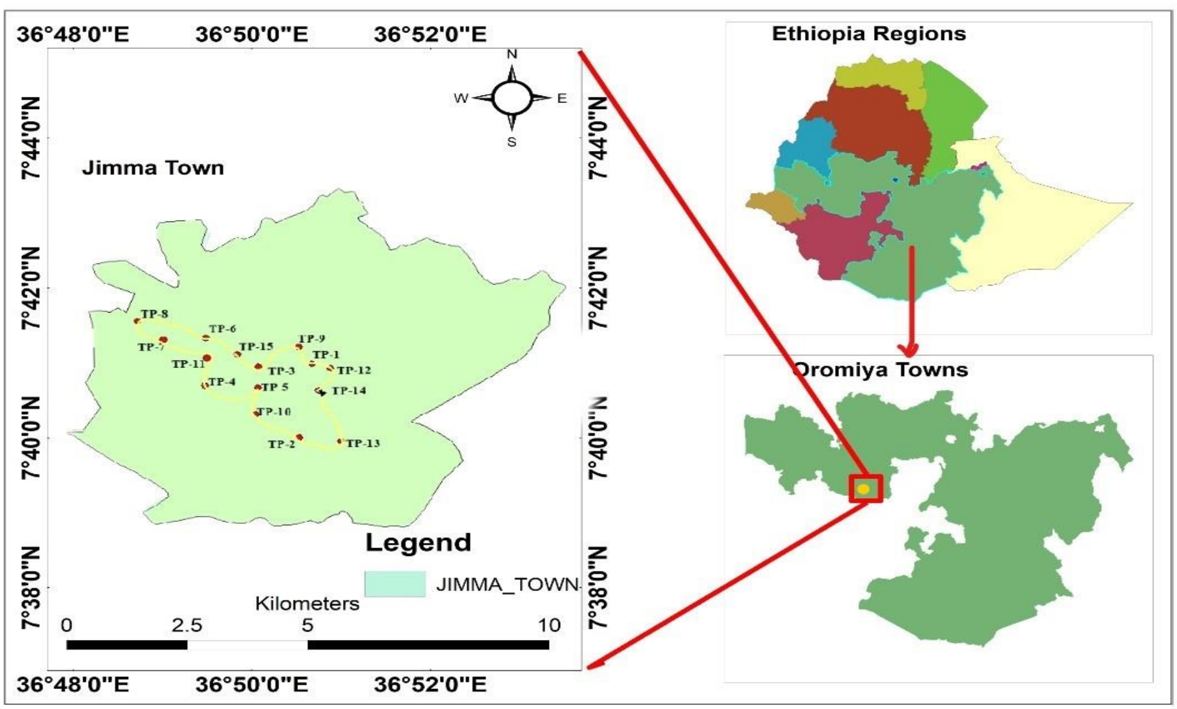

Figure 3.1: Study area location of Jimma Town (Arch GIS 10.4.1 ArcMap)

3.2 Research Design

To meet the objective of this research, generally the study design are divided in 5 main stages; (1) organizing literature review of different previous published researches and gathering as much as information as possible on the study subject and study area; (2) field identification; (3) sampling and data collection; (4) laboratory tests and analyzing the result from tests (5) conclusion and recommendation.

Field identifications were conducted on the study area to identify the properties of soils that are good indicator of their extensive potential these was done for sampling during the time of highly dry season where soils can be identified visually. The conducted field investigations are included of soil color, soil texture and lithological position. The engineering properties of soil were measured in this study,so it was a quantitative experiment. To examine the engineering properties of the soil, a laboratory expeiment program was designed to perform all of the basic soil index properties.

Thirty representative disturbed and undisturbed soil samples were collected from different locations and taken samples from 1.5-3.0 m depth. In particular, for all soil properties AASHTO, ASTM standard maual test laboratory procedures was performed. The laboratory test conducted on selected soil sample are; natural moisture content, grain size analysis, hydrometer, free swell tests, Atterberg limit, standard one dimensional consolidation test.

3.3 Sample Technique

The representative soil sample were used by selecting particular parameters to make it sure that the settings have specific characteristics as indicated for this study. Using field observation and some literature from the study area, systematic random sampling was used to collect soil samples, which were then analyzed using descriptive statistics to classify soil properties using laboratory test results. The amount of soil sample was determined according to ASTM standard test manual. Besides, large numbers of samples were collected to ensure that required detection limits to achieved and that sample can be for reanalysis if there is problem. After sampling carefully, disturbed and undisturbed soil samples are transported to the laboratory. For all types of laboratory tests, the sample collection procedure should be performed. Maintaining a constant surface and depth for test samples will minimize problems caused by different depth profiles. The data used for the study consist of current and past laboratory results of soils samples was collected from various parts of Jimma town, and the various geotechnical investigations conducted in different locations within the study area. The tests included Atterberg limits moisture content, particle size distribution and one-dimensional consolidation tests.

3.4 Sample Sites

For this study, thirty soil samples have collected from a different location. Those location are stated as follows: Maytric area, Bacho Bore, Awetu Village (Betseb Academy elementary School), Bossa Kitto, Hermata Merkato (near to Wema Hotel), Bossa A KG Model School, JiT/kitto furdisa, Kochi village, Arround main CBE, Sato Samaro, Ginjo Guduru, Technic area, RVU and Agri area) which can be well represented soil samples found in Jimma town. Are randomly selected and for each sample, all tests are performed for it in natural condition for both disturbed and undisturbed soil sample.

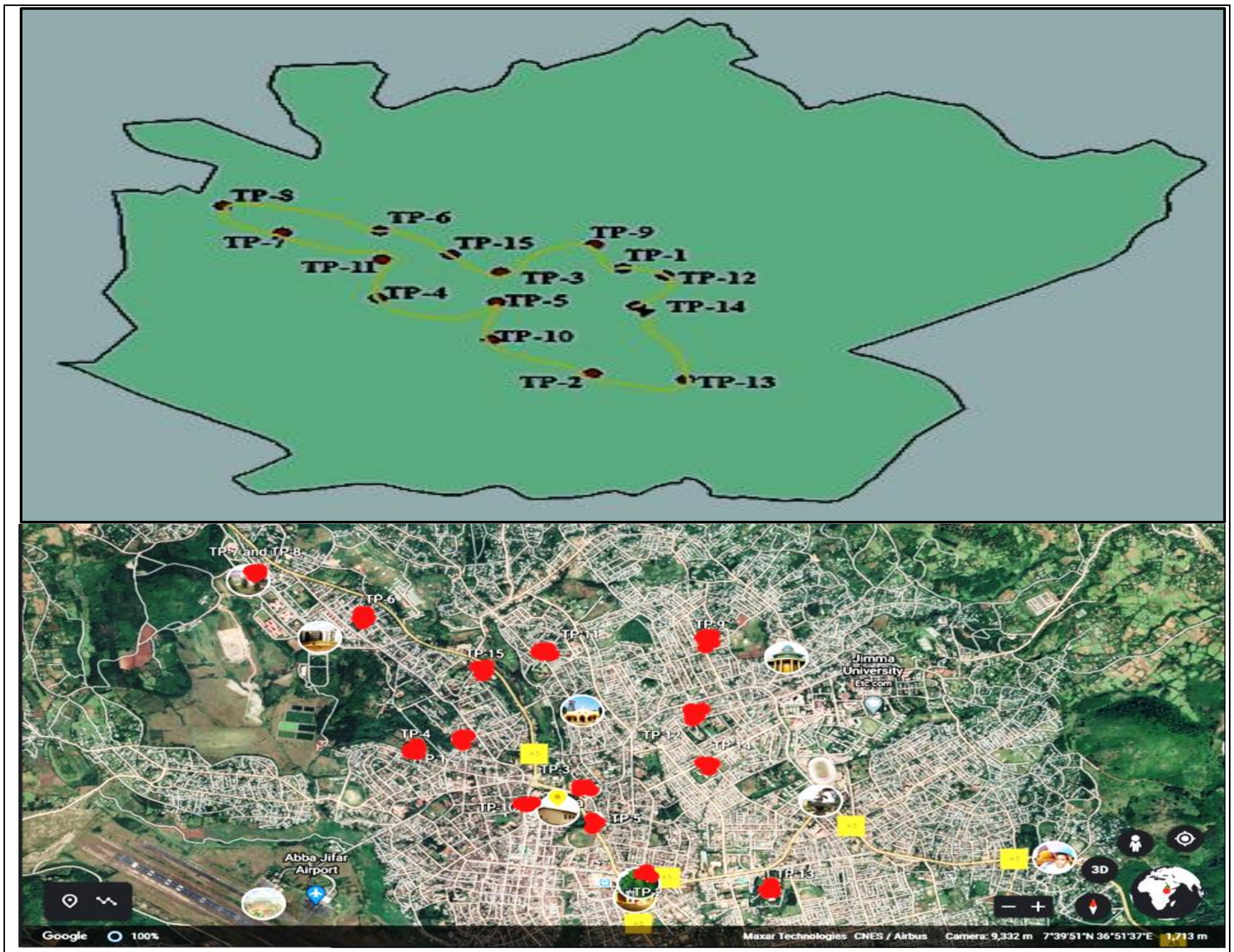

Figure 3.2: The geographical location sample test pits of the Jimma Town (Source: Arch GIS and Google earth)

3.5 Data Source

Primary data was obtained through laboratory tests and field investigation literature and materials used for this research from different source.

3.5.1 Field investigation

In this study, identify the soils of the study area during dry season through field investigation methods. According to the method [39, 40] expansive soils have the following properties: have a color of red, black and gray, polygon pattern of surface crack during dry season, a shiny surface when partly dry piece of soil is polished with finger, high dry strength and low wet strength and sickness and low traffic ability when wet. Based on this technique's soils sample of fifteen different location where identified.

3.5.2 Material

Soil is the essential source of material that used to examine by researcher in the study area. The soil used in this study was fine-grained soil, which is collected from Jimma town. The soil sample with represents soil sample of Jimma town has obtained from fifteen pits, which have stated above in sample size. A disturbed and undisturbed sample has collected from the hole at a depth of 1.5 to 3 m from ground level to avoid the inclusion of organic matter. Figure 1 in *appendix-2* shows that the over view of extracted source of material (soil) from different test pits. The index and engineering properties of soil sample are going to be determined as per AASHTO and ASTM standards of practice and briefly discussed in chapter four.

3.6 Sample Preparation

3.6.1 Preparations of disturbed and undisturbed soil sample for laboratory tests

Before testing the disturbed soil sample has prepared by the method described in AASHTO T87-86 (1996). This process involves: Air drying of samples and oven drying at 105±5ºC; breaking up the soil aggregates by a rubber covered mallet and adequately pulverized, then sieve analysis is conducted on properly pulverize natural soil. Sieves were conduct into three groups. The first team are soil samples passing, #10 (2.00 mm) sieve for specific gravity, soil samples passing #40 (4.25 mm) sieve for Atterberg limits and free swell and the third group are soil samples passing #200 (0.075 mm) for Hydrometer test. Disturbed soil sample preparation procedures were shown in *appendix-2* by figure 2.

Through this research, undisturbed soil samples were collected directly from the soil sample using cone cutter (steel tubes). Preparation of the sample began with removing the sample by opening the plastic case and separating the sample from the cone cutting tube. Then the sample cut one third (1/3) of its original height before being cut. The soil was trimmed to a size of 50 mm in diameter and 20 mm in height following the dimensions of the stainless-steel ring. Trimmer held the soil in place while using pre-tensioned steel wire to reduce soil thickness to the required dimensions. The soil was cut vertically against the trimmer wall to give it a smooth cylindrical shape shown in *appendix-2 by* Figure 3. Samples leftover from the trimming process are used for other tests, such as the Atterberg limits and the moisture content. The trimmed sample is, then placed inside the ring and assembled as in the oedometer apparatus.

3.7 Data collection process

Data collection concerned a plan for gathering data, information from field situations. A set of procedure followed to get the desired data or information from the fieldwork according to the ASTM standard manual to process and analyses the facts in a logical and scientific manner.

Thirty soil samples have collected from Jimma town. In collection of data, both disturbed and undisturbed samples have taken and collected in plastic bag from the depth of 1.5 to 3.0 m below the ground level. The amassed samples have been examined in the laboratory. Their index properties namely grain size distribution, specific gravity, liquid limit, plastic limit, dry density, initial moisture content and their classification are determined as per ASTM standard manual of practice. Samples of both disturbed and undisturbed were collected from fifteen test pits in different time from different locations. The sampling site was chosen to closely resemble the soils found in Jimma city. Selection of these sampling locations also considers visual soil classification, economic importance of sampling area, non-uniformity of the sample locations and coverage of the section. During excavation for sampling, it was observed that the ground water table is found far below 3.0 m depth. The locations of sample its coordinate system, elevation above mean sea level and terrain for different test pits are presented in Table 3.1.

Table 3.1: Sampling location and designation of sample test pits

Location	Test pit Code	Longitude (E)	Latitude (N)	Elevation (m)	Terrain	Color Description
Matric Village	TP-1	36º50`41.77‟	7º 40'54.59‟	1732.78	Rolling	Red
Bacho Bore	TP-2	36º50`31.20‟	7º 40'00.90‟	1720.59	Flat	Gray
Awetu Village	TP-3	36º50`04.96‟	7º 40'56.17‟	1723.03	Rolling	Red
Bossa Kitto	TP-4	36º49`30.24‟	7º 40'41.58‟	1738.88	Flat	Red
Hermata M.	TP-5	36º50`02.58‟	7º 40'19.49‟	1719.07	Flat	Gray
BAKG School	TP-6	36º49`23.10‟	7º 41'19.11‟	1752.29	Flat	Red
JiT/Stadium	TP-7	36º49`03.24‟	7º 41'17.19‟	1734.31	Flat	Gray
JiT/Dorm	TP-8	36º48`46.52‟	7º 41'31.69‟	1743.15	Rolling	Red
Kochi Village	TP-9	36º50`31.33‟	7º 41'11.07‟	1750.47	Rolling	Red
Arround CBE	TP-10	36º50`02.77‟	7º 40'19.10‟	1720.90	Flat	Gray
Sato Samaro	TP-11	36º49`39.15‟	7º 41'06.67‟	1755.65	Rolling	Red
Ginjo Guduru	TP-12	36º50`40.97‟	7º 40'51.47‟	1731.26	Flat	Black
Technic Area	TP-13	36º50`58‟	7º 39' 58‟	1744.07	Flat	Gray
Rift-valley Un.	TP-14	36º50`43.87‟	7º 40'37.63‟	1723.95	Rolling	Gray
Agri Area	TP-15	36º49`48.24‟	7º 41'06.55‟	1744.37	Rolling	Red

3.8 Study Variables

The independent variables of this study that were index properties such as Atterberg limits, dry density (γ_d), initial moisture content (w_n), specific gravity (G_s) has used as inputs. The dependent variable of this research is modeling for prediction of C_c based on soil index properties. Hence, the dependent variable C_c that is depending on the independent variables that were Atterberg limits (LL, PL and PI) since these variables is significant on dependent variable from the other index properties using statistical determination.

3.9 Laboratory Tests

Several tests have carried out such as the index soil test and oedometer in this research thesis. The samples have taken from Jimma at different areas of the town. The depth of the samples taken has varied in the range of 1.5-3 m. The physical (index properties) tests involved were moisture content, specific gravity, Atterberg limits, particle size distribution, and free swell test. In this study, the consolidation (oedometer) test was used to determine the compression index. One dimensional consolidometer having brass ring 50 mm in diameter and 20 mm height to be used. The specimen for consolidation test was prepared in initial moisture content and dry density. The laboratory test results were carefully examined and discussed after they were obtained. Then the output from analysis had been compared with standard specification of soil materials (ASTM and AASHTO), then categorized according to their test results. Finally, the determined output gives conclusion and recommendation.

3.9.1 Index properties of soil tests

The tests have performed in order to obtain the index soil properties such as moisture content, Specific gravity, Atterberg limits, particle size distribution, free swell and others. There were twenty different soils samples from ten test pits used for the entire test conducted. All the tests performed in this research were accordance to ASTM and AASHTO the results have discussed in Chapter four.

Moisture Content (MC)

Moisture content test has conducted for natural soil sample according to the standard test procedure of ASTM (D-2216-98) the following process has used to determine moisture content of the tested soil: Disturbed small representative soil sample covered with plastic was taken from the site; obtained soil sample was weighed and kept in oven dried for at least for 16 hours; then the sample was then reweighed, and the weight of dry soil divided the difference in weight is giving moisture content of the soil.

Specific Gravity (Gs)

Specific gravity tests have conducted using the small pycnometer jar method as shown in *Appendix-2 by* Figure 4. This method is more accurate for fine -grained soil compare to the large pycnometer jar method. The value for the Gs has used for the calculation of the soil parameters such as the moist density or the initial void ratio.

Atterberg Limits

The Atterberg limits of the soil are composed of two different tests, which were LL and PL. These were determined through the standard Casagrande method and plastic limit method. The values of the plastic and the liquid limit were used for correlation with several parameters obtained from oedometer test. The LL and PL values were used in determining the plasticity index.

a. Liquid limit (LL)

Liquid limit test where conducted according to the standard test procedure of ASTM (D4318-98), and the test are performed by the following process: 250 g of air-dried soil sample passing through sieve #40 (opening 425μm) was obtained soaked at least for 16 hr. to ensure that the soil grained had absorbed water and soften through; Then the mixed soil paste was placed on the Casagrande cup and grooved by standard grooving tool; Then the cup has lifted up and dropped by turning the crank until the two parts of the soil come into contact at the bottom of the groove. For one test point, it needs three trials by increasing 1-3 % of its moisture content. The number of blows at which that occurred has recorded, and a little quantity of the soil has taken and its moisture content determined. The values of the moisture content (determined) and the corresponding number of blows has then plotted on a semi-logarithmic graph, and the liquid limit has identified as the moisture content corresponding to 25 blows.

b. **Plastic limit (PL**)

Plastic limit test was conducted according to the standard test procedure of ASTM (D4318-99), and the following process performs the test: A portion of the natural soil used for the liquid limit test has retained for the determination of plastic limit. Retained soil sample paste was remolded and rolled into the threads on glass plate until the threads started to crack at a diameter of about 3 m. The moisture content at which the soil sample begins to crumble at the specified width was recorded as plastic limit.

c. Plastic index (PI)

Plastic index of the natural soil sample has calculated by subtracting the result of plastic limit from liquid limit.

$$PI = LL - PL \quad \text{--} \text{Eq. (3.1)}$$

Free swell test

The test included of determining the free swell for the natural soil and stabilizing the soil sample. Both AASHTO and ASTM have not yet standardized this analysis. Holtz and Gibbs, (1956) proposed the method for measuring the expansion potential of cohesive soils. The free swelling test is the simplest test that is carried out to examine the swelling properties of the soil. This test was performed by slowly pouring 10 ml of oven dry soil that has passed the No.40 (0.425 mm) sieve into 100 ml graduated cylinder filled with distilled (tap) water. The final volume of the suspension is read after 24 hours. Soils with a free swell of less than 50% are unlikely to have any expansive properties, while soils with a free swell of more than 50% can cause swelling problems. Values of 100% or more are associated with clay that could swell considerably. Finally, Figure 6 showed the free swell test procedure in Appendix-2 and the value of the free swell value was calculated according to the Equation (3.2).

$$\text{Free swell} = \frac{\text{Vf}-\text{Vi}}{\text{Vi}} * 100 ------------------------- \text{Eq.}\,(3.2)$$

Where: VI = initial reading and VF = final reading after 24 hours. This test tries to give a reasonable approximation of the degree of expansion of a soil sample.

3.9.2 **Grain Size Distribution**

This test was performed to determine the percentage of grains of different sizes found in a soil. Mechanical or sieve analysis is carried out to determine the distribution of coarse particles of grater-size. The hydrometer method is used for determination of the distribution of the most exceptional particles (ASTM D 422-63).

Wet sieve analysis

Wet sieve analysis test has carried for natural soil sample, and the test has conducted by the following procedure: 500 gm to 1000 gm of the natural soil sample is taken and washed on sieve size of 75μm; After removed the soil sample, the retained soil on sieve size of 75μm was taken and oven dried over the night; weighing the dried soil sample and recording the weight; Clean all of the sieves and stack them in ascending order of sieve number (#4 sieves at the top, #200 sieves at the bottom). Place the pan in front of the #200 sieves. Carefully pour the dried soil sample into the top sieve, place the cap over it; and place the sieve stack in the mechanical shaker, and shake it, after 10 minutes remove the stack from the shaker and finally record the weight of the soil retained on each sieve.

Hydrometer test

For determining the distribution of fine particles (silt and clay) 50g of air-dried soil sample passing through sieve 75µm is used. The soil sample is socked in a chemical solution of 125 ml (40g/lit) (Sodium hexa-metaphosphate) for 24 hours. Hydrometer readings were taken at 1,2, 5, 8, 15, 30, 60, 240 minutes and 24 hours and the test procedures were shown in *Appendix-2* by Figure 7.

3.9.3 Consolidation (Oedometer) Test

Tests were performed with an oedometer to determine the magnitude of the decrease in soil volume that was confined laterally when it was subjected to different vertical pressures as part of this study. The results of the experiments will provide the compression curve (pressure-void relationship). These data are used to determining the compression index (Cc), recompression index (Cs) and the preconsolidation pressure (Pc) of the soil. The oedometer tests were carried out as specified by ASTM D-2435-03 and using a standard floating ring method [41]. The samples were placed in the stainless-steel ring measuring 50 mm in diameter and 20 mm in height. The ratio of lever arm of the oedometer machine is 10:1, which indicates that the given ratio should multiply the weight load transfer.

Porous stones were placed on the upper and lower sides of the sample to allow water to enter the soil. The porous stones held together in vacuum distilled water to saturate the porous stone and facilitate the permeability of the porous stone for a period. The test was carried out at room temperature, which was maintained at 25 ºC+- 1 ºC.

i. Saturation stage

In the consolidation test, the specimens were first subjected to a saturation process. At this stage, the samples were left in the metal case in the presence of water for 24 hours. However, this is an assumption made by Terzaghi that all pores within the soil have become completely saturated with water. The initial dial gauge reading was used as a reference before the saturation process was started. It is observed during the saturation process that the soil tended to expand after the water had poured into the metal shell. To prevent the soil from swelling further, several lightweights were added one by one until the dial gauge reading reached the initial value before the saturation process. These applied pressures have been added carefully and just enough to prevent the soil from expanding further. The soils are saturated for 24 hours and the reading was checked again until it reached a constant value before the consolidation began.

ii. Loading and unloading stages

The consolidation tests carried out consisted of two stages of loading and unloading processes. In each test, the specimen was loaded up to1600 kPa and in between of the loading, the sample was unloaded at100, 200, 400 and 800 kPa respectively. At 400 kPa, the sample was unloaded to 200 kPa before loaded it back to 800 kPa. After the load has reached at this point, the soil was unloaded back to 600 kPa. The summary of the loading and unloading stages are presented in Chapter four. In this test, the duration to complete loading and unloading stages was not be completed without observing the creep behaviour for 24 hours at the end of the loading or unloading stage. The compression and expansion values were measured by an observation from the dial gauge reading. Creep is a condition in which the soil experiences a set in the soil particles. It is important to monitor the creep to ensure that the next compression of the soil is not due to the influence of the creep, but to the compression by the weight loaded on the soil. A plot of settlement (mm) versus time (min) and the gradient that was observed before any loading or unloading intent. If the gradient was less than 0.002, then Figure 8 in *Appendix-2* shows that the loading or unloading stages can be carried out since the increment load changes are not so significant and the soil has reached the equilibrium state.

3.10 Data processing and analysis

The data Processing and analysis to be carried out in this study was presented and explained using tables, charts, and graphs. The results of laboratory tests were analyzed and compared to the standards and current standard proposed by ASTM, AASHTO. The result obtained was organized and interpreted using MS-Excel and numerical modeling according to established objective and presented as a chart, table and graph. Regression analysis and artificial neural network are the two approaches that to get the correlation between compression index (C_c) and soil index properties (i.e. LL, PL and PI).

Regression analysis is used to explain variability in the dependent variables by means of one or more of the independent or control variables. it can used to predict the value of dependent variable based on value of the independent variables. To correlate the linear of the measured compression index from the soil index properties by using a computer program Microsoft excel and (SPSS-20).

In this study, compression index (Cc) is the dependent variables whereas the LL, PL, and PI are regressor variables. To carry out statistical analysis, Microsoft® excel, SPSS-20 were used. Thirty numbers of samples are used in correlating Cc with LL, PL, and PI. While caring out the statistical analysis different regression models (i.e., LR, MLR) are used and those models with a higher value of coefficient of determination (R^2) are accepted.

A multiple linear regression (MLR) model of compression index was built to test the relationship between Cc and its determinants. The ANN model was compared to this model. The following multiple regression equation was used to predict the Cc for the dataset as follows:

$$yi = \beta 0 + \beta 1x1i + \beta 2x2i + \cdots + \beta pxpi + ei \text{ ---Eq (3.3)}$$

Where for a set of i successive observations, the predicted and variable y is a linear combination of an offset βo, a set of k predictor variables x with matching β coefficients, and a residual error e. The β values are usually calculated using the ordinary least squares method. When the regression equation is used in a predictive model, e is omitted because its expected value is zero. While curvilinear relationships can be integrated into regression models through polynomial terms, regression models are inherently linear. Known relationships can be pre-specified by transforming a nonlinear predictor variable into a more linear form before using it in the model.

Artificial neural networks are the numerical models that conduct many analyses. ANN's conduct to determine the output value, aim identifying, make out data of multi factorial pattern, and finishing the recognize form through fruitful training. The input and testing layer with the set of validation data presented in Ann's methodology through learning procedure, which is called trained a network. Initialization; training, adaptation and performance are learning functions in Ann's analyses. During the training process, a network is continuously updated by training functions, which recurrent utilize observed values to the net until a desired error criterion is found. The lowest possible error can be determined by using an error criterion till to the specific independent variables corral to their target variables. In addition, weights and the biases were obtained from the network training.

The observed values of the LL, PL, PI and C_c from the experimental results were taken as an input, the ANN mechanism was processed in the hidden layer, and the outputs were in the form of compression index. Figure 9 in *Appendix-2* shows the mechanism of ANN modeling. By changing hidden layers number, the R value changes. In this trained, the maximum R value is obtained by giving 20 hidden layers for the ANN modeling. Coefficient of determination (R^2-value) determined from the output. To find out the output values the simulation process is performed after R value was predicted. The simulation diagram of current problem where liquid limit, plastic limit and plasticity index are given as input variables is given in Figure 10 in *Appendix-2*. The high coefficient analyses of multiple determinations were selected. Derived equations for compression index, which is applicable to the study area and then comparison is made between the experimental results and the calculated results. Finally, from the developed correlation overall conclusions are drawn about the result obtained.

CHAPTER FOUR

4 RESULTS AND DISCUSSION

4.1 Index properties test of soils

The properties and characteristics of the soils vary from point to point. Index properties were used to identify and classify the soil. The various properties of soils, which has considered as index properties investigated in this study are natural moisture content, specific gravity, Atterberg limits, free swell and particle size distributions. The test results of all index properties were summarized in the Tables (4.1, 4.2, 4.3 and 4.4).

Table 4.1 illustrates the natural moisture content of different soil samples for disturbed soil of the study area. The NMC of the soil samples varied from small to large and the soils had different colors, which is ranged between 36.74 and 68.78% is the result of the study area. Table 4.2 summarizes the specific gravity of the soil samples. The results indicate that all soil samples conform to standard (ASTM) and the Gs, which vary from 2.6 to 2.9 for clayey and silty soils as suggested by Das [27]. The specific gravity of clay is between 2.60-2.76 and for silty it varies from 2.68-2.73. The specific gravity values showed a variation within a limited range at 1.5 to 3 m depths and at different locations.

The result of the Atterberg limit of soil sample used presented in Table 4.3 shows which was determined by using Casagrande's and plastic limit method. The liquid limit is between 58 and 106%; the plastic limit ranged from 24.8-52.3% and the plastic index between 31 and 62%. The test outcome displays, which the soils in the study area are highly plastic with high plasticity index values. Free swell test results for oven-dried (OD) samples at a temperature of 105º ±5º C are summarized in Table 4.4. The investigated free swell of the study area ranges from 40 to 110%. The soils are mostly in between 40% and 80% except for TP-12 and TP-13 at 1.5 m and 3.0 m that were typically black and light gray soils. In this study, there is a moderate expansive character, which has slightly bear upon the construction of structures.

Table 4.1: Natural moisture content of soil samples

Test Pits code	Depth (m)	Color	NMC (%)	Test Pits code	Depth (m)	Color	NMC (%)
TP-1	1.5	Red	43.90	TP-8	2.5	Red	46.88
	2.5	Red	47.41	TP-9	1.5	Red	43.26
TP-2	2.5	Gray	57.00		3	Red	44.78
	3	Gray	44.45	TP-10	1.5	Gray	45.51
TP-3	1.5	Red	43.96		3	Gray	47.50
	2.5	Red	47.50	TP-11	1.5	Red	43.57
TP-4	1.5	Red	47.39		2.5	Red	39.98
	2.5	Red	47.50	TP-12	1.5	Black	60.82
TP-5	1.5	Gray	45.91		3	Black	68.78
	2.5	Gray	66.62	TP-13	1.5	Gray	39.86
TP-6	1.5	Red	39.14		2.5	Gray	46.81
	2.5	Red	45.70	TP-14	1.5	Gray	52.87
TP-7	1.5	Black	40.89		2.5	Gray	56.47
	2.5	Gray	57.07	TP-15	1.5	Red	36.74
TP-8	1.5	Red	43.00		2.5	Red	54.21

Table 4.2: Specific gravity of the soil of the study area

Test Pit code	Depth (m)	Gs	Test Pit code	Depth (m)	Gs
TP-1	1.5	2.72	TP-8	2.5	2.61
	2.5	2.7	TP-9	1.5	2.69
TP-2	2.5	2.62		3	2.65
	3	2.6	TP-10	1.5	2.65
TP-3	1.5	2.76		3	2.61
	2.5	2.73	TP-11	1.5	2.61
TP-4	1.5	2.73		2.5	2.65
	2.5	2.71	TP-12	1.5	2.68
TP-5	1.5	2.69		3	2.7
	2.5	2.66	TP-13	1.5	2.63
TP-6	1.5	2.7		2.5	2.61
	2.5	2.68	TP-14	1.5	2.75
TP-7	1.5	2.69		2.5	2.73

	2.5	2.65	TP-15	1.5	2.68
TP-8	1.5	2.64		2.5	2.71

Table 4.3: Atterberg limits of the soils of sample

Test Pit code	Depth (m)	LL (%)	PL (%)	PI (%)	Test Pit code	Depth (m)	LL (%)	PL (%)	PI (%)
TP-1	1.5	81.30	36.60	44.70	TP-8	2.5	75.60	33.60	42.00
	2.5	77.30	37.30	40.00	TP-9	1.5	65.70	30.70	35.00
TP-2	2.5	59.50	28.50	31.00		3	83.50	38.50	45.00
	3	59.80	24.80	35.00	TP-10	1.5	67.40	31.40	36.00
TP-3	1.5	61.00	30.00	31.00		3	79.20	32.20	47.00
	2.5	60.00	29.00	31.00	TP-11	1.5	70.20	33.20	37.00
TP-4	1.5	79.70	44.70	35.00		2.5	71.00	32.00	39.00
	2.5	87.00	46.00	41.00	TP-12	1.5	101.00	52.30	48.70
TP-5	1.5	67.00	32.50	34.50		3	106.00	45.00	61.00
	2.5	72.30	34.80	37.50	TP-13	1.5	102.00	40.00	62.00
TP-6	1.5	63.00	32.00	31.00		2.5	92.00	36.00	56.00
	2.5	58.00	27.00	31.00	TP-14	1.5	77.00	36.00	41.00
TP-7	1.5	65.00	25.00	40.00		2.5	80.00	39.00	41.00
	2.5	90.00	40.00	50.00	TP-15	1.5	67.00	29.00	38.00
TP-8	1.5	77.00	37.00	40.00		2.5	65.00	30.00	35.00

Table 4.4: Free swell value of the soil samples

Test Pits code	Depth (m)	Test Condition	Free Swell (%)	Test Pits code	Depth (m)	Test Condition	Free Swell (%)

TP-1	1.5	OD	50	TP-8	2.5	OD	50
	2.5	OD	50	TP-9	1.5	OD	45
TP-2	2.5	OD	85		3	OD	40
	3	OD	70	TP-10	1.5	OD	70
TP-3	1.5	OD	50		3	OD	80
	2.5	OD	45	TP-11	1.5	OD	60
TP-4	1.5	OD	50		2.5	OD	50
	2.5	OD	50	TP-12	1.5	OD	90
TP-5	1.5	OD	80		3	OD	100
	2.5	OD	70	TP-13	1.5	OD	110
TP-6	1.5	OD	45		2.5	OD	95
	2.5	OD	40	TP-14	1.5	OD	50
TP-7	1.5	OD	80		2.5	OD	40
	2.5	OD	70	TP-15	1.5	OD	50
TP-8	1.5	OD	50		2.5	OD	50

4.2 Particle size distribution

Grain size distributions of the soil are given in *appendix-1* Table E-1 and Figure 4.1. The gradation curve for the tests carried out at 1.5 m and 3 m depths for each test pit is provided in

Appendix-1. From the particle size results, it was observed that there are a number of particle size variations. Grain size analysis yielded of percentage of finer than 0.075 mm (a clay content and silt fraction) ranging from 86.96-99.33%, sand fraction 0.67-12.89% and gravel content from 0.0 – 0.41% summarized in *Table-E*.

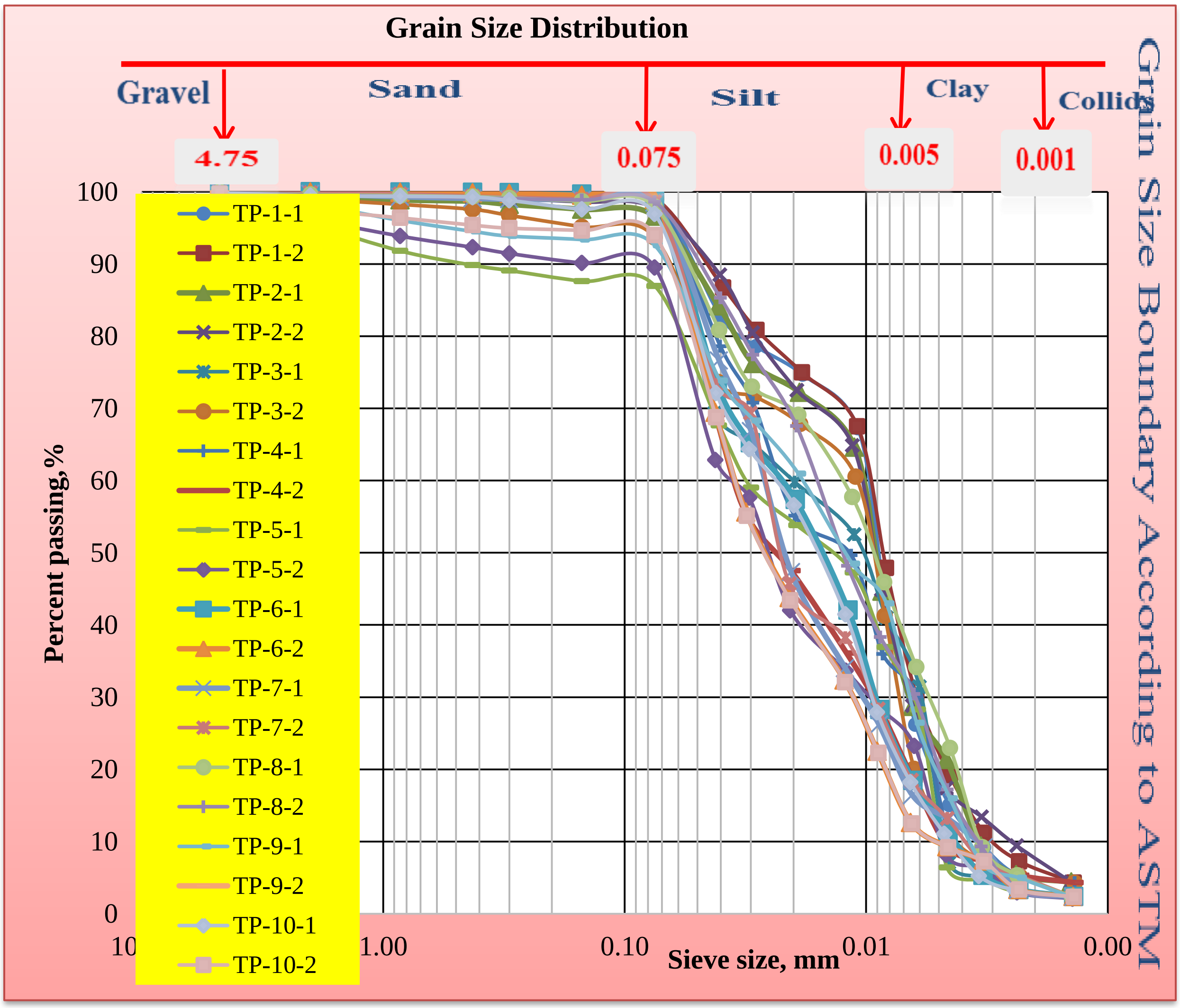

Figure 4.1: Summary of combined grain size distribution curves from sieve and hydrometer analysis for ten test pits at 1.5 and 3 m depths

4.3 Classification of the soil

For both the classification test results are summarized in Table 4.5. The gradation and the plasticity of the soil sample were determined for classification soil properties of the study area shown in Table 4.5. Most of the soils of the study area were in CH and three soil samples were in MH region as USCS classification scheme [42]. From visual observations and field tests, the soils of the study area were classified as clay with high plasticity. The soils are classified as CH or MH (clay with high plasticity, clay with high elastic) as USCS. According to AASHTO, [43] classification the soil is classified as A-7-5 and A-7-6 which are clayey soils.

Table 4.5: Classifications of soils based on USCS and AASHTO classification system

Test Pits code	Depth (m)	LL (%)	PI (%)	Particle size (%)	Classification style		Remark
					USCS	AASHTO	
TP-1	1.5	81.30	44.70	99.13	CH	A-7-5	Clay soils
	2.5	77.30	40.00	99.15	CH	A-7-5	Clay soils
TP-2	2.5	59.50	31.00	96.63	CH	A-7-6	Clay soils
	3	59.80	35.00	97.73	CH	A-7-6	Clay soils
TP-3	1.5	61.00	31.00	97.95	CH	A-7-5	Clay soils
	2.5	60.00	31.00	93.68	CH	A-7-6	Clay soils
TP-4	1.5	79.70	35.00	99.33	MH	A-7-5	Clay soils
	2.5	87.00	41.00	99.09	MH	A-7-5	Clay soils
TP-5	1.5	67.00	34.50	86.96	CH	A-7-5	Clay soils
	2.5	72.30	37.50	89.51	CH	A-7-5	Clay soils
TP-6	1.5	63.00	31.00	99.23	CH	A-7-5	Clay soils
	2.5	58.00	31.00	98.95	CH	A-7-6	Clay soils
TP-7	1.5	65.00	40.00	98.5	CH	A-7-6	Clay soils
	2.5	90.00	50.00	98.64	CH	A-7-5	Clay soils
TP-8	1.5	77.00	40.00	97.95	CH	A-7-5	Clay soils
	2.5	75.60	42.00	98.62	CH	A-7-5	Clay soils
TP-9	1.5	65.70	35.00	92.57	CH	A-7-5	Clay soils
	3	83.50	45.00	92.24	CH	A-7-5	Clay soils
TP-10	1.5	67.40	36.00	96.93	CH	A-7-5	Clay soils
	3	79.20	47.00	94.02	CH	A-7-5	Clay soils

TP-11	1.5	70.20	37.00	85.7	CH	A-7-5	Clay soils
	2.5	71.00	39.00	92.3	CH	A-7-5	Clay soils
TP-12	1.5	101.00	48.70	87.2	MH	A-7-5	Clay soils
	3	106.00	61.00	90.7	CH	A-7-5	Clay soils
TP-13	1.5	102.00	62.00	96.93	CH	A-7-5	Clay soils
	2.5	92.00	56.00	94.02	CH	A-7-5	Clay soils
TP-14	1.5	77.00	41.00	85.7	CH	A-7-5	Clay soils
	2.5	80.00	41.00	92.3	CH	A-7-5	Clay soils
TP-15	1.5	67.00	38.00	87.2	CH	A-7-6	Clay soils
	2.5	65.00	35.00	90.7	CH	A-7-5	Clay soils

For both soil classification schemes (USCS and AASHTO) of the plasticity chart were shown in Figures 4.2 and 4.3. The soil found in Jimma town is highly plastic clay except for soils TP-4 and TP-12-1 from all test pits that is highly elastic in Figure 4.2. Most soil samples of the study area were falls in A-7-5 subgroup, which the plasticity index is equal to, or less than the liquid limit minus 30 and below the A-line in Figure 4.3. In addition, some soil samples fall in A-7-6 subgroup, for which the PI is greater than the LL minus 30 and above or equal to the A-line. Therefore, the classifications of soil properties are to group the soil with similar properties, to facilitate communication and to shorthand notation.

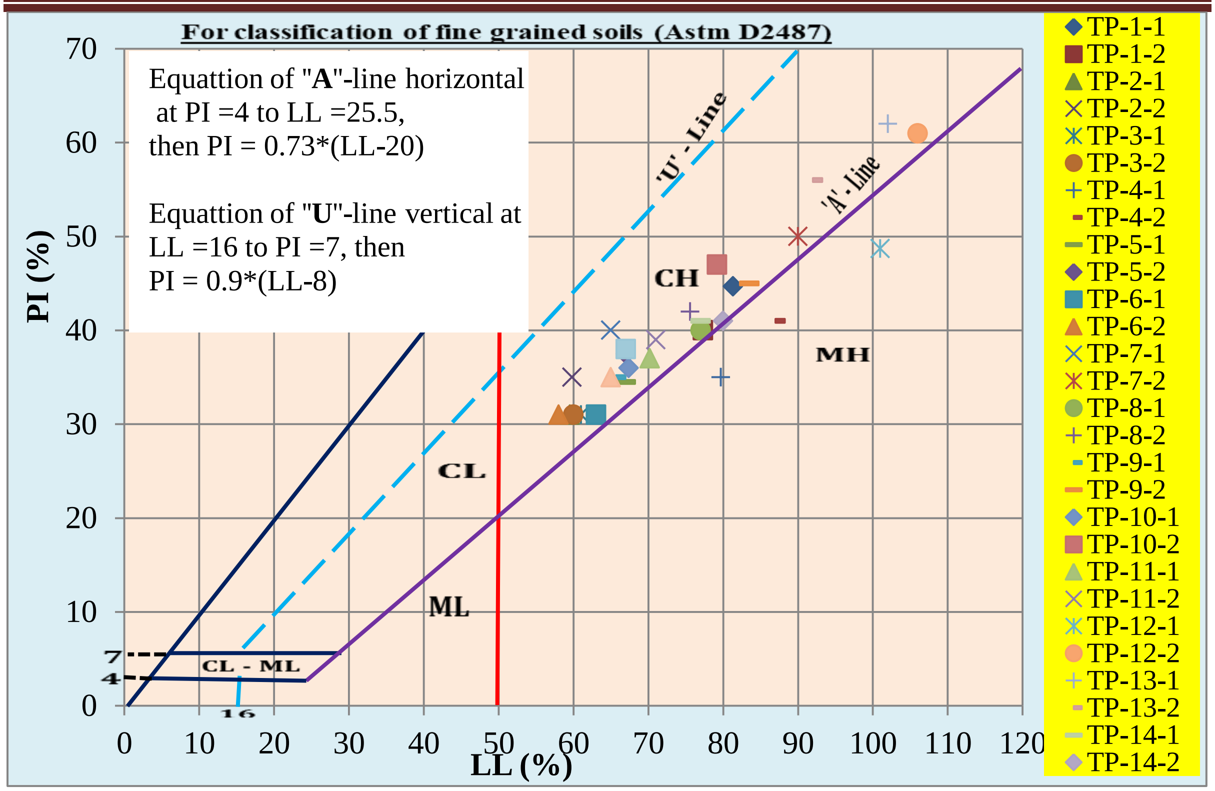

Figure 4.2: Plasticity chart for USCS of the soil

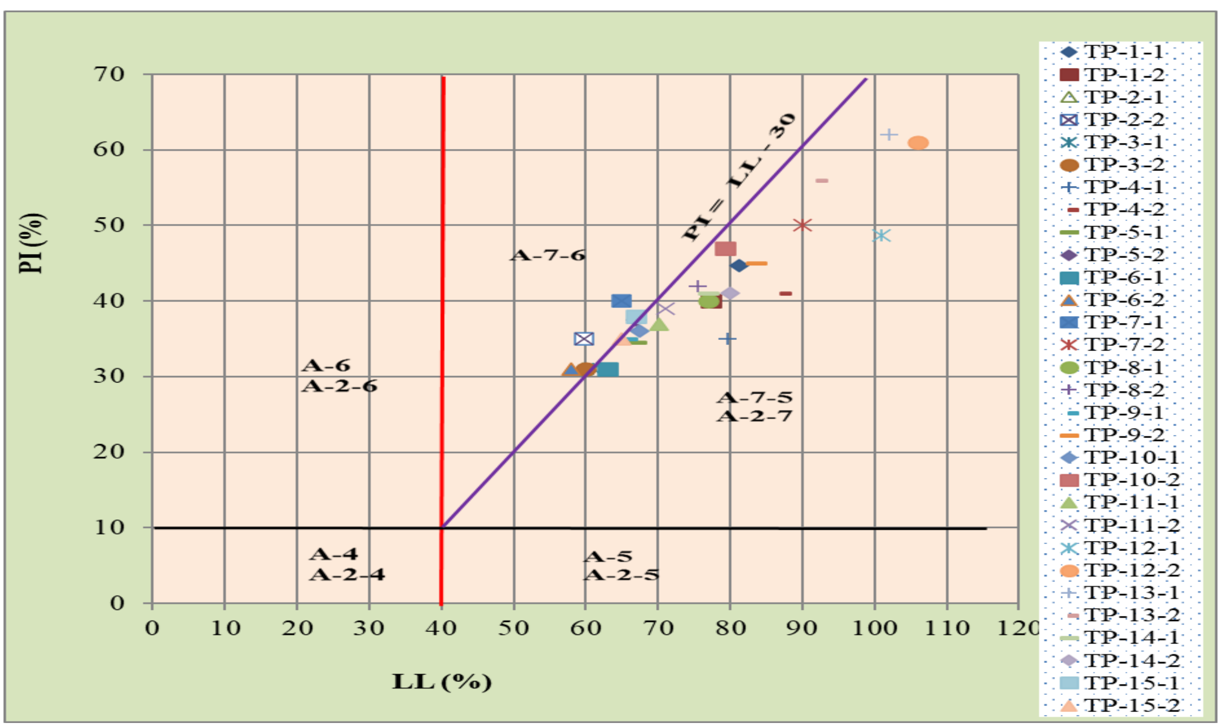

Figure 4.3: Plasticity chart of the soils according to AASHTO system of classification

4.4 Consolidation test

The summary of consolidation test results for five test pits are given in Table 4.6 and the value of ten test pits (TP-6 to TP-15) test results were presented in *Appendix-1* Table A-2.

Table 4.6: Results of consolidation test for ten soil samples for study area

Test pit code	Depth (m)	w_n (%)	e_o	LL (%)	PI (%)	C_c	C_s
TP-1	1.5	33.5	1.21	81.3	44.7	0.287	0.02
	2.5	31.3	1.33	77.3	40.0	0.274	0.06
TP-2	2.5	47.9	1.31	59.5	31.0	0.232	0.05
	3	45.5	1.3	59.8	35.0	0.227	0.07
TP-3	1.5	48.7	1.23	61.0	31.0	0.248	0.03
	2.5	39..6	1.19	60.0	31.0	0.244	0.03
TP-4	1.5	41.5	1.29	79.7	35.0	0.286	0.03
	2.5	43.1	1.31	87.0	41.0	0.31	0.03
TP-5	1.5	47.9	1.41	67.0	34.5	0.264	0.06
	2.5	43.9	1.36	72.3	37.5	0.243	0.05

[1]Natural water content and initial void ratio is calculated after consolidation test

Results of compressibility parameters for the thirty undisturbed soil samples collected from fifteen test pits around Jimma town summarized in *appendix-1* by Table A-2. The test results of collected data test in the study area is conducted for oedometer test with the value of Cc ranged between 0.227 and 0.33, the value of C_r ranged between 0.114 and 0.128 which obtained from four soil samples and the Cs values lies in a range of 0.02 to 0.11.

The results revealed that clays in the study area are highly plastic with a marginal degree of expansion and it have also relatively a moderate to high free swell values. Correlation between results of the fifteen station and collected data shows that the C_c values in general increases with increasing LL and PI of a soil. This serves to suggest that the soil compressibility generally increases with plasticity and vice versa.

Generally, the results of compression index (C_c) and recompression index (C_r) the soil of Jimma town is natural normally consolidated and the 13.33% was over consolidated from the thirty soil samples of the study area.

Pressure -Void ratio curve

The summary of pressure-void ratio curve is presented in Figures 4.4, 4.5, and *Appendix-1*

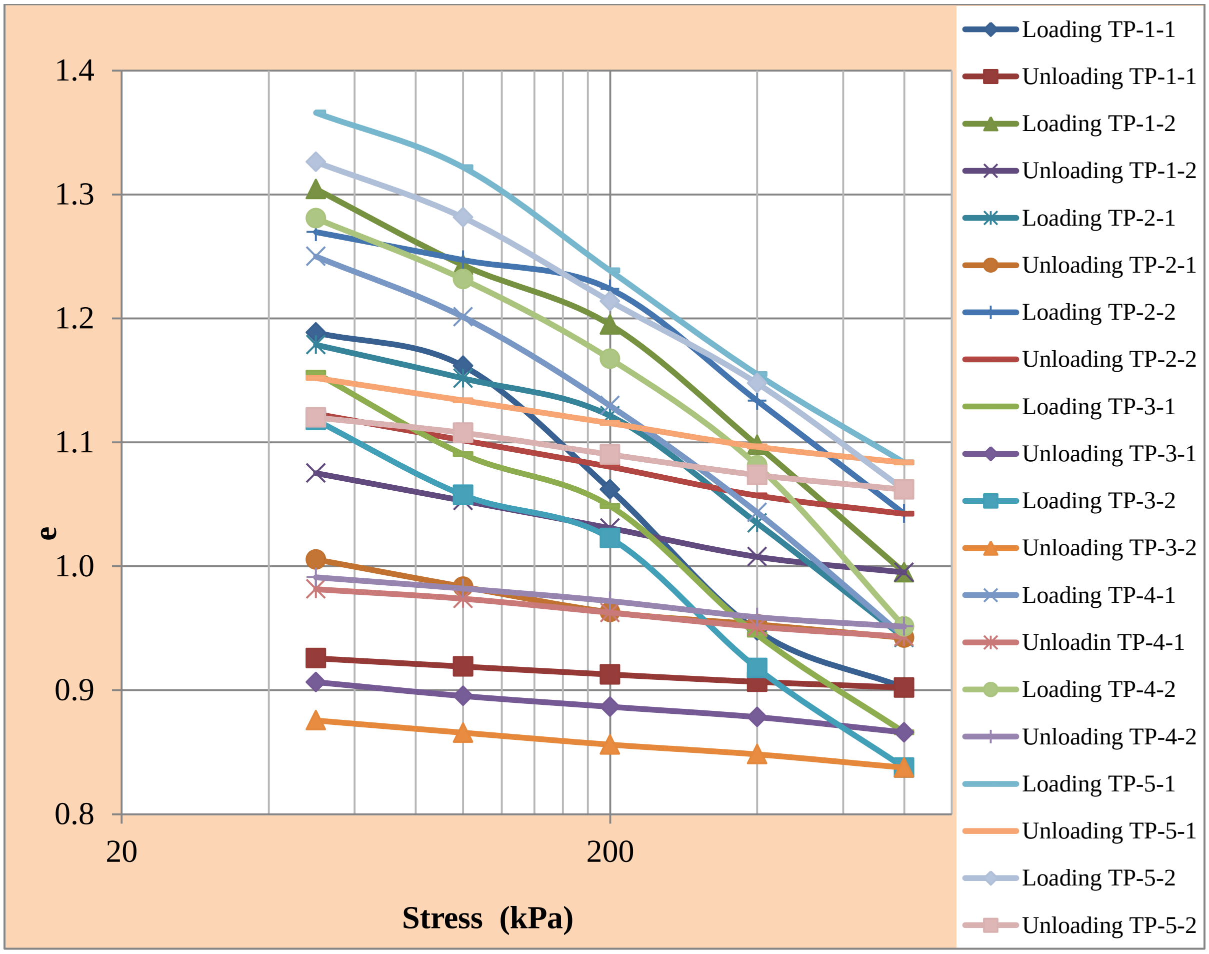

Figure 4.4: Plot of void ratio versus log-pressure curve for soil samples for five samples of the study area

The compression curves for soil samples in a standard e-log σc' space was shown in Figure 4.5. The preconsolidation stress, σc is the effective stress that separates the boundary line of soft and stiff deformation of soil with response to loading. The consolidation of the curves illustrated a slight concave upon reaching the virgin compression line. The C_c has described by the change of the void ratio, e and the log scale. It can clearly observe that the initial void ratio of TP-3 was lower than TP-1, TP-2, TP-4 and TP-5 as summarized in *Appendix-1*, Table A-4, which indicates that the soil is relatively denser. This indicates the soil that has lower initial void ratio tend to has higher preconsolidation pressure as indicated in Figure 4.5(b) for TP-3-2.

Generally void ratios for all of samples were reduced to lower value since increasing intensity of loadings at each steps of loading brought soil grains more closely to each other.

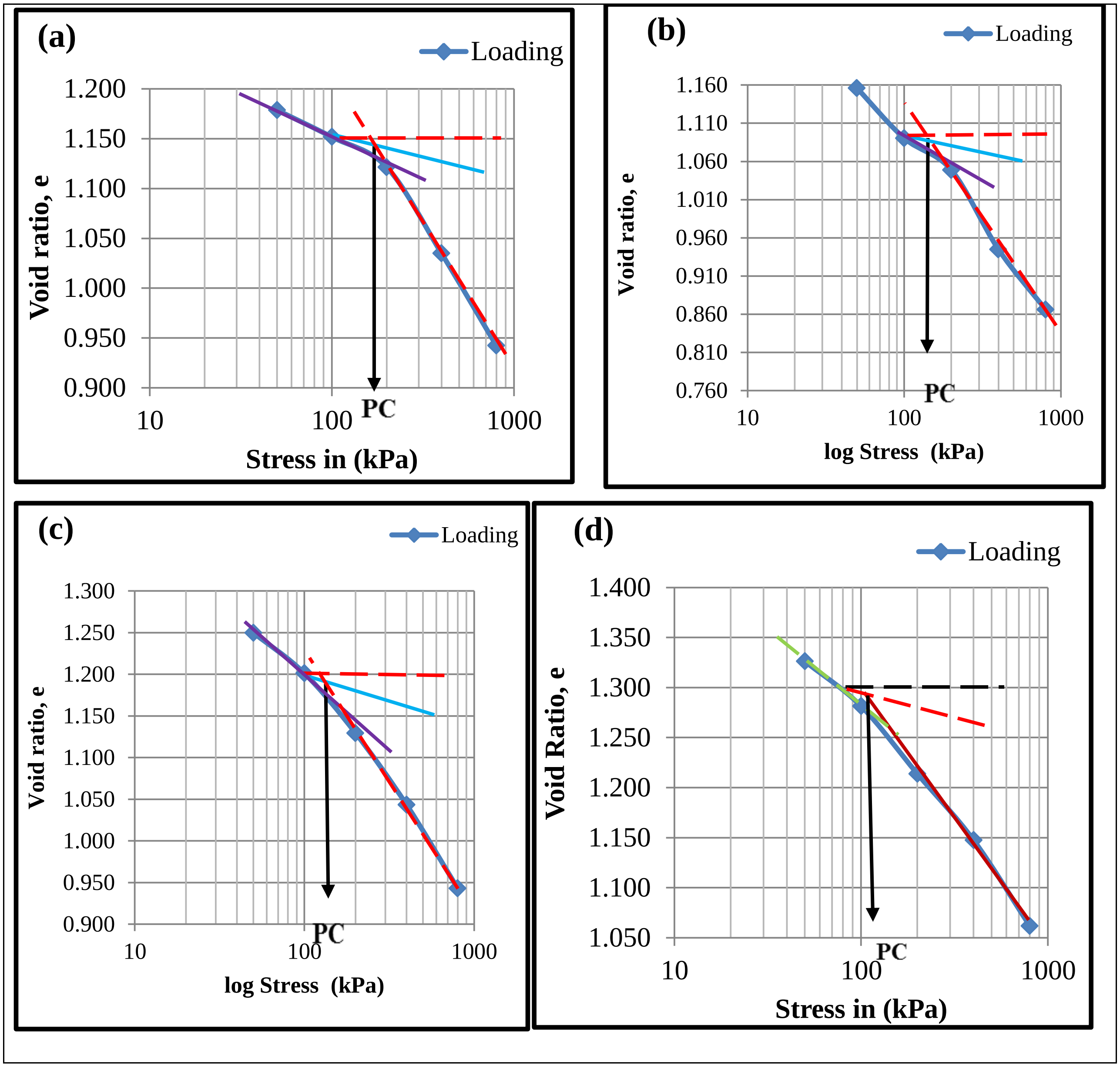

Figure 4.5: Plot of the preconsolidation stress (a) e- log σ for TP-2-1; (b) e- log σ for TP-3-2; (c) e -log σ for TP-4-1; and (d) e- log σ for TP-5-2

4.4.1 Numerical Modeling

4.4.1.1 Regression analysis

The linear regression discussed was (i.e., the regression between Cc and with soil index parameters) had shown that the compression index is significantly affected by liquid limit, plastic limit and plasticity index. The remaining parameters such as natural moisture content, specific gravity and void ratio has not affected the Cc in a significant amount.

In the Figure 4.6 the scatter plot of Cc with LL, PL, PI, NMC and e_o are presented. The available test points are not sufficient to give reliable relationships between the independent and dependent variables. Nevertheless, different models (linear and non-linear) have been employed to examine the trend of the scatter in Figure 4.6.

Figure 4.6(a) shows that the compression index is increased with the increment of liquid limit and have a good relationship between Cc and LL as R^2 = 0.845. Figure 4.6(c) indicates the Cc is increased with PI increased and have a positive relationship between Cc and PI as the value of R^2 = 0.741. Figure 4.6(b) shows that the compression index is increased with the increment of plastic limit but it not intrinsic variable on Cc value as LL and PI. Figure 4.6(d and e) shows that the compression index is decreased with the decreasing of NMC and e_o but it not intrinsic variable on Cc value, since the R-value of e_o and NMC is less than 50% (i.e. e_o =20% and NMC =17%). In developing correlations, the first step is creating a scatter plot of the data; visually assess the strength and form of the relationship.

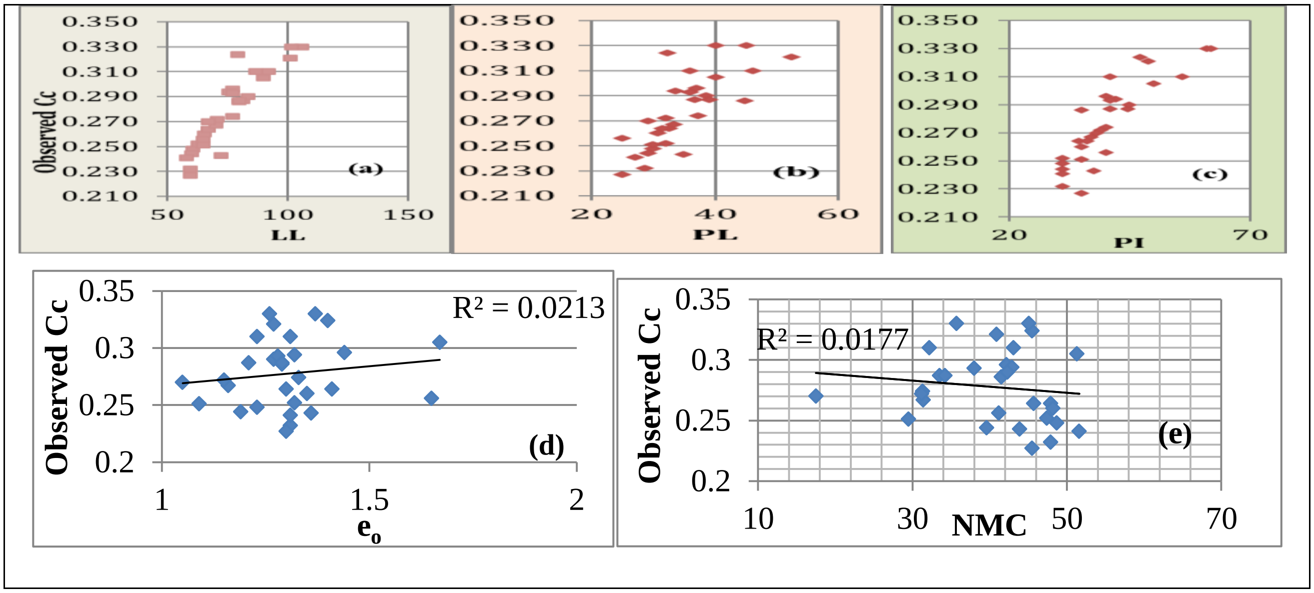

Figure 4.6: Scatter plot of Cc versus LL, PL, PI, NMC and e_o

The multiple regressions were conducted clay soils after incorporating data inside of Jimma is used for parametric study on compression index. The adjusted coefficient of determination mentioned in the following sections of the multiple regressions describes the amount of variance in Y, which could be explained by the regression equation in Chapter three (*Section 3.10*, *Equation 3.3*). In this study, the developed equation for multiple regressions of C_c with LL (%), PI (%), and PL (%) for clay soils, with N = 30, R^2 = 0.798 and standard error = 0.012 is:

Cc = 0.0018*LL +0.0004*PI + 0.1231 --Eq (4.1)

The multiple regression of C_c with LL and PI indicated that Cc has good correlation with the parameters by achieving adjusted coefficient of determination of 79% with 30 samples (refer to Equation 4.1). But PL is not affecting the Cc in significant amount in case of multilinear regression.

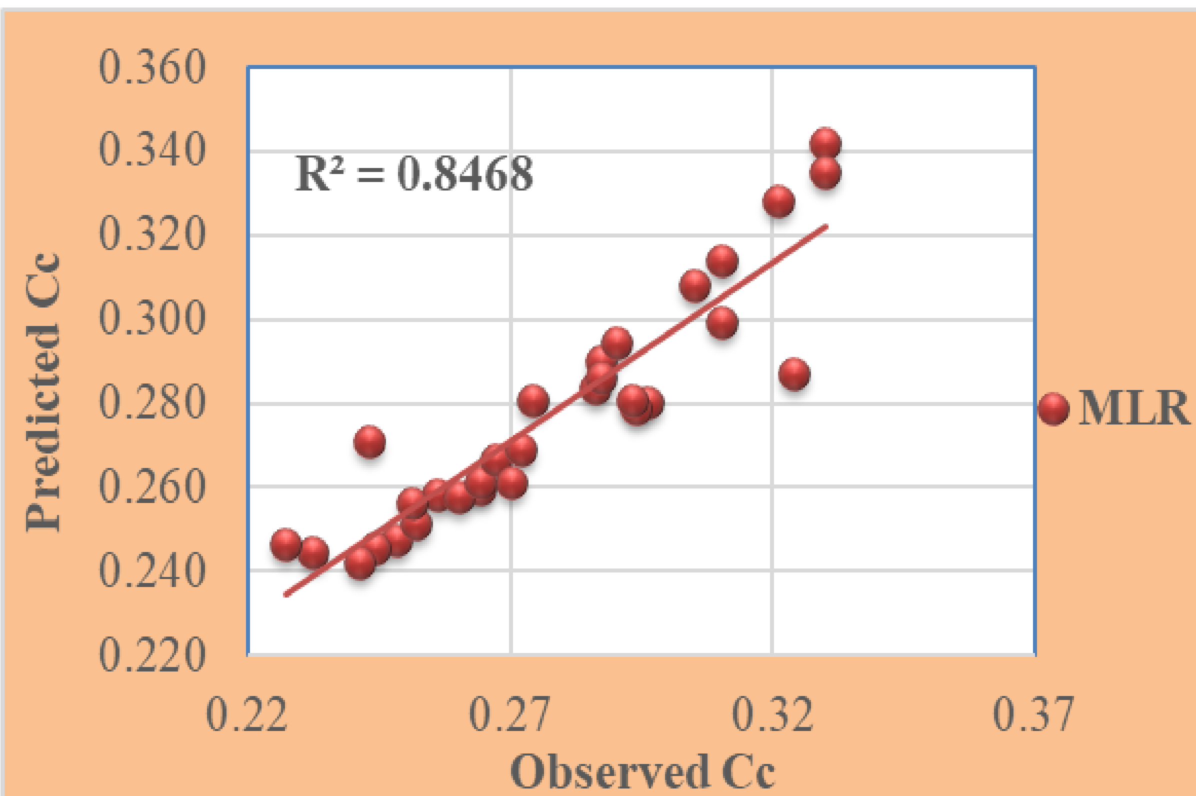

Figure 4.7: The predicted compression index versus the observed compression index proposed through multilinear regression analysis model

Three different values of C_C predicted when LL, PL and PI are given as inputs are shown in Table 4.7.

Table 4.7: Predicted values of Cc using regression model LL, PL and PI as input

Test pit code	Observed Cc	Pred. Cc LL as input	Pred. Cc PL as input	Pred. Cc PI as input	Test pits code	Observed Cc	Pred. Cc LL as input	Pred. Cc PL as input	Pred. Cc PI as input
Tp-1-1	0.287	0.290	0.284	0.290	Tp-8-2	0.294	0.278	0.273	0.282
Tp-1-2	0.274	0.282	0.286	0.276	Tp-9-2	0.260	0.258	0.263	0.261
Tp-2-1	0.232	0.245	0.255	0.248	Tp-9-2	0.290	0.294	0.291	0.291
Tp-2-2	0.227	0.245	0.242	0.261	Tp-10-1	0.264	0.261	0.266	0.264
Tp-3-1	0.248	0.248	0.261	0.248	Tp-10-2	0.324	0.286	0.268	0.297
Tp-3-2	0.244	0.246	0.257	0.248	Tp-11-1	0.267	0.267	0.272	0.267
Tp-4-1	0.286	0.287	0.313	0.261	TP-11-2	0.272	0.269	0.268	0.273
Tp-4-2	0.310	0.302	0.317	0.279	TP-12-1	0.321	0.331	0.339	0.303
Tp-5-1	0.264	0.260	0.269	0.259	TP-12-2	0.330	0.341	0.314	0.340
Tp-5-2	0.243	0.271	0.278	0.268	Tp-13-1	0.330	0.333	0.296	0.343
Tp-6-1	0.252	0.252	0.268	0.248	Tp-13-2	0.310	0.312	0.282	0.325
Tp-6-2	0.241	0.242	0.250	0.248	TP-14-1	0.293	0.281	0.282	0.279
Tp-7-1	0.256	0.256	0.243	0.276	TP-14-2	0.287	0.287	0.292	0.279
Tp-7-2	0.305	0.308	0.296	0.307	Tp-15-1	0.270	0.260	0.257	0.270
Tp-8-1	0.296	0.281	0.285	0.276	Tp-15-2	0.251	0.256	0.261	0.261

4.4.1.2 Artificial neural network (Ann)

Atterberg limits detected LL, PL and PI were given as input and observed C_c was given as target for the ANN modeling. After the values were given as input, the training process will take place in the developed hidden layer to predict the R-value. From the trained results the output values are obtained and the trained model results were shown in *appendix-1*. Figure 4.7 shows the R value after training process.

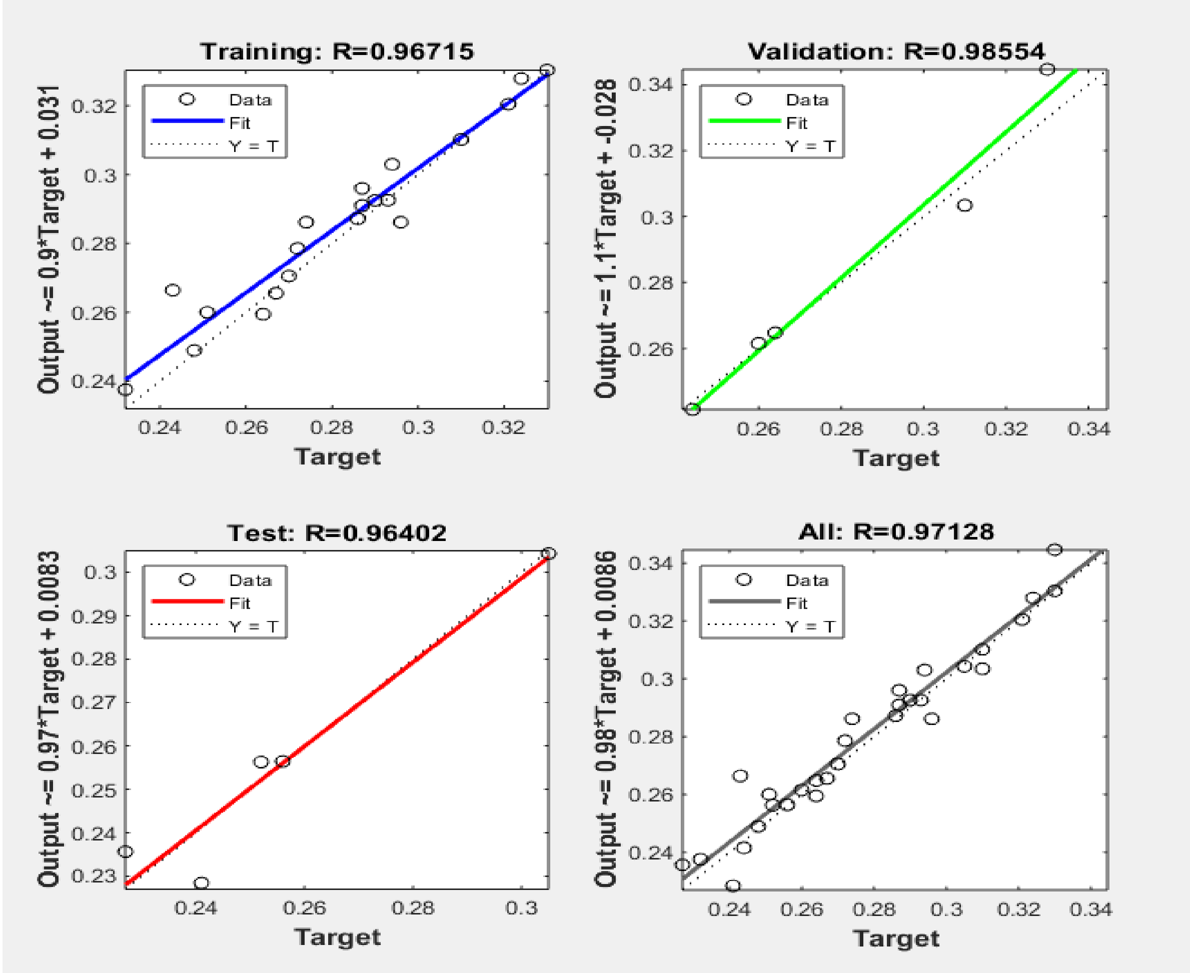

Figure 4.8: Output after training

Three different type of predicted values of compression index (Cc) using ANN model when liquid limit, plastic limit as input and plasticity index as input are shown in Table 4.8

Table 4.8: Predicted values of compression index using Ann Model

Test pit code	**Cc observed**	**Pred. Cc LL as input**	**Pred. Cc PL as input**	**Pred. Cc PI as input**	**Test pits code**	**Cc observed**	**Pred. Cc LL as input**	**Pred. Cc PL as input**	**Pred. Cc PI as input**
Tp-1-1	0.287	0.287	0.292	0.287	Tp-8-2	0.294	0.294	0.289	0.301
Tp-1-2	0.274	0.274	0.283	0.277	Tp-9-2	0.26	0.260	0.259	0.263
Tp-2-1	0.232	0.227	0.241	0.243	Tp-9-2	0.29	0.290	0.290	0.291
Tp-2-2	0.227	0.231	0.231	0.263	Tp-10-1	0.264	0.272	0.269	0.264
Tp-3-1	0.248	0.249	0.257	0.243	Tp-10-2	0.324	0.324	0.288	0.325

Tp-3-2	0.244	0.243	0.251	0.243	Tp-11-1	0.267	0.287	0.290	0.260
Tp-4-1	0.286	0.299	0.285	0.263	TP-11-2	0.272	0.257	0.286	0.275
Tp-4-2	0.31	0.295	0.327	0.298	TP-12-1	0.321	0.321	0.328	0.320
Tp-5-1	0.264	0.264	0.290	0.259	TP-12-2	0.33	0.330	0.326	0.330
Tp-5-2	0.243	0.243	0.243	0.260	Tp-13-1	0.33	0.330	0.311	0.330
Tp-6-1	0.252	0.252	0.286	0.243	Tp-13-2	0.31	0.310	0.301	0.305
Tp-6-2	0.241	0.239	0.240	0.243	TP-14-1	0.293	0.293	0.301	0.298
Tp-7-1	0.256	0.262	0.232	0.277	TP-14-2	0.287	0.287	0.292	0.298
Tp-7-2	0.305	0.305	0.311	0.307	Tp-15-1	0.27	0.264	0.251	0.262
Tp-8-1	0.296	0.293	0.284	0.277	Tp-15-2	0.251	0.262	0.257	0.263

Predicted vs observed Cc that obtained through ANN trained model is shown in figure 4.8.

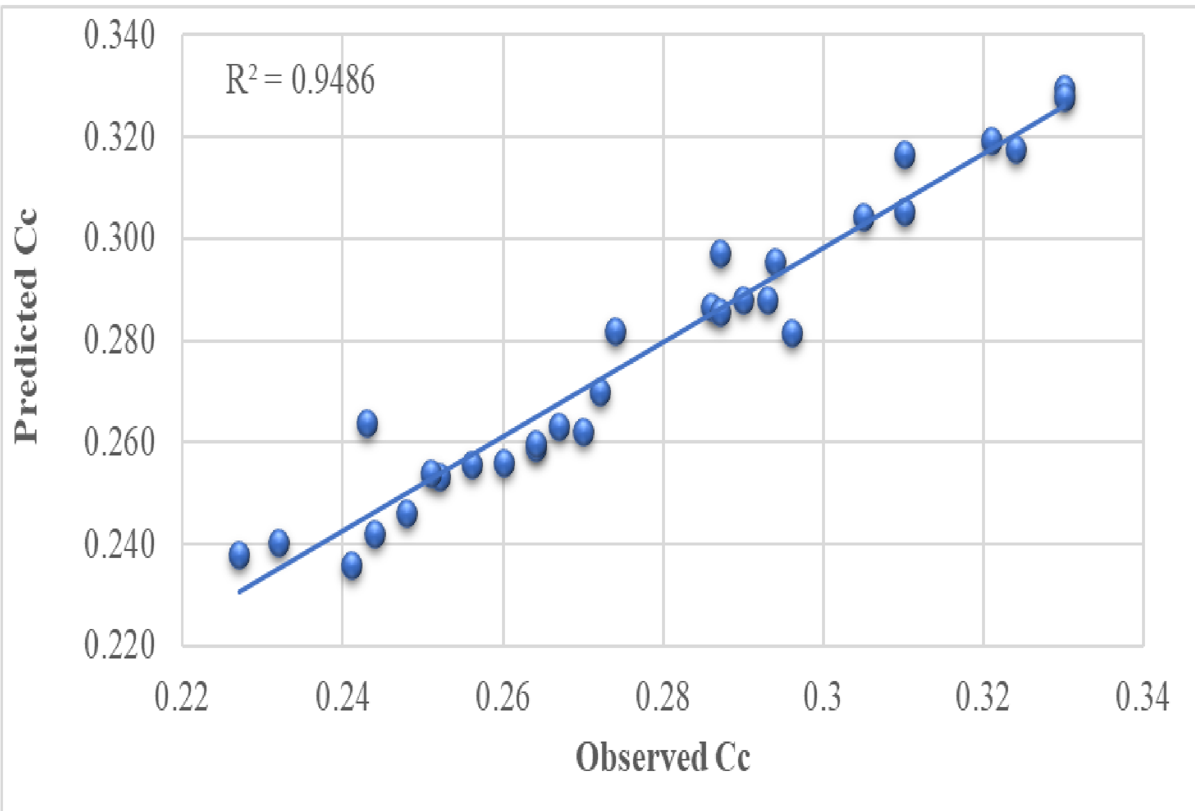

Figure 4.9: The predicted compression index versus the observed compression index by ANN trained model

Correlations using the ANN

The relation between the observed and predicted compression index with liquid limit, plastic limit and plasticity index as input presented in Appendix I, Figures 1, 2 and 3. Correlation between Cc and (LL, PL and PI) was arrived based on the plot, represented in following equation 4.2, 4.3 and 4.4.

Cc = 0.0021 (LL) + 0.1219 -- (4.2)

Cc = 0.0035 (PL) + 0.1547-- (4.3)

Cc = 0.0031 (PI) + 0.1536 -- (4.4)

4.4.2 Comparison of Predicted Cc by Microsoft excel, SPSS-20 and Matlab-ANN

The value of Cc can determine from oedometer using the slope of the linear portion of the e-log p curve as discussed in Chapter two *sections 2.4.7*.

In this study the value of Cc found from Oedometer tests and the predicted Cc are almost similar as it is shown in Tab.4.9 below.

The values of compression index predicted using the ANN model and another numerical model were shown in Table 4.9 and Figure 4.10. The accuracy of proposed model was also checked by calculating the correlation coefficient (R-value, MSE) and it was found that for ANN model was 0.9486 whereas for models proposed using multilinear perception and regression analysis were 0.8734 and 0.8468 respectively. It was found that compression index values predicted using the Ann model has better distribution around the equality line in comparison of another model. It can be calculated that proposed models are much accurate and are good agreement with laboratory value.

Table 4.9: Comparison of value of Cc found from oedometer test and predicted Cc by LR (Microsoft excel), NN- MLP (SPSS-20) and Matlab-Ann analysis

Test pit code	**Observed C_c**	**RA**	**MLP**	**ANN**	**Test pits code**	**Observed Cc**	**RA**	**MLP**	**ANN**
Tp-1-1	0.287	0.290	0.3	0.297	Tp-8-2	0.294	0.279	0.287	0.295
Tp-1-2	0.274	0.281	0.288	0.282	Tp-9-2	0.260	0.258	0.257	0.256
Tp-2-1	0.232	0.245	0.244	0.240	Tp-9-2	0.290	0.294	0.304	0.288
Tp-2-2	0.227	0.247	0.248	0.238	Tp-10-1	0.264	0.261	0.262	0.260
Tp-3-1	0.248	0.247	0.246	0.246	Tp-10-2	0.324	0.287	0.298	0.318

Tp-3-2	0.244	0.246	0.245	0.242	Tp-11-1	0.267	0.267	0.269	0.263
Tp-4-1	0.286	0.284	0.286	0.287	TP-11-2	0.272	0.269	0.273	0.270
Tp-4-2	0.310	0.299	0.306	0.305	TP-12-1	0.321	0.328	0.321	0.319
Tp-5-1	0.264	0.260	0.259	0.259	TP-12-2	0.330	0.342	0.323	0.329
Tp-5-2	0.243	0.271	0.274	0.264	Tp-13-1	0.330	0.335	0.322	0.328
Tp-6-1	0.252	0.251	0.249	0.253	Tp-13-2	0.310	0.314	0.316	0.317
Tp-6-2	0.241	0.242	0.243	0.236	TP-14-1	0.293	0.281	0.288	0.288
Tp-7-1	0.256	0.258	0.262	0.256	TP-14-2	0.287	0.286	0.294	0.286
Tp-7-2	0.305	0.308	0.314	0.304	Tp-15-1	0.270	0.261	0.263	0.262
Tp-8-1	0.296	0.280	0.287	0.282	Tp-15-2	0.251	0.256	0.256	0.254

In general, the proposed model through numerical modeling (i.e., ANN, MLP, LR and MLR) were determined based on the highest value of determination coefficient (R^2), mean squared error (MSE), square standard error (SSE), standard error (SE). The correlation coefficient with least standard error is considered, and the following relationships are found in Table 4.10.

Table 4.10: Summary of R^2-Value for Regression analysis, MLP and Ann Model

Model equation	$\mathbf{R^2}$	**SE**	**N**	**model used**
$C_c = 0.0021\ LL + 0.1219$	0.845	0.018	30	
$C_c = 0.0035\ PL + 0.1547$	0.589	0.0194	30	LR
$C_c = 0.0031\ PI + 0.1536$	0.741	0.0154	30	
$Cc = 0.0018(LL) + 0.0004(PI) + 0.1231$	0.847	0.012	30	MLR
$C_c = 0.002\ (LL) + 0.1238$	0.912	SSE = 0.0012, MSE = 0.0065	30	
$C_c = 0.0034\ (PL) + 0.1551$	0.621		30	ANN
$C_c = 0.003\ (PI) + 0.1576$	0.812		30	

As the Figure 4.10 indicated that, ANN model shows more goodness of fit and it has higher reliability based on the least MSE, which is 0.0065, square standard error 0.0012, R^2-value 0.948 and adjusted R^2-value 0.946, than the multilinear perception that is R^2-value 0.873 and the regression analysis R^2-value 0.847 from these three numerical models.

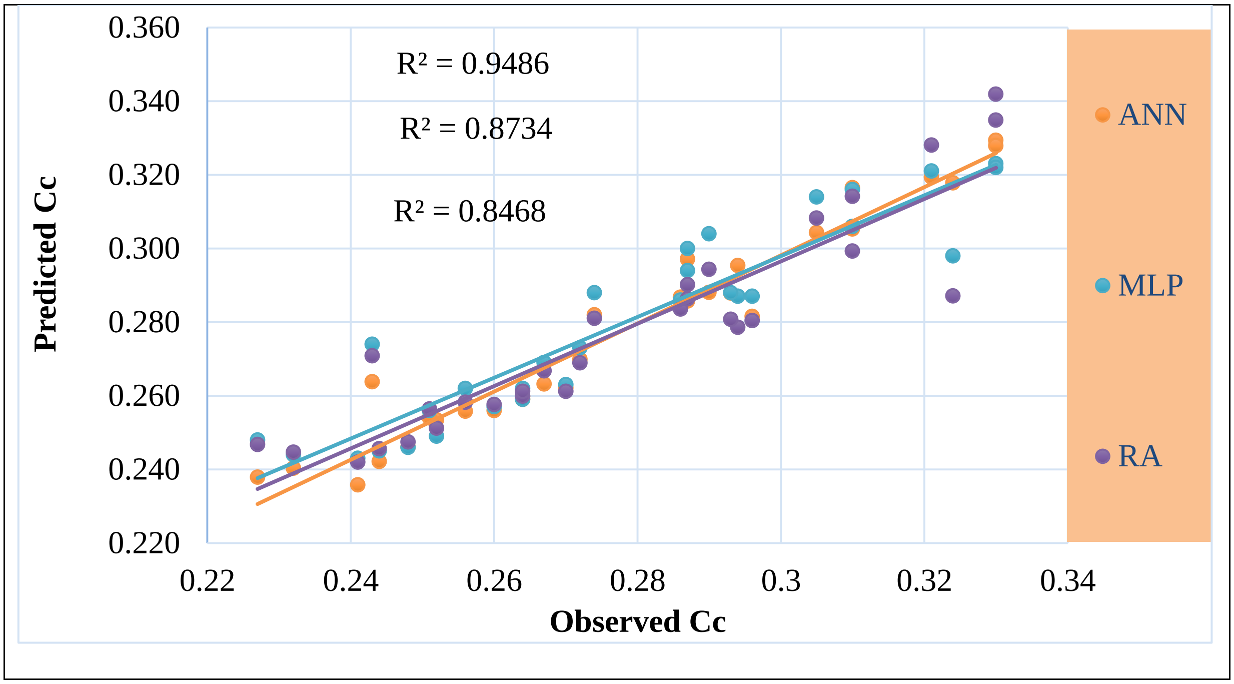

Figure 4.10: Comparison of different mathematical models in one plot

4.4.3 Comparison of the Jimma soils of current study with the previous research work

The research objective was to develop a model that will allow the prediction of compression index from index test results. The predicted values of Cc depend on the test results. One dimensional consolidation was done on thirty test samples at loading intensities of 50 kPa to 800 kPa. The compression index (Cc) is one of the very important compressibility parameters in settlement estimation for the engineering design purpose. The correlation between Cc and other soil properties were developed empirical equation by various investigators. However, most of the researchers recommended Cc = 0.006 (LL-10); but the best correlation of compression index with Atterberg limits suggested by Terzaghi. The Cc values of medium to soft clay soil ranged between 0.15 and 1.0 [2]. The results of the compression index (Cc) for this study ranged between 0.227 and 0.33. C_c values is found to be relatively almost similar those obtained for undisturbed soil samples by Jebril [26] which ranged between 0.238 to 0.399 of Cc values, but the value of Cc is less that obtained by Alemineh [44] and the soils are soft clay that is highly compressible that 0.585 and 0.711 value of Cc when comparison with current study. Therefore, the soil of study area was high to very high compressibility according to Bell [25].

Comparison of Correlation of Compression index

The accuracy of present ANN model was checked by comparing the laboratory values of C_c with predicted values of C_c. It was found that for mean target value for input data was 0.2776 while the mean target value 0.2774. Slamet Widodo and Nesamatha were proposed the mean target value of 1.098 and 0.5409 from predicted compression index.

The proposed model performance was checked by determining the coefficient of correlation (R-value, MSE) and it was found that for present ANN model was 0.948 whereas for proposed models by Slamet Widodo and Nesamatha were 0.854 and 0.963 respectively. The values of compression index predicted using the present ANN model and other proposed models were shown in Figure 4.11. It was found that compression index values predicted using the Nesamatha model has better distribution around the equality line in comparison of present study model.

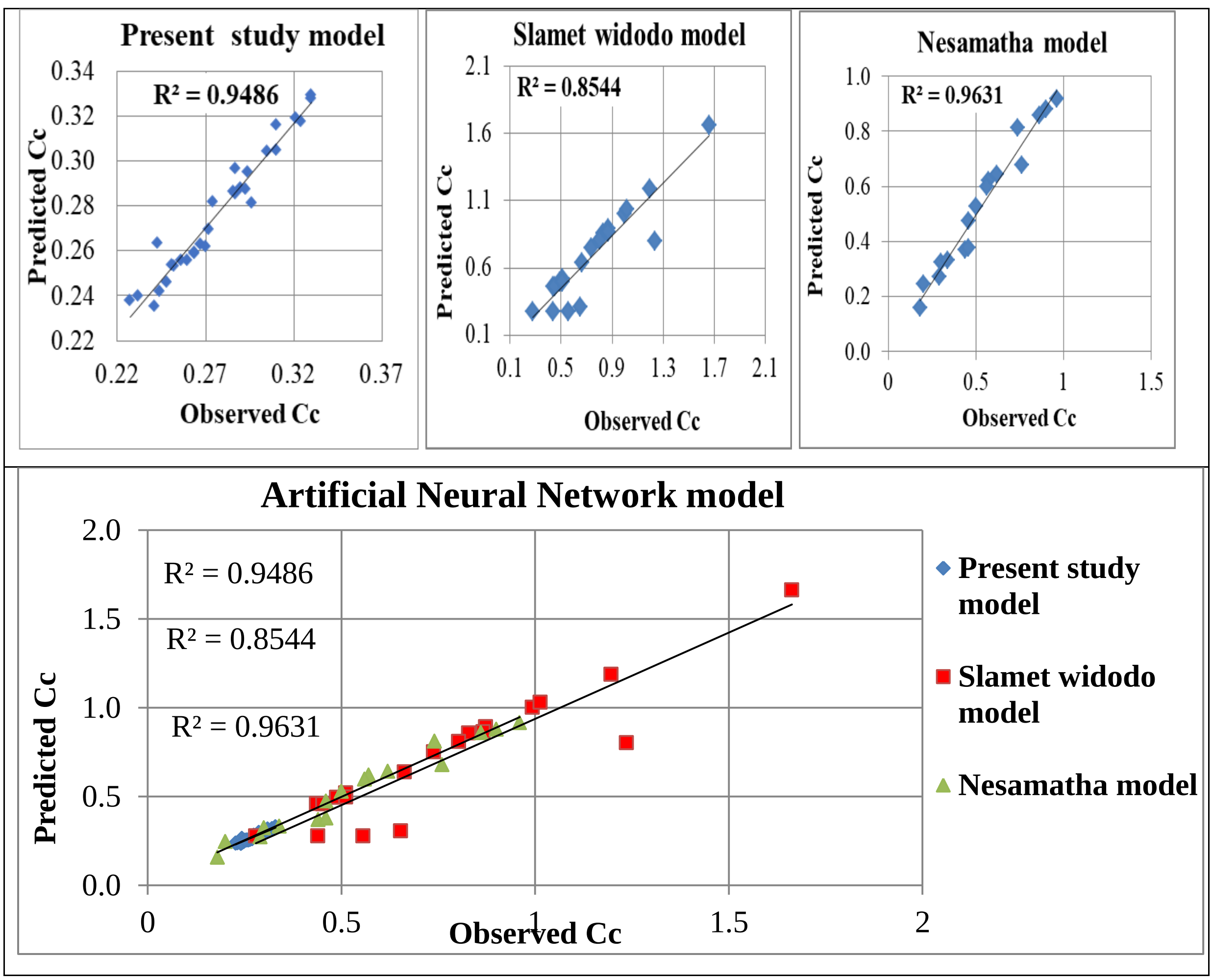

Figure 4.11: Comparison of different empirical equations using ANN model

CHAPTER FIVE

5 CONCLUSION AND RECOMMENDATION

5.1 Conclusions

The main objective of this thesis was to obtain valid relationships between index properties and compression index of Jimma clay soil. However, from regression analysis Cc has a strong correlation with Atterberg limits by achieving coefficient of determination of 84%, 58% and 74% respectively while parameters like void ratio, dry unity weight and natural moisture content have little influence on the compression index in this study. That means, the variables NMC, e and γ_d cannot predict about 50% of the compression index in the regression analysis, therefore cannot be used to accurately predict the compression index in the study area

From ANN model for LL, PL and PI the R^2 (correlation coefficient) is 91%, 62% and 81% respectively which is the Cc has extremely strong correlation with Atterberg limits. In this study, the ANN model is the best fit to achieving the great R-value than the regression analysis model. Therefore, compression index can be computed from known value of LL, PL and PI by the correlation equations.

The statistical analysis and Ann analysis shows that there is a relatively good correlation between the independent variables (LL, PL and PI) and the dependent variable (Cc). However, poor correlation is observed between Cc and PL as compared with the other variables. The developed correlations generally show that liquid limit, plastic limit, and plasticity index of soil affect the compression of soil behavior. This study however, indicates the existence of a relatively good correlation between index properties (LL, PL and PI) and compression index (Cc). The proposed model that obtained from the correlation between C_c and LL, PI is given as Cc = 0.0018(LL) + 0.0004(PI) +0.1231, R^2 = 0.847 with 0.012 of standard error through multilinear regression analysis.

In the MATLAB software, 70 percent of both normalized output and input data were entered into network as training and the remaining 30 percent entered as test (the training is an observer one). If the value of predicated output is close to the actual one entered in to output part, indicating the ideal predication of the network and ensure that the MSE is low and R value is high. Therefore, in this study the predicted output of the network is close to the target.

From the statistical analysis and ANN analysis, one observes a relatively good indicative correlation between Cc and liquid limit (LL), Cc and plastic limit (PL) and Cc and plasticity index (PI) while parameters like e, γ_d and w_n have little influence on the compression index in this study. From the developed correlations one would be in a position to determine the compression index from the index properties for undisturbed soil samples of Jimma town.

In this study, ANN’s (curve fitting) practice has been made to predict the compression index based on the geotechnical characteristics of different test pits data collected from Jimma town. ANN is a powerful tool in predicting the consolidation parameters and the best fit model than conventional methods are obtained. In the proposed ANN model, the soil properties such as the liquid limit, plastic limit and the plasticity index are input parameters.

The proposed model of the ANN results compared with the experimental values and the predicted compression index values have found close to the experimental values. In this research, the observed compression index is performed by ANN proposed model to obtained the predicted Cc. Hence, Cc = 0.002 (LL) + 0.1238, R^2 = 0.912 and Cc = 0.003 (PI) + 0.1576, R^2 = 0.812. By engineer judgement one of the formulae proposed in this study may be used for computing Cc due to absence of consolidation test data.

5.2 Recommendation

In this research it is observed that, there is a relationship between compressibility parameters and index properties for undisturbed soil samples of Jimma. To get reliable correlation it is essential to enhance the number of test samples and the coverage of sites in Jimma where different clay soil is found.

The fact encountered in trying to perform the current research has divulgence areas where further efforts may be come out in the future. The recommendations in relation to the subject study were discussed as following:

1. It is recommended to perform this prediction with the large number of samples of oedometer test and compressibility parameters such as recompression index (Cr) which are not covered by this research.
2. It also recommended conducting such a study in other parts of the Ethiopia.

REFERENCE

[1] Akayuli C. and B. Ofosu, "Empirical Model for Estimating Compression Index for Physical properties of weathered Birimian Phyllites," Electronic Journal of Geotechnical Engineering, vol. 18, pp. 6135-6144, 2013.

[2] Jain V. and D. Mahabir, "Correlation of Plasticity Index and Compression Index of Soil," International Journal of Innovations in Engineering and Technology, vol. 5, no. 3, pp. 263-270, 2015.

[3] Norlia M. I. "Determination of Plasticity Index and Compression Index of Soil at Perlis," 2012.

[4] Zumrawi M., "Prediction of Swelling Characteristics of Expansive Soils," Sudan Engineering Society Journal, vol. 2, p. 58, 2014.

[5] Patil A. and R. Panse, "Establishing relationship between Swelling Pressure and Free Swell Index of Soils," 2016.

[6] Yoon G.L. and Kim B., "Empirical correlations of compression index for marine clay from regression analysis," Canadian Geotechnical Journal, vol. 41, pp. 1213-1221, 2004.

[7] Abbasi N., "Prediction of compression behaviour of normally consolidated fine-grained soils," World Applied Sciences Journal, vol. 18, no. 1, pp. 06-14, 2012.

[8] Jumikis A., Soil Mechanics, Florida: Robert E. Krieger Publishing Company, 1984.

[9] George M., Applied Statistics and Probability for Engineers, third edition ed., John Wiley & Sons, Inc. USA, 2003.

[10] Sridharan A. and H. Nagaraj, "Compressibility behavior of remolded, fine grained soils and correlation with index properties," Canadian Geotechnical journal Proquest Science journals, vol. 37, no. 3, pp. 712-722, 2000.

[11] Bae W. and T. Heo, "Prediction of compression index using regression analysis of transformed variables method," Mar Georesources Geotechnology, vol. 29, no. 1, pp. 76-94 [Google Scholar], 2011.

[12] Lav M. and Ansel, "Regression analysis of soil compressibility," Turkish Journal of Engineering and Environmental, vol. 25, pp. 101-109, 2001.

[13] Amith N. and S. Dedalal, "The Role of plasticity index in Predicting Compression behaviour of clay," Electronic Journal of Geotechnical Engineering, vol. 9, 2004.

[14] Nesamatha R. and Arumairaj, "Numerical Modeling for Prediction of Compression Index from Soil Index properties," 2015.

[15] Lee C., S. Hong, Kim D. and Lee W., "Assessment of compression index of Busan and Incheon clays with sedimentation state," Marine Georesources & Geotechnology, vol. 33, no. 1, p. 2332, 2015.

[16] Widodo S. and A. Ibrahim, "Estimation of Primary Compression index (Cc) using physical properties of Soft Soil," 2012.

[17] Jacob C., Patricia C., G. Stephen and West Leona, Applied Multiple Regression or correlation Analysis for the behavioral Sciences, 2013, pp. 17-736.

[18] Amardeep and S. Noor, "Soil Compression Index Prediction Model for Fine Grained Soils," International Journal of Innovations in Engineering and Technology, vol. 1, no. 4, pp. 34-37, 2012.

[19] Demir A., "New computational network models for better predictions of the soil compression index," Acta Geotech Slov, vol. 12, no. 1, p. 59–69, 2015.

[20] Isik N. S., "Estimation of swell index of fine-grained soils using regression equations and artificial neural networks," Scientific Research and Essay, vol. 4, no. 10, pp. 1047-1 056, 2009.

[21] Park H. and S. Lee, "Evaluation of the compression index of soils using an artificial neural network," Computers and Geotechnics, vol. 38, pp. 472-481, 2011.

[22] Kalantary F. and A. Kordnaeij, "Prediction of Compression Index Using Artificial Neural Network," Scientific Research and Essays, vol. 7, no. 31, pp. 2835-2848, 2012.

[23] Namdarvand F. and G. Sayyad, "Estimation of soil compression coefficient using artificial neural network and multiple regressions." International Research Journal Applied Basic Science, vol. 4, no. 10, p. 3232–3236 [Google Scholar], 2013.

[24] Barnes G.E., Compressibility and Consolidation in Soil Mechanics, Palgrave, London. https://doi.org/10.1007/978-1-349-13258-4_6, 1995.

[25] Bell F., Engineering Geology, Second edition, 2007.

[26] Jibril J. "In-depth Investigation into Engineering Characteristics of Jimma Soils," Addis Ababa, 2014.

[27] Barja Das. Principles of Geotechnical Engineering, 5th ed., Sacramento: California state university, 2006.

[28] Budhu M., Soil Mechanics and Foundations, New York NY: John Wiley & Sons, Inc, 2000.

[29] Terzaghi K. P. and G. Mesri, Soil Mechanics in Engineering Practice, Wiley & Sons Inc. International Edition, 1996.

[30] Arora K.R., "Soil Mechanics and Foundation Engineering," New Delhi, India, Standard Publishers Distributors, 2004.

[31] Murthy V., Soil Mechanics and Foundation Engineering, UBS Publishers Distributors Ltd, 2001.

[32] Bowles J., Foundation Analysis and Design, Fifth Edition, McGraw- Hill Companies Inc, 1996.

[33] Onyejekwe S. and X. Kang, Assessment of empirical equations for the compression index of fine-grained soils in Missouri, Official journal of the IAEG. doi: 10.1007/s10064-014-0659, 2014.

[34] Das B.M, Advanced Soil mechanics, Second edition. ed., Francis, Taylor, 1997.

[35] Casagrande A. and Fadum, "Closure to Applications of Soil Mechanics in Designing Building Foundation Transactions," vol. 109, ASCE, 1944, p. 467.

[36] Taylor D. W., Fundamentals of Soil Mechanics, Wiley, Ed., New York, 1948.

[37] Jain V. Kumar and M. Dixit, "Prediction of compression Index (Cc) of fine-grained remoulded soils from basic soil Properties," International Journal of Applied Engineering Research, vol. 11, no. 1, pp. 592-598, 2016.

[38] Taga H. and A. Alptekin, "Prediction of Compression and Swelling Index Parameters of Quaternary Sediments from Index Tests at Mersin District," Open Geosciences, vol. 11, pp. 482-491, 2019.

[39] Chen F., Foundation on Expansive Soils Developments in Geotechnical Engineering, vol. 12, Elsevier Publications, 1988.

[40] Nelson J. and D. Miller, "Expansive Soils: Problems and Practice in Foundation and Pavement Engineering," John Wiley and Sons, Inc., New York, 1992.

[41] ASTM, "ASTM D2435/D2435-11, Standard test methods for onedimensional consolidation properties of soils using incremental loading," ASTM International West Conshohocken, PA, 2011.

[42] ASTM, "American Society for Testing and Materials," vol. vol.04.08, Philadelphia, PA, 1995.

[43] AASHTO, "American Association for State Highway and Transportation Officials," in Standard Specifications for Transportation Materials and Methods of Sampling and Testing, Twenty-Six ed., 2006.

[44] Sorsa A., Senadheera S. and B. Yoseph, "Engineering Characterization of Subgrade Soils of Jimma Town, Ethiopia, for Roadway Design," vol. 10, p. 94, 2020.

[45] Jemal Z., "Correlation between Undrained Shear Strength with Index Properties of Jimma Clay Soils," Ababa University, Addis Ababa, 2012.

[46] Sefu H., "Correlation of Dynamic cone penetration with undrained shear strength of clay," Jimma, 2018.

[47] Pal S. K. and A. Ghosh, "Volume Change Behavior of Fly Ash–Montmorillonite Clay Mixtures," International Journal of Geomechanics, vol. 14, pp. 59-68, 2014.

[48] Arpan L. and P. Sujit Kumar, "Geotechnical Characteristics of Two Different Soils and their Mixture and Relationships between Parameters," Electronic Journal of Geotechnical Engineering, vol. 17, 2012.

APPENDIX-1

I. Artificial Neural Network Trained Results

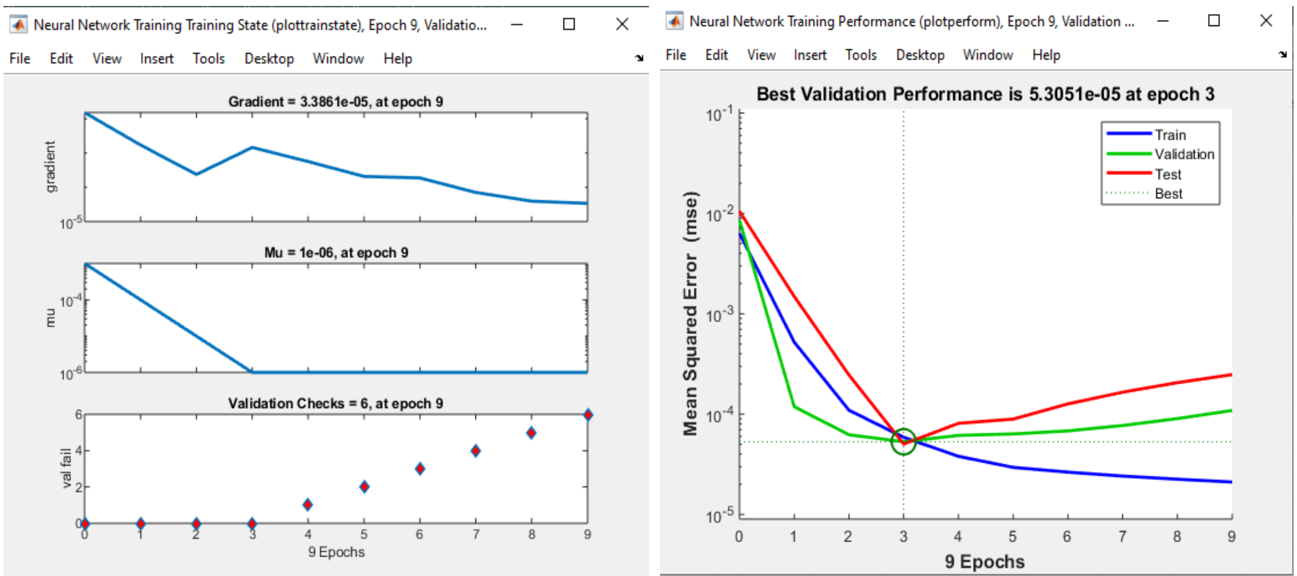

Figure of training state and performance for validation through neural network

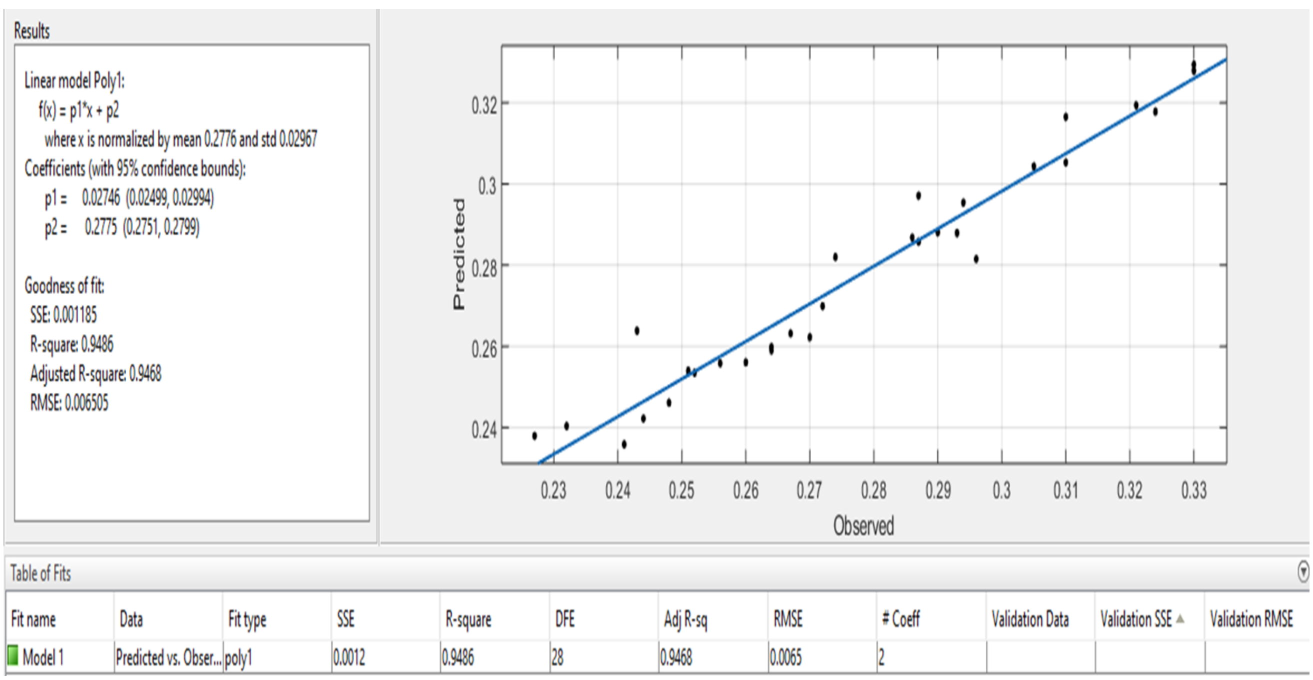

Figure of the predicted compression index versus the observed compression index by ANN trained model

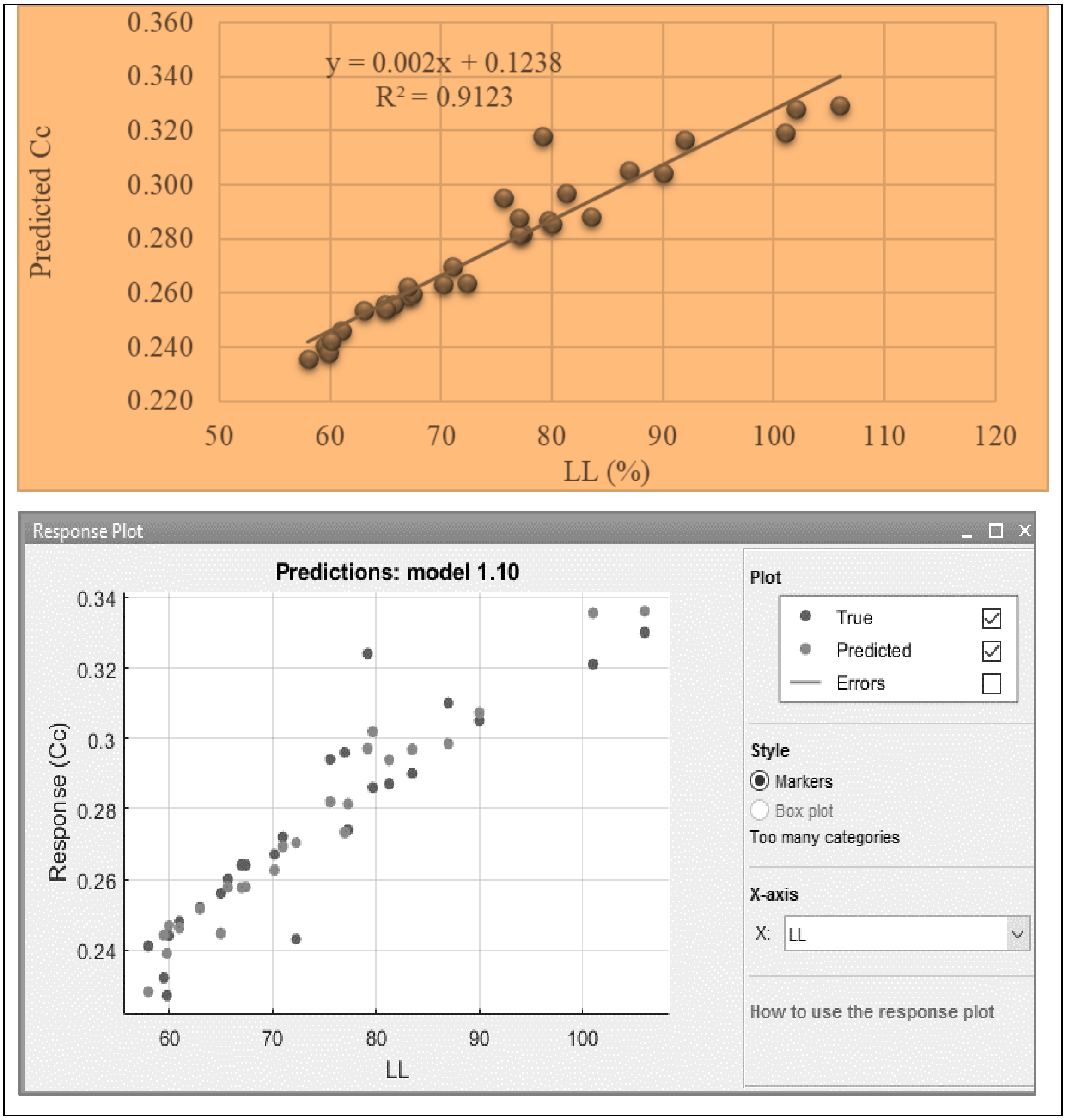

Figure 1: predicted and observed compression index from ANN model using liquid limit (LL)

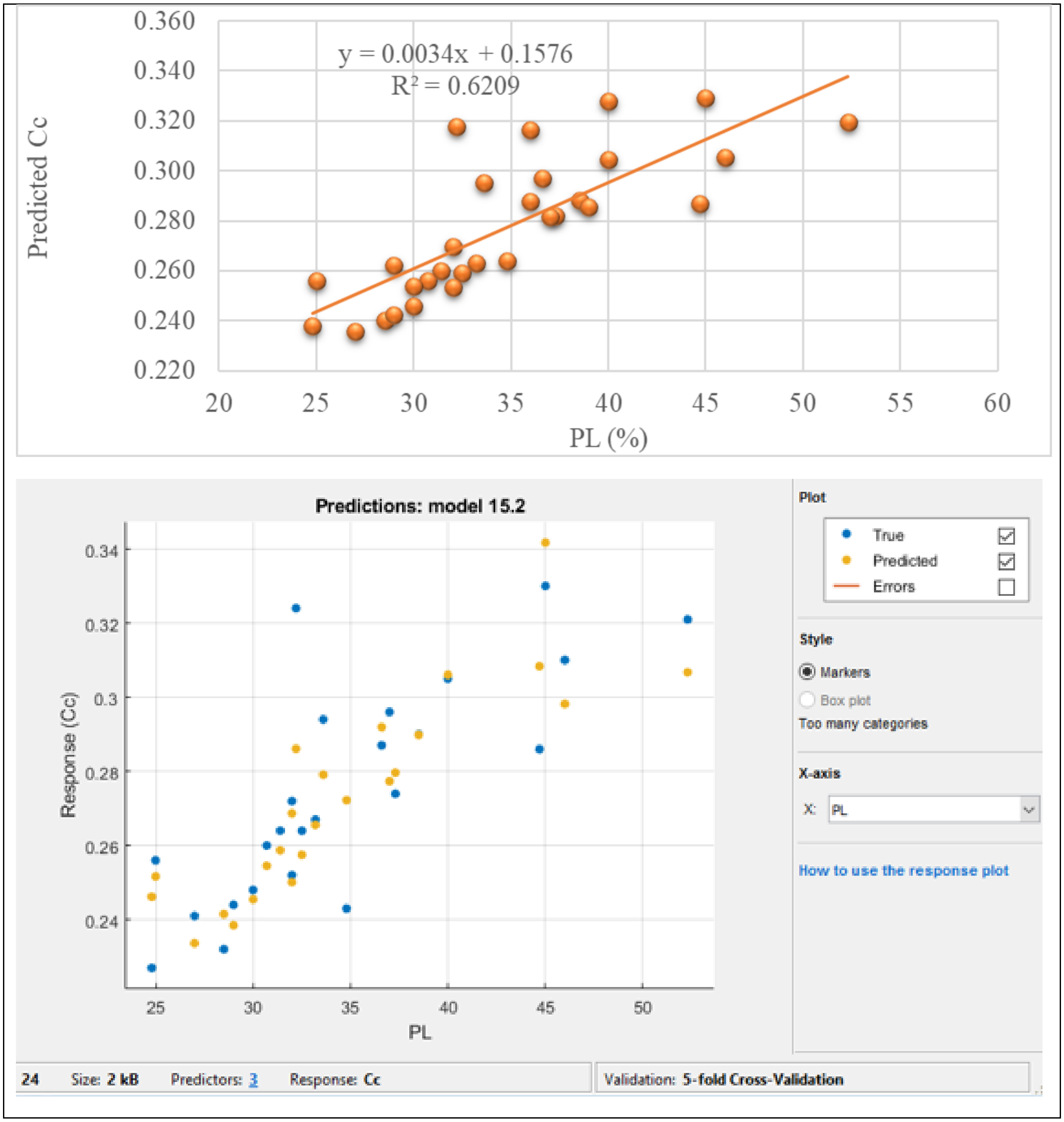

Figure 2: Predicted and observed compression index from ANN model using plastic limit (PL)

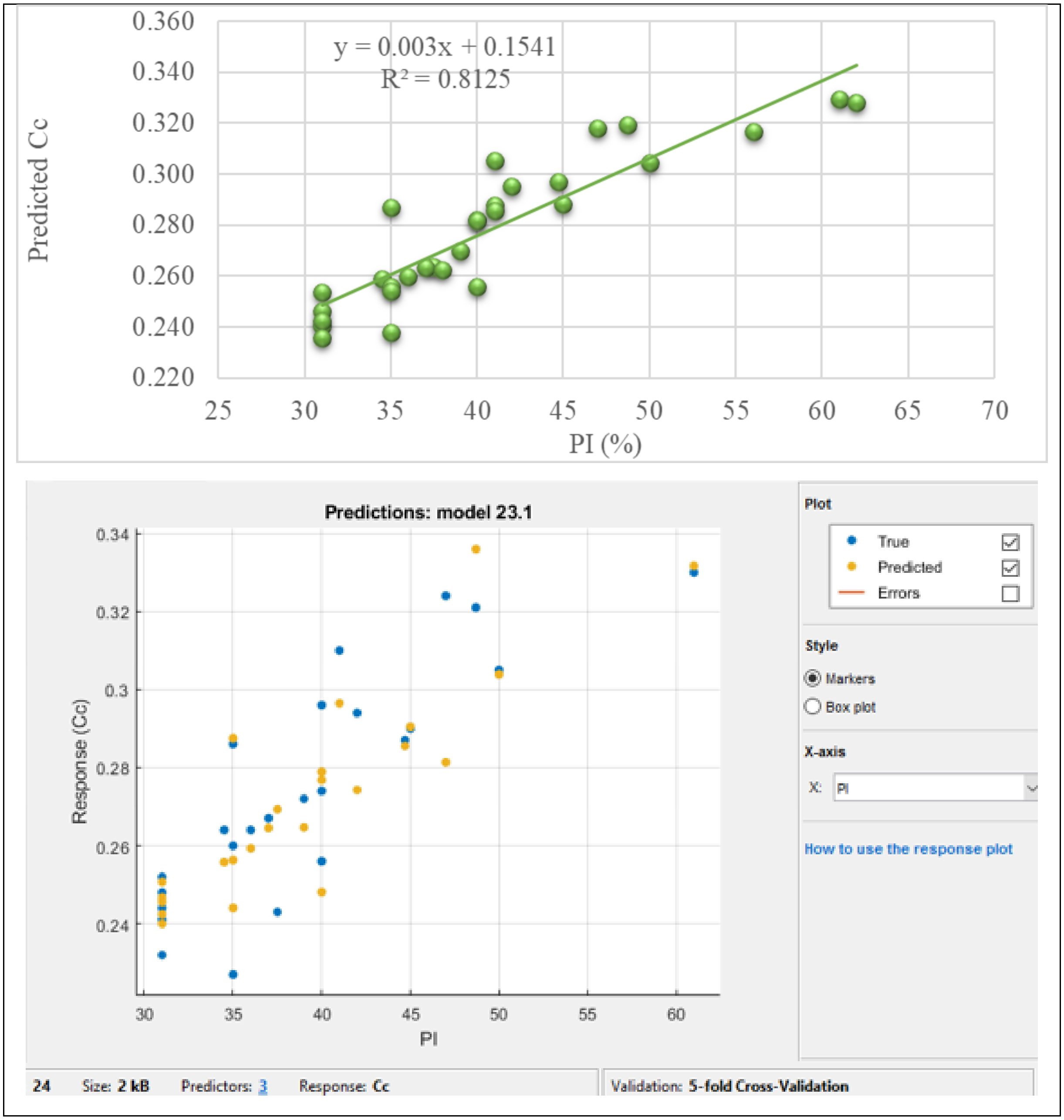

Figure 3: Predicted and observed compression index from ANN model using plasticity index (PI)

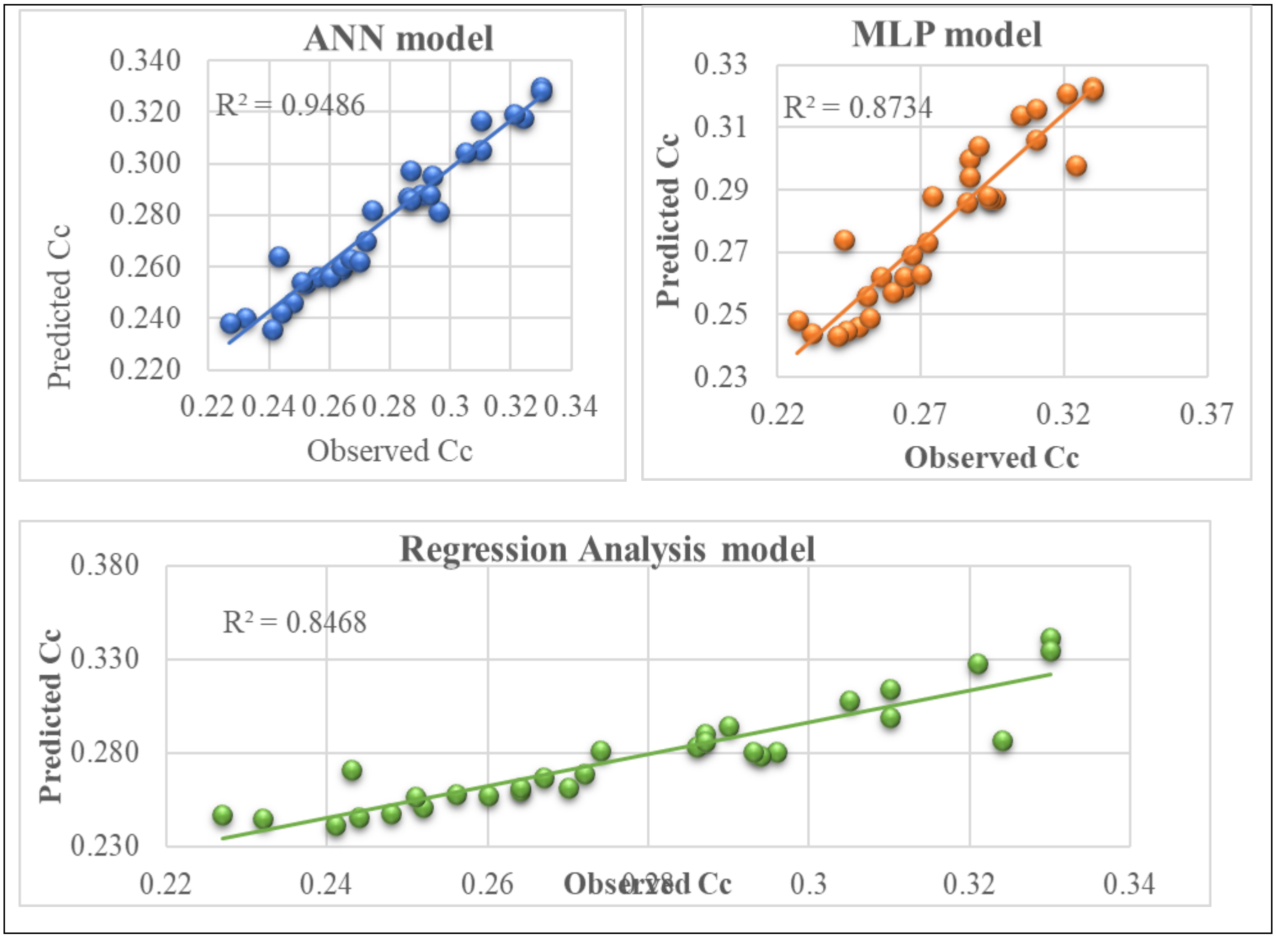

Figure 4: The plot of different mathematical model for relationship between predicted and observed target values of the study.

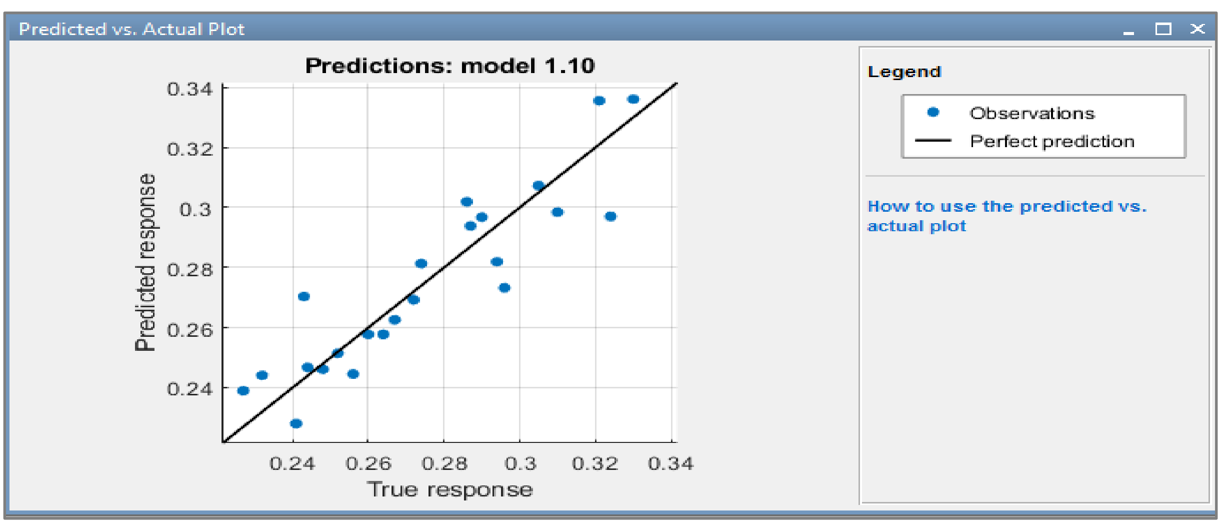

Figure 5: The predicted compression index versus the observed compression index by ANN trained mode

A. One Dimensional consolidation test results

Table A-1 Plot of void ratio –log pressure curve for all samples and calculation of consolidation test

Determination of dry unit weight,void ratio and Height of solids after test for TP-1 to TP-5										
Test Designation	TP-1-1	TP-1-2	TP-2-1	TP-2-2	TP-3-1	TP-3-2	TP-4-1	TP-4-2	TP-5-1	TP-5-2
Specimen wet mass + ring	132.4	127.4	133.6	132.4	139.9	136.2	134	133.6	132.6	131.39
Specimen dry mass + ring	116.2	113.2	112.3	112.2	116.3	116.8	114.6	113.8	111.6	112
Mass of ring (g)	67.8	67.8	67.8	67.8	67.8	67.8	67.8	67.8	67.8	67.8
Specimen Height, L (cm)	2	2	2	2	2	2	2	2	2	2
Specimen diameter, D (cm)	5	5	5	5	5	5	5	5	5	5
Area of ring cm^2	19.625	19.625	19.625	19.625	19.625	19.625	19.625	19.625	19.625	19.625
Volume of ring cm^3	39.25	39.25	39.25	39.25	39.25	39.25	39.25	39.25	39.25	39.25
Bulk density, (g/cm^2)	1.65	1.52	1.68	1.65	1.84	1.74	1.69	1.68	1.65	1.62
Water Content,w (%)	33.5	31.3	47.9	45.5	48.7	39.6	41.5	43.0	47.9	43.9
Dry density, (g/cm2)	1.23	1.16	1.13	1.13	1.24	1.25	1.19	1.17	1.12	1.13
Height of solid, (cm)	0.91	0.86	0.87	0.87	0.90	0.91	0.87	0.86	0.83	0.85
Initial void ratio, e	1.21	1.33	1.31	1.30	1.23	1.19	1.29	1.31	1.41	1.36
Gs	2.72	2.7	2.62	2.6	2.76	2.73	2.73	2.71	2.69	2.66

Determination of dry unit weight,void ratio and Height of solids after test for TP-6 to TP-12												
Test Designation	TP-6-1	TP-6-2	TP-7-1	TP-7-2	TP-9-1	TP-9-2	TP-10-1	TP-10-2	TP-11-1	TP-11-2	TP-12-1	TP-12-2
Specimen wet mass + ring (g)	135	136.8	123.5	127.4	134.5	133.6	133.8	130.8	130.2	131.3	133.2	128.6
Specimen dry mass + ring (g)	113.4	113.3	102	107.2	112.8	113.7	113.1	111.102	115.3	116.2	114.2	112.6
Mass of ring (g)	67.8	67.8	67.8	67.8	67.8	67.8	67.8	67.8	67.8	67.8	67.8	67.8
Specimen Height, L (cm)	2	2	2	2	2	2	2	2	2	2	2	2
Specimen diameter, D (cm)	5	5	5	5	5	5	5	5	5	5	5	5
Area of ring cm^2	19.625	19.625	19.625	19.625	19.625	19.625	19.625	19.625	19.625	19.625	19.625	19.625
Volume of ring cm^3	39.25	39.25	39.25	39.25	39.25	39.25	39.25	39.25	39.25	39.25	39.25	39.25
Bulk density, (g/cm^2)	1.71	1.76	1.41	1.52	1.70	1.68	1.68	1.61	1.59	1.62	1.67	1.55
Water Content,w (%)	47.4	51.6	41.2	51.3	48.2	43.4	45.7	45.5	31.4	31.2	40.9	35.7
Dry density, (g/cm2)	1.16	1.16	1.00	1.00	1.15	1.17	1.15	1.10	1.21	1.23	1.18	1.14
Height of solid, (cm)	0.86	0.87	0.76	0.75	0.85	0.88	0.87	0.85	0.93	0.93	0.88	0.85
Initial void ratio, e	1.32	1.31	1.65	1.67	1.35	1.27	1.30	1.37	1.16	1.15	1.27	1.37
Gs	2.7	2.68	2.7	2.68	2.69	2.66	2.65	2.61	2.61	2.65	2.68	2.7

Table A-2: Results of Consolidation Test for all soil samples

		Oedometer test results						Classification schemes		
TP code	Depth(m)	w_n	e_o	γ_d	γ_b	C_c	C_s	USCS	AASHTO	Remark
TP-1	1.5	33.5	1.21	1.23	1.65	0.287	0.02	CH	A-7-5	Clay soils
	2.5	31.3	1.33	1.16	1.52	0.274	0.06	CH	A-7-5	Clay soils
TP-2	2.5	47.9	1.31	1.13	1.68	0.232	0.05	CH	A-7-6	Clay soils
	3	45.5	1.3	1.13	1.65	0.227	0.07	CH	A-7-6	Clay soils
TP-3	1.5	48.7	1.23	1.24	1.84	0.248	0.03	CH	A-7-5	Clay soils
	2.5	39..6	1.19	1.25	1.74	0.244	0.03	CH	A-7-6	Clay soils
TP-4	1.5	41.5	1.29	1.19	1.69	0.286	0.03	MH	A-7-5	Clay soils
	2.5	43.1	1.31	1.17	1.68	0.31	0.03	MH	A-7-5	Clay soils
TP-5	1.5	47.9	1.41	1.12	1.65	0.264	0.06	CH	A-7-5	Clay soils
	2.5	43.9	1.36	113	1.62	0.243	0.05	CH	A-7-5	Clay soils
TP-6	1.5	47.4	1.32	1.16	1.71	0.252	0.04	CH	A-7-5	Clay soils
	2.5	51.6	1.31	1.16	1.76	0.241	0.04	CH	A-7-6	Clay soils
TP-7	1.5	41.2	1.65	1	1.41	0.256	0.11	CH	A-7-6	Clay soils
	2.5	51.3	1.67	1	1.52	0.305	0.05	CH	A-7-5	Clay soils
TP-8	1.5	42.2	1.44	1.09	1.55	0.296	0.04	CH	A-7-5	Clay soils
	2.5	42.9	1.32	1.13	1.62	0.294	0.04	CH	A-7-5	Clay soils
TP-9	1.5	48.2	1.35	1.15	1.70	0.26	0.04	CH	A-7-5	Clay soils
	3	42.3	1.27	1.17	1.68	0.29	0.04	CH	A-7-5	Clay soils
TP-10	1.5	45.7	1.3	1.15	1.68	0.264	0.07	CH	A-7-5	Clay soils
	3	45.5	1.4	1.1	1.61	0.324	0.07	CH	A-7-5	Clay soils
TP-11	1.5	31.4	1.16	1.21	1.59	0.267	0.02	CH	A-7-5	Clay soils
	2.5	31.2	1.15	1.23	1.62	0.272	0.02	CH	A-7-5	Clay soils
TP-12	1.5	40.9	1.27	1.18	1.67	0.321	0.06	MH	A-7-5	Clay soils
	3	35.7	1.37	1.14	1.55	0.33	0.07	CH	A-7-5	Clay soils
TP-13	1.5	45.1	1.26	1.16	1.69	0.33	0.06	CH	A-7-5	Clay soils
	2.5	322	1.23	1.17	1.55	0.31	0.07	CH	A-7-5	Clay soils
TP-14	1.5	38	1.28	1.21	1.67	0.293	0.09	CH	A-7-5	Clay soils
	2.5	34.2	1.29	1.19	1.6	0.287	0.08	CH	A-7-5	Clay soils
TP-15	1.5	17.5	1.05	1.31	1.54	0.27	0.08	CH	A-7-6	Clay soils
	2.5	29.5	1.09	1.26	1.68	0.251	0.02	CH	A-7-5	Clay soils

Where: w_n is the natural moisture content after test, e_o is the initial void ratio that obtain after consolidation test, γ_d dry unit weight of soil, γ_b bulk unit weight of soil, C_c compression index and C_s is swelling (recompression) index

Table A-3: Results of Laboratory Test for all soil samples

		Laboratory Test Results						
TP code	Depth(m)	Gs	NMC (%)	LL (%)	PL (%)	PI (%)	FS (%)	*#200 (P %)*
TP-1	1.5	2.72	43.9	81.3	36.6	44.7	50	99.13
	2.5	2.7	47.41	77.3	37.3	40	50	99.15
TP-2	2.5	2.62	57	59.5	28.5	31	85	96.63
	3	2.6	44.45	59.8	24.8	35	70	97.73
TP-3	1.5	2.76	43.96	61	30	31	50	97.95
	2.5	2.73	47.5	60	29	31	45	93.68
TP-4	1.5	2.73	47.39	79.7	44.7	35	50	99.33
	2.5	2.71	47.5	87	46	41	50	99.09
TP-5	1.5	2.69	45.91	67	32.5	34.5	80	86.96
	2.5	2.66	66.62	72.3	34.8	37.5	70	89.51
TP-6	1.5	2.7	39.14	63	32	31	45	99.23
	2.5	2.68	45.7	58	27	31	40	98.95
TP-7	1.5	2.69	40.89	65	25	40	80	98.5
	2.5	2.65	57.07	90	40	50	70	98.64
TP-8	1.5	2.64	43	77	37	40	50	97.95
	2.5	2.61	46.88	75.6	33.6	42	50	98.62
TP-9	1.5	2.69	43.26	65.7	30.7	35	45	92.57
	3	2.65	44.78	83.5	38.5	45	40	92.24
TP-10	1.5	2.65	45.51	67.4	31.4	36	70	96.93
	3	2.61	47.5	79.2	32.2	47	80	94.02
TP-11	1.5	2.61	43.57	70.2	33.2	37	60	85.7
	2.5	2.65	39.98	71	32	39	50	92.3
TP-12	1.5	2.68	60.82	101	52.3	48.7	90	87.2
	3	2.7	68.78	106	45	61	100	90.7
TP-13	1.5	2.63	39.86	102	40	62	110	96.93
	2.5	2.61	46.81	92	36	56	95	94.02
TP-14	1.5	2.75	52.87	77	36	41	50	85.7
	2.5	2.73	56.47	80	39	41	40	92.3
TP-15	1.5	2.68	36.74	67	29	38	50	87.2
	2.5	2.71	54.21	65	30	35	50	90.7

Table A-4: Summary of applied pressure and void ratio for twelve soil samples of study area

Test Pits code	TP-1		TP-2		TP-3		TP-4		TP-5	
	TP-1-1	TP-1-2	TP-2-1	TP-2-2	TP-3-1	TP-3-2	TP-4-1	TP-4-2	TP-5-1	TP-5-2
Stress, kPa	Void ratio, e	Void ratio, e	Void ratio, e	Void ratio, e	Void ratio, e	Void ratio, e	Void ratio, e	Void ratio, e	Void ratio, e	Void ratio, e
Loading Stage										
50	1.189	1.304	1.179	1.270	1.156	1.118	1.250	1.281	1.366	1.326
100	1.162	1.243	1.152	1.247	1.090	1.058	1.201	1.232	1.322	1.281
200	1.062	1.195	1.121	1.224	1.049	1.023	1.130	1.167	1.239	1.214
400	0.948	1.098	1.035	1.134	0.945	0.918	1.043	1.081	1.155	1.148
800	0.902	0.995	0.942	1.042	0.866	0.838	0.943	0.951	1.084	1.062
Unloading Stage										
800	0.902	0.995	0.942	1.042	0.866	0.838	0.943	0.951	1.084	1.062
400	0.907	1.008	0.953	1.057	0.878	0.848	0.951	0.959	1.096	1.074
200	0.913	1.031	0.963	1.080	0.887	0.856	0.963	0.972	1.116	1.090
100	0.919	1.053	0.984	1.102	0.895	0.866	0.974	0.982	1.134	1.108
50	0.926	1.075	1.006	1.123	0.907	0.876	0.982	0.991	1.152	1.120

Figure A-1The void ratio versus stress curve for both loading and unloading for six tests (TP-1 to TP-6)

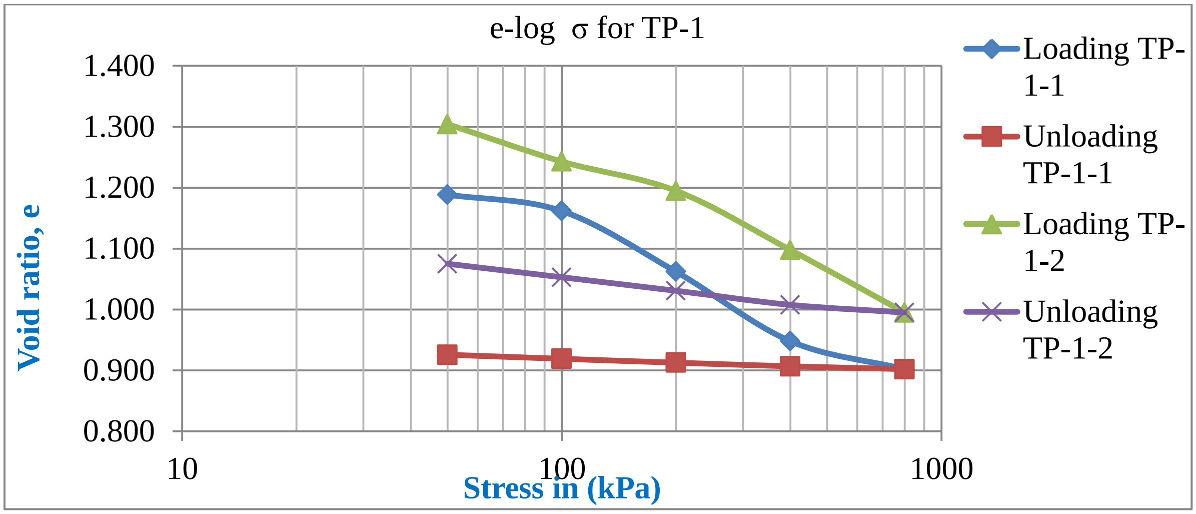

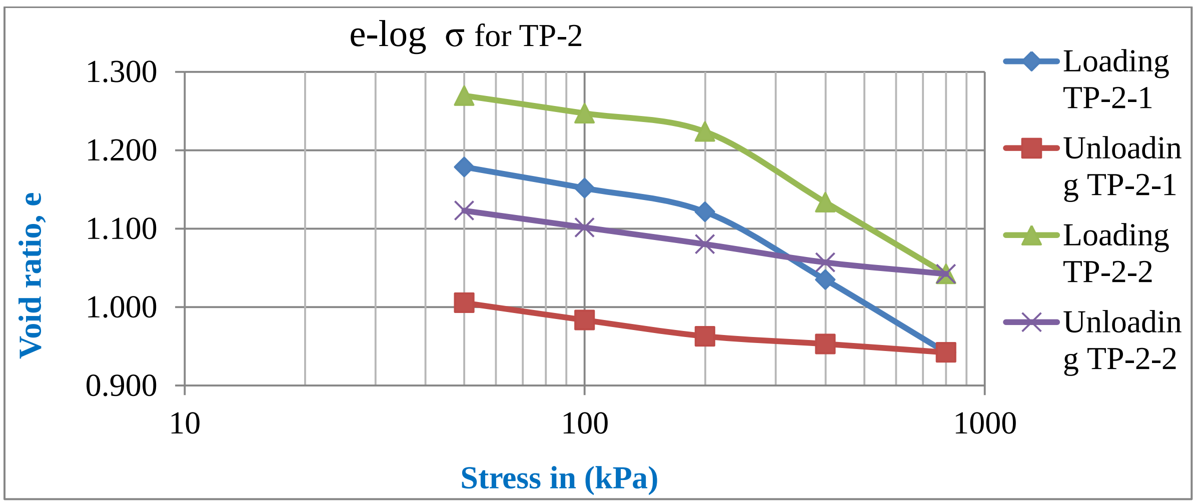

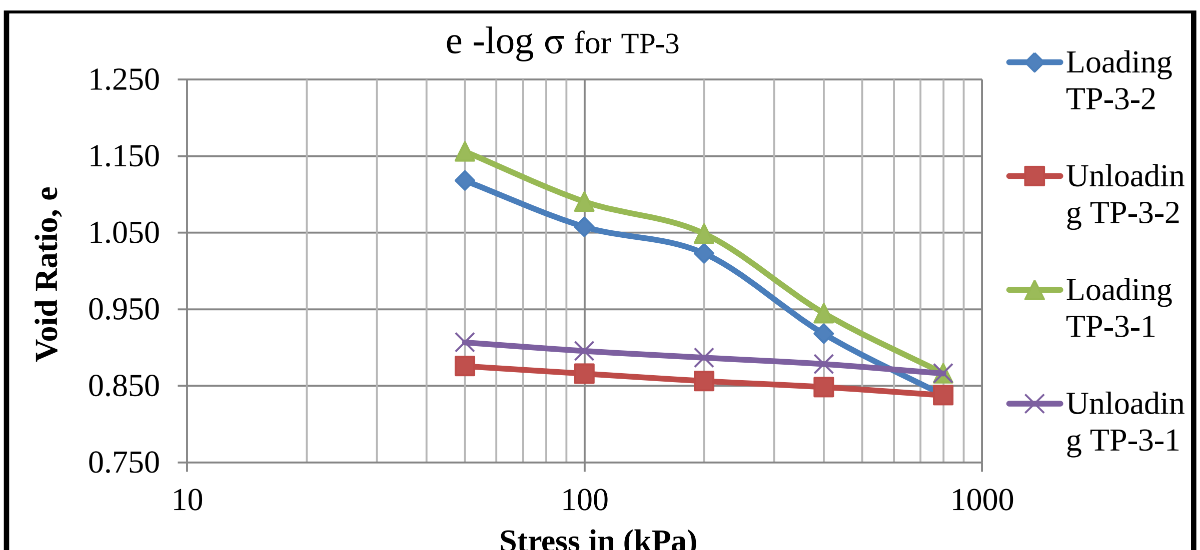

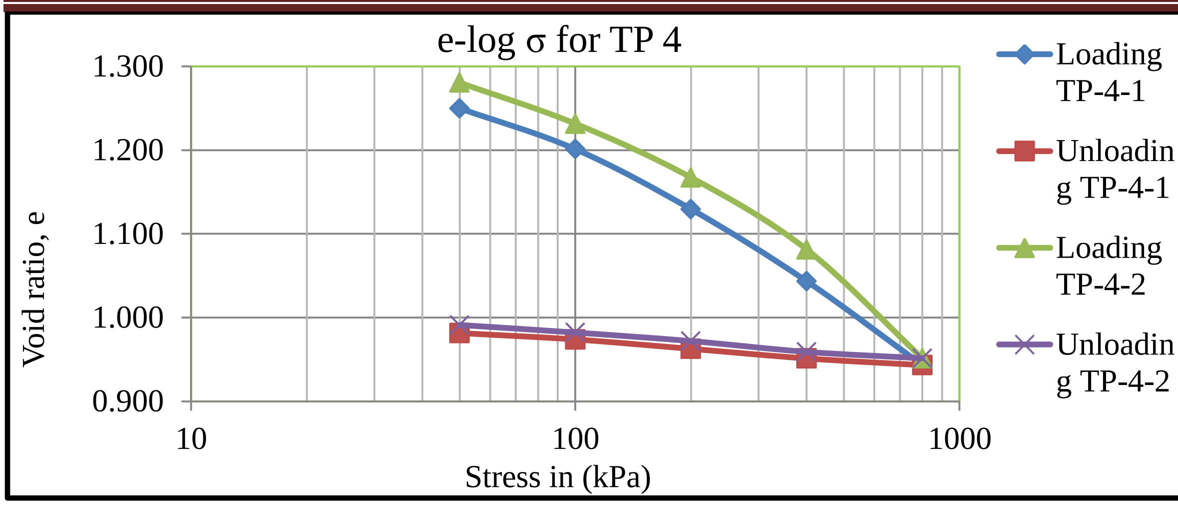
e-log σ for TP 4
Void ratio, e
1.300
1.200
1.100
1.000
0.900
10
100
1000
Stress in (kPa)
Loading TP-4-1
Unloading TP-4-1
Loading TP-4-2
Unloading TP-4-2

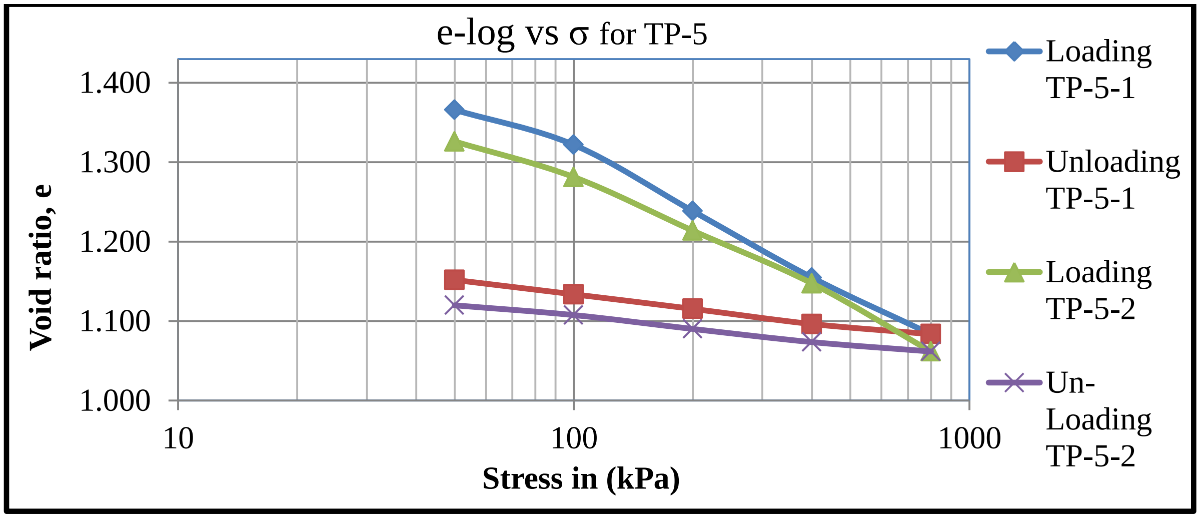
e-log vs σ for TP-5
Void ratio, e
1.400
1.300
1.200
1.100
1.000
10
100
1000
Stress in (kPa)
Loading TP-5-1
Unloading TP-5-1
Loading TP-5-2
Un-Loading TP-5-2

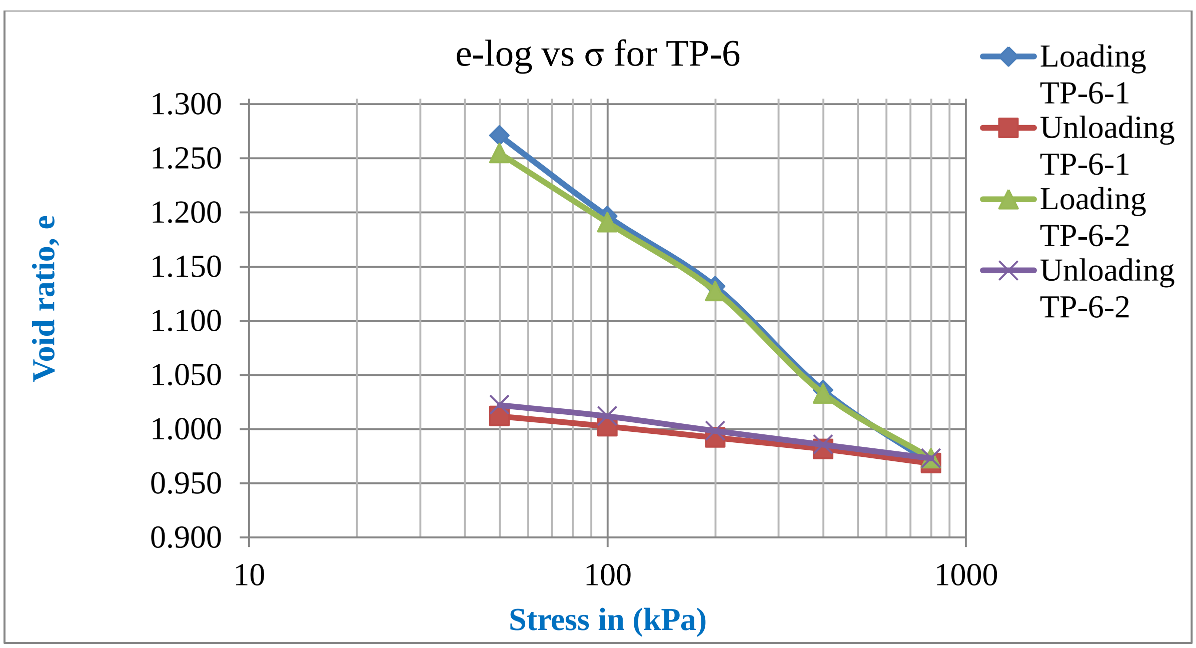
e-log vs σ for TP-6
Void ratio, e
1.300
1.250
1.200
1.150
1.100
1.050
1.000
0.950
0.900
10
100
1000
Stress in (kPa)
Loading TP-6-1
Unloading TP-6-1
Loading TP-6-2
Unloading TP-6-2

Log time versus dial reading for different loading for TP-1-2

Load increment	50 kPa	100 kPa
Time (min)	Deformation	Deformation
0.00	0.318	0.574
0.10	0.332	0.578
0.25	0.334	0.584
0.50	0.338	0.588
1.00	0.344	0.596
2.00	0.426	0.61
4.00	0.438	0.614
8.00	0.456	0.616
15.00	0.476	0.626
30.00	0.496	0.642
60.00	0.506	0.662
120.00	0.546	0.684
240.00	0.562	0.704
480.00	0.568	0.73
1440.00	0.574	0.74

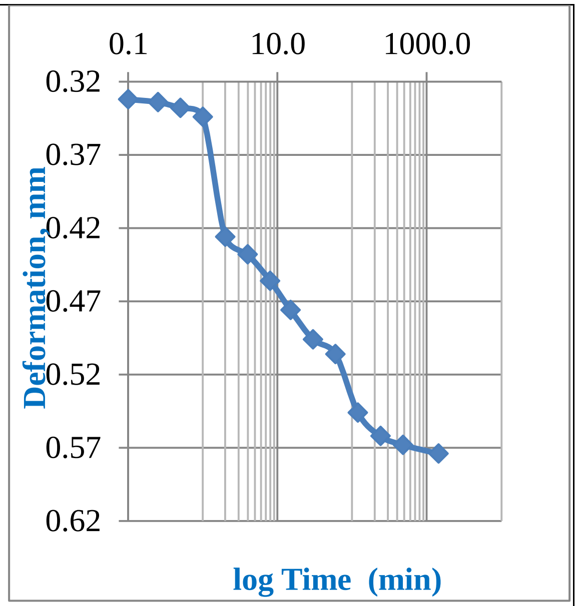

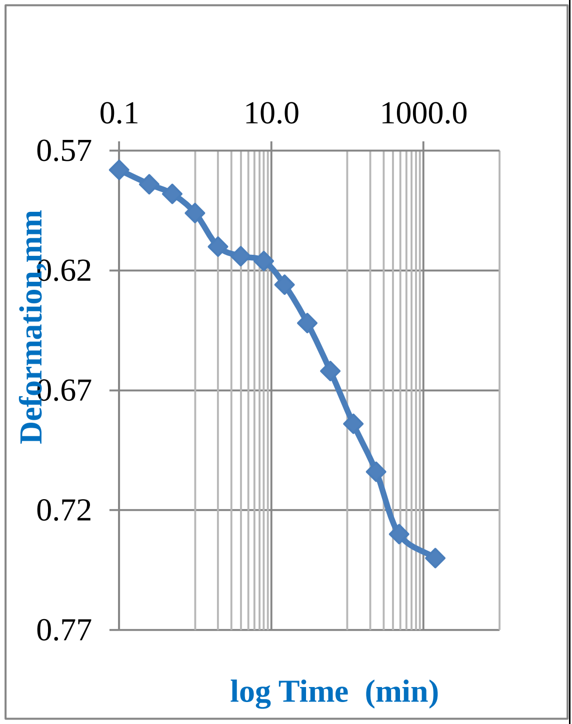

Load increment	200 kPa	400 kPa	800 kPa
Time (min)	Deformation	Deformation	Deformation
0.00	0.74	0.88	1.562
0.32	0.744	0.892	1.588
0.50	0.746	0.898	1.592
0.71	0.748	0.942	1.618
1.00	0.752	0.964	1.646
1.41	0.758	0.996	1.686
2.00	0.766	1.212	1.734
2.83	0.772	1.274	1.796
3.87	0.776	1.286	1.874
5.48	0.782	1.352	1.914
7.75	0.796	1.416	2.02
10.95	0.824	1.472	2.16
15.49	0.848	1.514	2.2
21.91	0.872	`	2.23
37.95	0.88	1.562	2.24

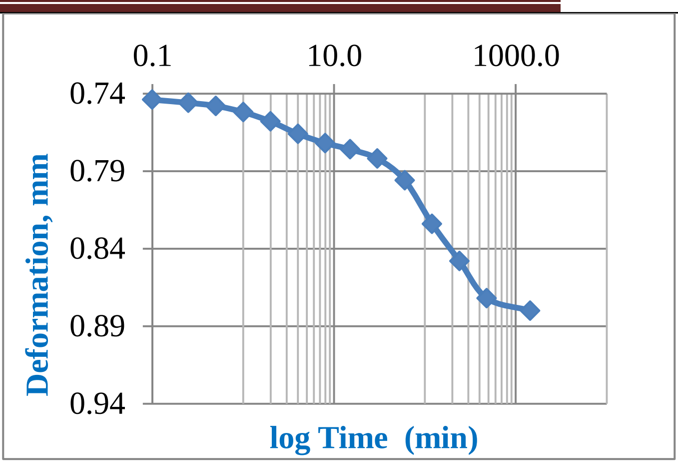

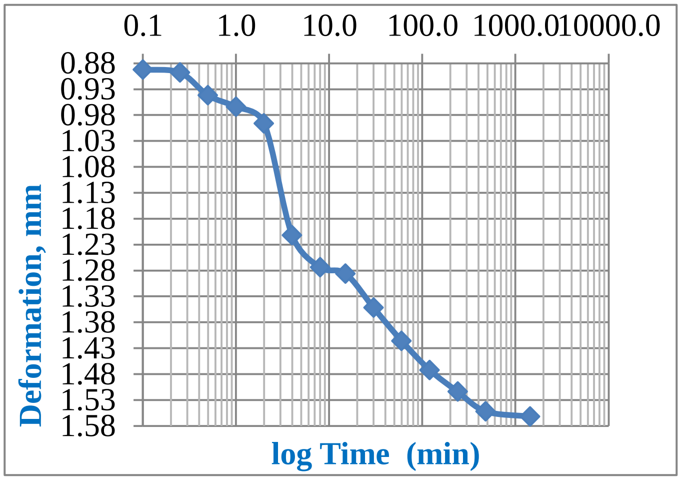

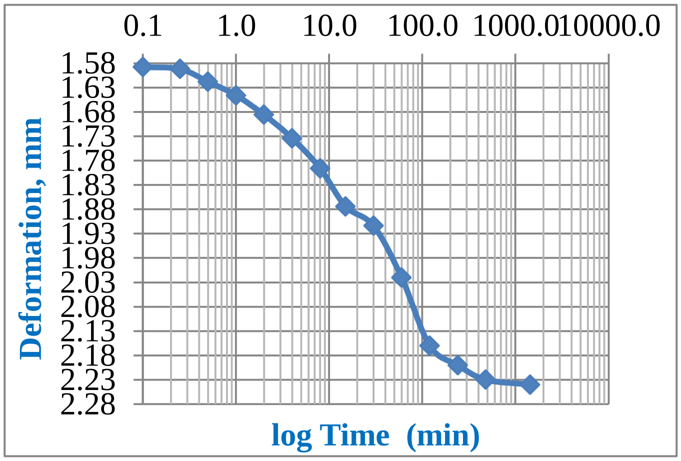

Square time versus dial reading for different loading for TP-1-1

Load increment	50 kPa	100 kPa
√Time	Deformation	Deformation
0.00	0.218	0.374
0.32	0.346	0.41
0.50	0.35	0.44
0.71	0.358	0.458
1.00	0.358	0.464
1.41	0.359	0.476
2.00	0.36	0.486
2.83	0.36	0.498
3.87	0.362	0.504
5.48	0.364	0.512
7.75	0.366	0.52
10.95	0.37	0.526
15.49	0.372	0.532
21.91	0.374	0.534
37.95	0.374	0.54

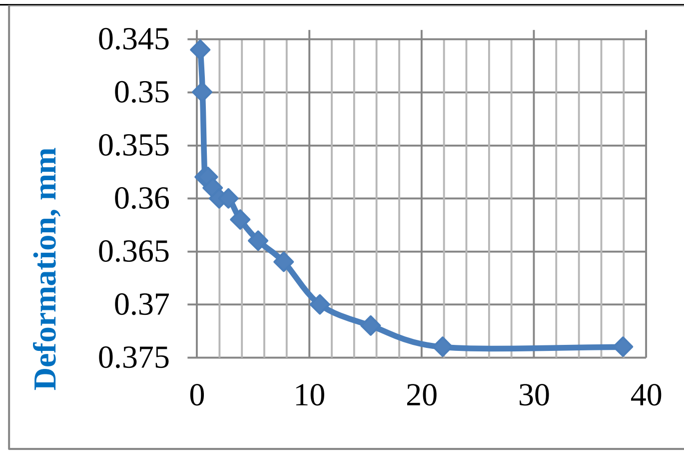

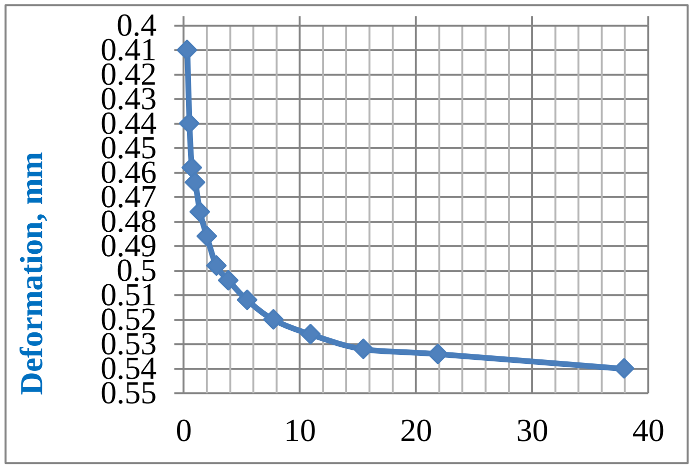

Load increment	200 kPa	400 kPa	800 kPa
√Time	Deformation	Deformation	Deformation
0.00	0.54	1.328	2.922
0.32	0.594	2.236	2.976
0.50	0.858	2.436	3.03
0.71	0.896	2.548	3.074
1.00	0.962	2.666	3.113
1.41	1.216	2.700	3.15
2.00	1.226	2.754	3.186
2.83	1.246	2.762	3.218
3.87	1.262	2.772	3.246
5.48	1.276	2.858	3.273
7.75	1.29	2.869	3.294
10.95	1.304	2.897	3.312
15.49	1.312	2.908	3.324
21.91	1.324	2.91	3.338
37.95	1.328	2.922	3.352

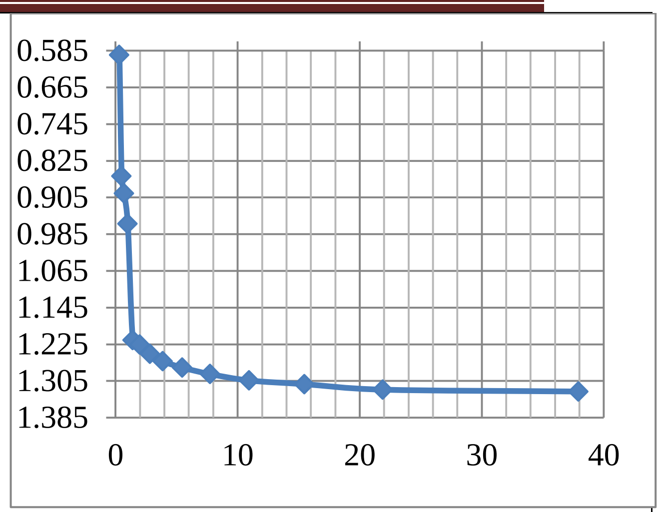

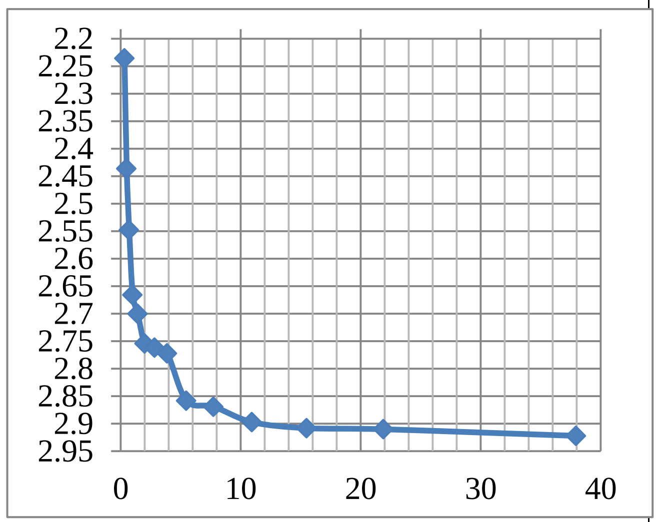

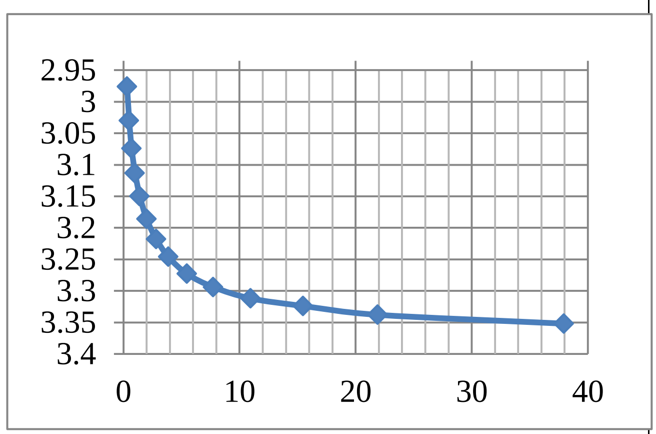

Table A1-1: Calculation of consolidation coefficient versus effective pressure by using square root method for TP-1-1

Pressure (kPa)	Do	Deformation dial reading at 90% consolidation	Deformation Dial reading Representing 100% Primary Consolidation	Deformation dial reading at 50% consolidation	Time for Root 90% consolidation	Time for 90% consolidation	Thickness of specimen at 50% consolidation	Half-thickness of specimen at 50% consolidation	Coefficient of consolidation Cv (m^2/year)
50	0.350	0.358	0.359	0.354	1.4	2.0	19.646	9.823	*21.94*
100	0.440	0.498	0.504	0.472	2	4.0	19.528	9.764	*10.62*
200	0.858	1.226	1.267	1.062	2	4.0	18.938	9.469	*9.99*
400	2.436	2.754	2.789	2.613	2	4.0	17.387	8.694	*8.42*
800	3.030	3.218	3.239	3.134	2	4.0	16.866	8.433	*7.92*
400	3.334	3.320	3.318	3.326	3.87	15.0	16.674	8.337	*2.07*
200	3.276	3.269	3.268	3.272	3.87	15.0	16.728	8.364	*2.08*
100	3.218	3.210	3.209	3.214	3.87	15.0	16.786	8.393	*2.10*
50	3.160	3.154	3.153	3.157	2	4.0	16.843	8.422	*7.90*

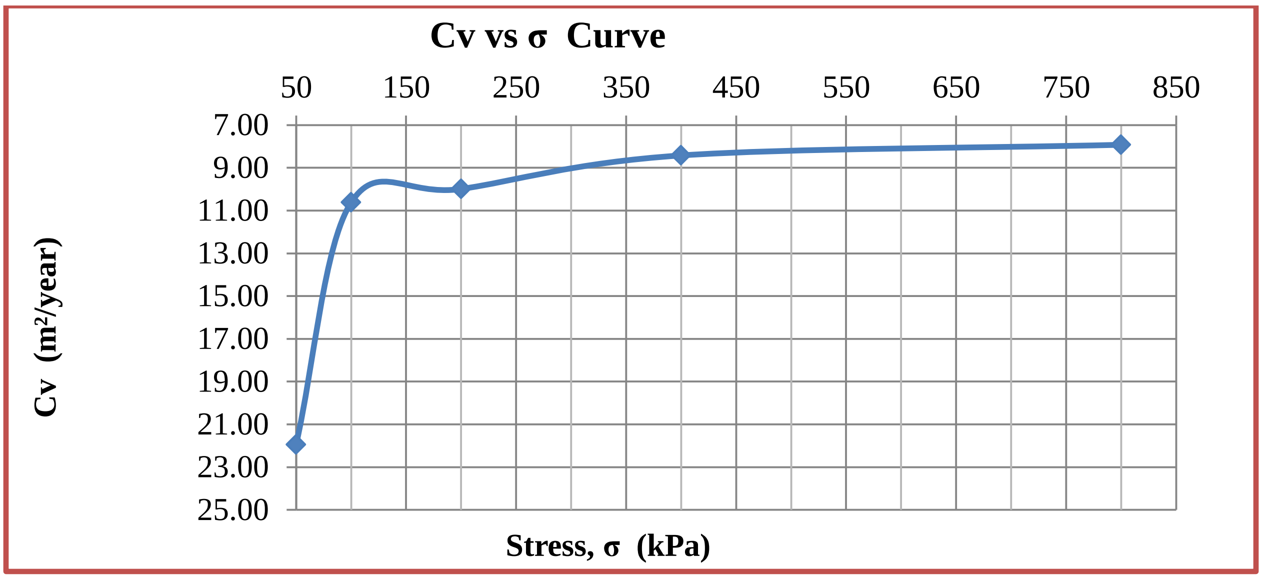

FigureA1-1: Consolidation coefficient versus effective pressure by using square root method for TP-1-1

Square time versus dial reading for different loading for TP-2-1

Load increment	50 kPa	100 kPa
√Time	Deformation	Deformation
0.00	0.328	1.174
0.32	0.778	1.176
0.50	0.784	1.178
0.71	0.794	1.182
1.00	0.846	1.184
1.41	0.854	1.188
2.00	0.876	1.196
2.83	0.888	1.201
3.87	0.988	1.224
5.48	1.106	1.244
7.75	1.124	1.263
10.95	1.156	1.283
15.49	1.172	1.303
21.91	1.172	1.328
37.95	1.174	1.338

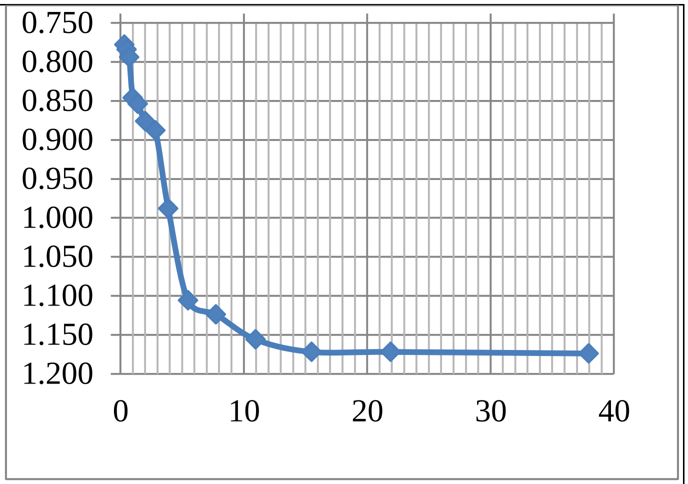

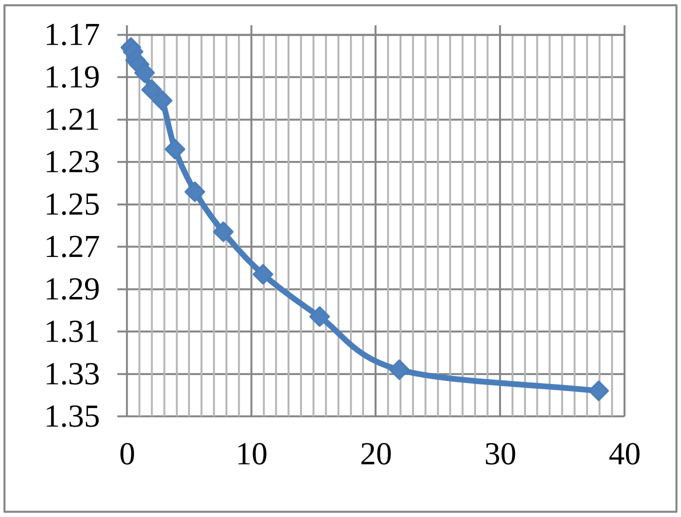

Load increment	200 kPa	400 kPa	800 kPa
√Time	Deformation	Deformation	Deformation
0.00	1.338	1.487	1.982
0.32	1.342	1.488	2.158
0.50	1.346	1.49	2.192
0.71	1.348	1.54	2.238
1.00	1.352	1.562	2.246
1.41	1.358	1.596	2.286
2.00	1.366	1.612	2.296
2.83	1.372	1.663	2.334
3.87	1.376	1.8	2.374
5.48	1.38	1.814	2.41
7.75	1.398	1.826	2.42
10.95	1.426	1.877	2.56
15.49	1.446	1.914	2.6
21.91	1.47	1.956	2.63
37.95	1.487	1.982	2.66

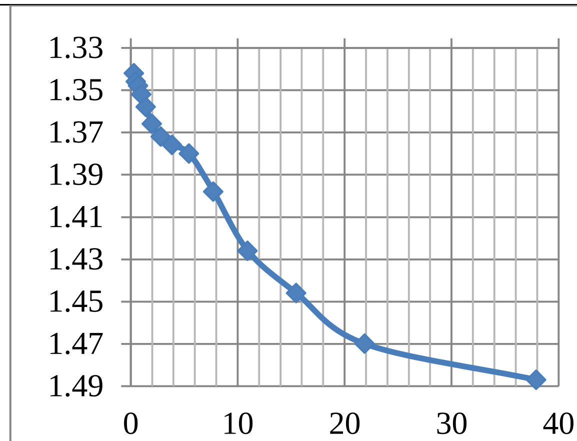

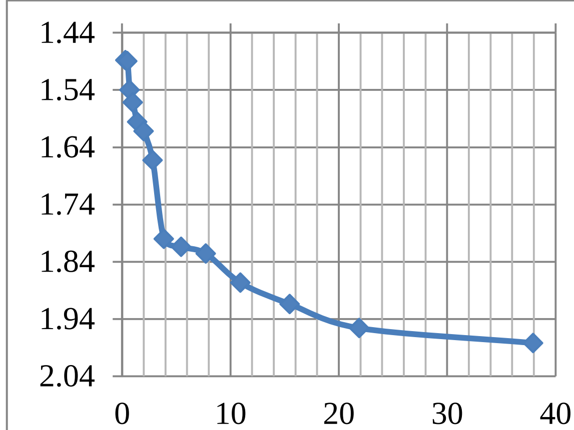

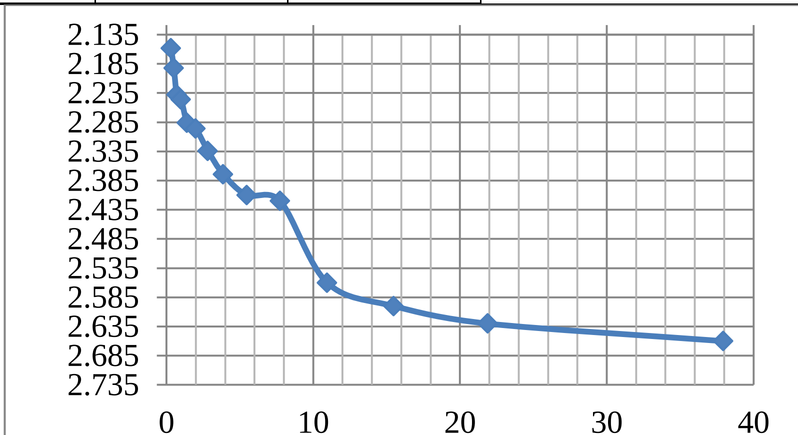

TableA1-2: Calculation of consolidation coefficient versus effective pressure by using square root method for TP-2-1

Pressure (KPa)	Do	Deformation dial reading at 90% consolidation	Deformation Dial reading Representing 100% Primary Consolidation	Deformation dial reading at 50% consolidation	Time for Root 90% consolidation	Time for 90% consolidation	Thickness of specimen at 50% consolidation	Half-thickness of specimen at 50% consolidation	Coefficient of consolidation Cv (m^2/year)
50	0.784	0.876	0.886	0.835	2	4.0	19.165	9.582	*10.23*
100	1.178	1.263	1.272	1.225	7.745	60.0	18.775	9.387	*0.65*
200	1.346	1.376	1.379	1.363	3.87	15.0	18.637	9.319	*2.58*
400	1.540	1.814	1.844	1.692	5.48	30.0	18.308	9.154	*1.24*
800	1.920	2.374	2.424	2.172	3.87	15.0	17.828	8.914	*2.36*
400	2.622	2.566	2.560	2.591	5.48	30.0	17.409	8.705	*1.12*
200	2.496	2.370	2.356	2.426	10.95	119.9	17.574	8.787	*0.29*
100	2.305	2.183	2.169	2.237	15.492	240.0	17.763	8.881	*0.15*
50	2.126	1.958	1.939	2.033	21.91	480.0	17.967	8.984	*0.07*

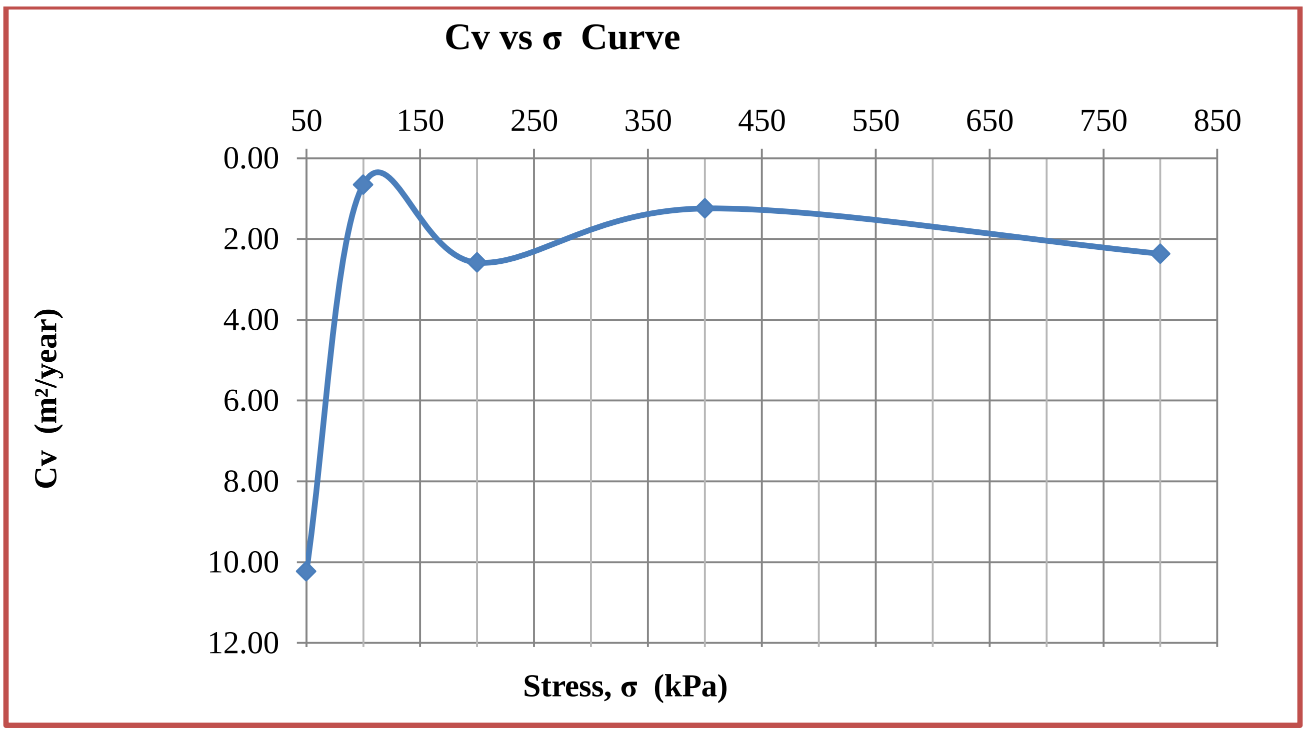

FigureA1-2: Consolidation coefficient versus effective pressure by using square root method for TP-2-1

<u>Square time versus dial reading for different loading for TP-3-2</u>

Load increment	50 kPa	100 kPa
√Time	Deformation	Deformation
0.00	0.116	0.754
0.32	0.338	0.816
0.50	0.432	0.876
0.71	0.532	0.894
1.00	0.548	0.912
1.41	0.576	0.932
2.00	0.624	0.952
2.83	0.638	1.028
3.87	0.652	1.038
5.48	0.705	1.05
7.75	0.716	1.071
10.95	0.726	1.082
15.49	0.736	1.094
21.91	0.746	1.098
37.95	0.754	1.104

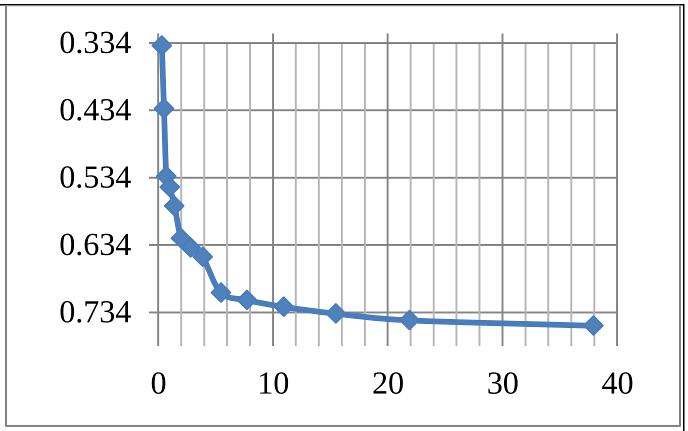

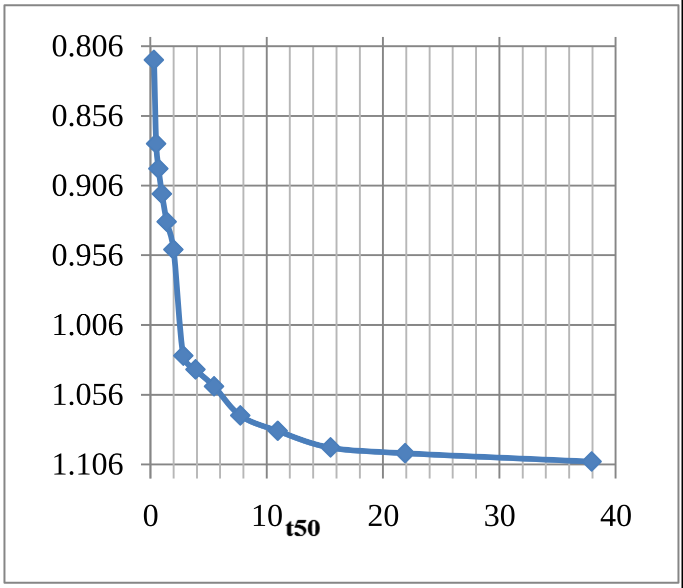

Load increment	200 kPa	400 kPa	800 kPa
√Time	Deformation	Deformation	Deformation
0.00	1.104	1.4	2.134
0.32	1.28	1.636	2.236
0.50	1.284	1.691	2.334
0.71	1.296	1.714	2.416
1.00	1.33	1.738	2.442
1.41	1.335	1.814	2.465
2.00	1.347	1.846	2.532
2.83	1.352	1.92	2.565
3.87	1.36	1.959	2.575
5.48	1.366	2.018	2.604
7.75	1.37	2.045	2.648
10.95	1.388	2.062	2.704
15.49	1.392	2.102	2.766
21.91	1.398	2.124	2.798
37.95	1.4	2.134	2.808

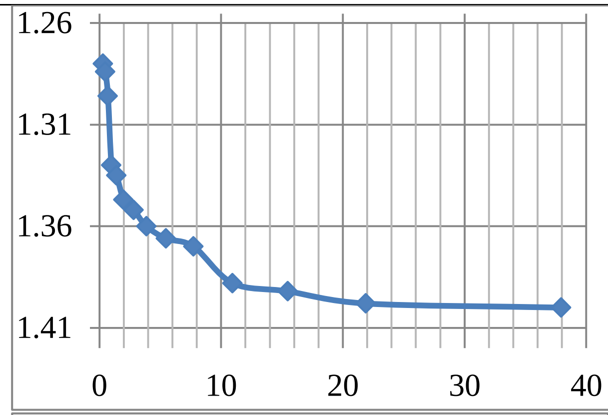

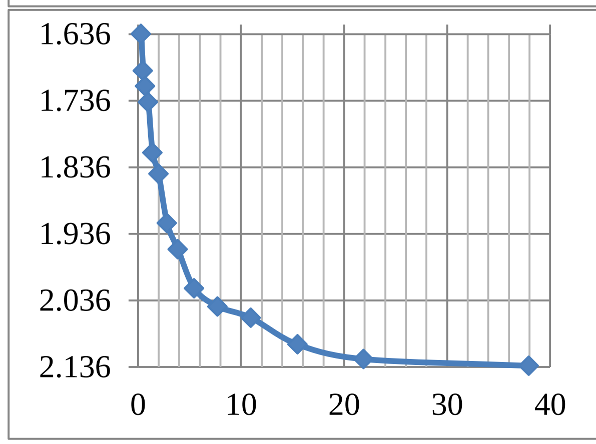

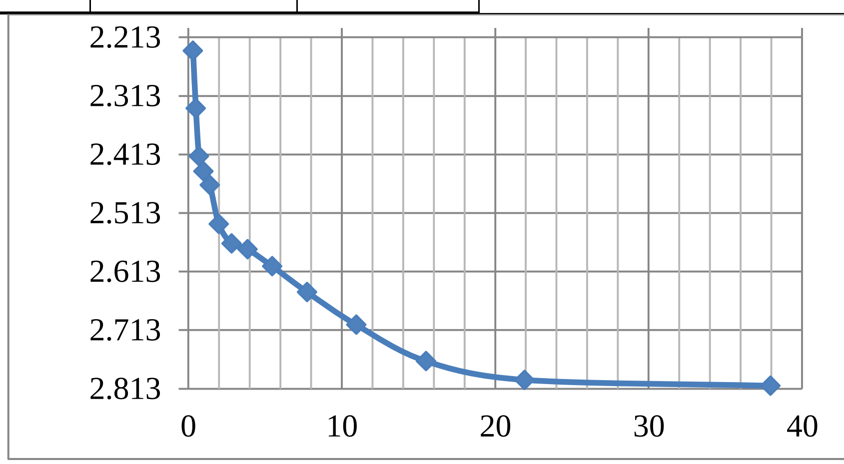

TableA1-3: Calculation of consolidation coefficient versus effective pressure by using square root method for TP-3-2

Pressure (KPa)	Do	Deformation dial reading at 90% consolidation	reading Representing 100% Primary Consolidation	Deformation dial reading at 50% consolidation	Time for Root 90% consolidation	Time for 90% consolidation	Thickness of specimen at 50% consolidation	Half-thickness of specimen at 50% consolidation	Coefficient of consolidation Cv (m^2/year)
50	0.532	0.705	0.724	0.628	3.87	15.0	19.372	9.686	*2.79*
100	0.876	1.038	1.056	0.966	3.87	15.0	19.034	9.517	*2.70*
200	1.330	1.366	1.370	1.350	5.48	30.0	18.650	9.325	*1.29*
400	1.691	2.018	2.054	1.873	5.48	30.0	18.127	9.064	*1.22*
800	2.416	2.575	2.593	2.504	3.87	15.0	17.496	8.748	*2.28*
400	2.792	2.754	2.750	2.771	3.87	15.0	17.229	8.615	*2.21*
200	2.692	2.660	2.656	2.674	3.87	15.0	17.326	8.663	*2.23*
100	2.618	2.584	2.580	2.599	7.75	60.1	17.401	8.700	*0.56*
50	2.524	2.512	2.511	2.517	1.41	2.0	17.483	8.741	*17.13*

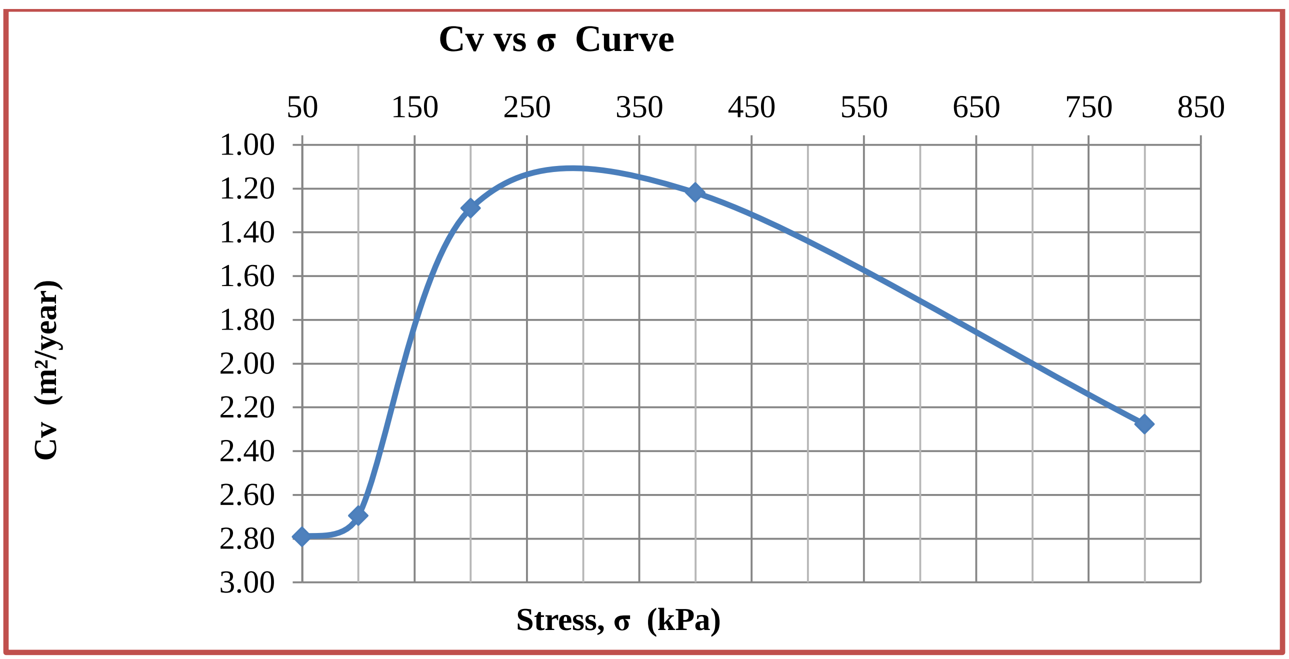

FigureA1-3: Consolidation coefficient versus effective pressure by using square root method for TP-3-2

Square time versus dial reading for different loading for TP-5-2

Load increment	50 kPa	100 kPa
√Time	Deformation	Deformation
0.00	0.032	0.336
0.32	0.216	0.454
0.50	0.234	0.474
0.71	0.246	0.486
1.00	0.260	0.498
1.41	0.270	0.51
2.00	0.282	0.523
2.83	0.293	0.538
3.87	0.300	0.546
5.48	0.306	0.557
7.75	0.310	0.564
10.95	0.316	0.574
15.49	0.324	0.586
21.91	0.332	0.598
37.95	0.336	0.603

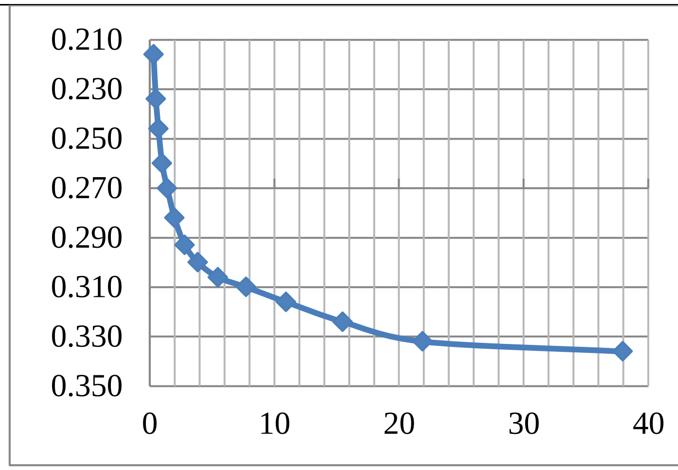

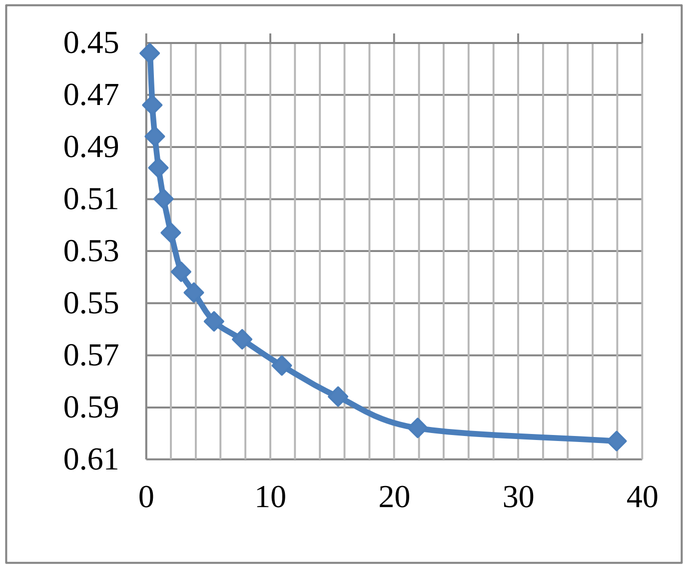

Load increment	200 kPa	400 kPa	800 kPa
√Time	Deformation	Deformation	Deformation
0.00	0.603	0.993	1.558
0.32	0.794	1.174	1.814
0.50	0.816	1.248	1.854
0.71	0.832	1.286	1.88
1.00	0.848	1.302	1.908
1.41	0.866	1.315	1.941
2.00	0.883	1.355	1.985
2.83	0.903	1.38	2.04
3.87	0.927	1.422	2.089
5.48	0.931	1.446	2.142
7.75	0.945	1.476	2.185
10.95	0.967	1.508	2.222
15.49	0.978	1.546	2.244
21.91	0.985	1.554	2.284
37.95	0.993	1.558	2.288

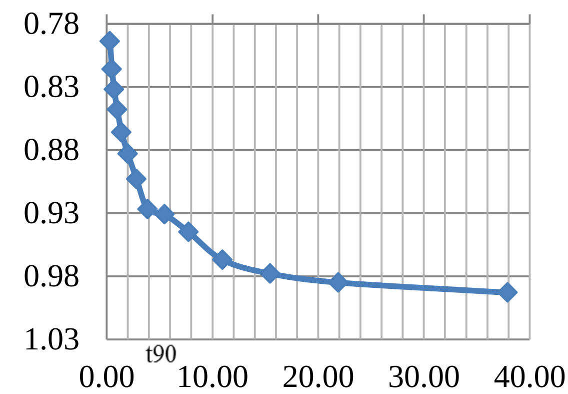

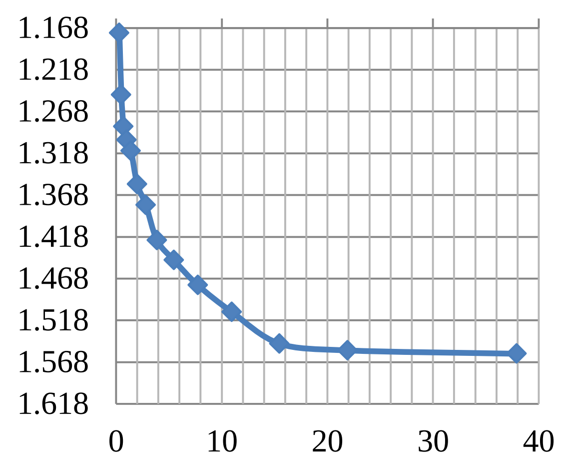

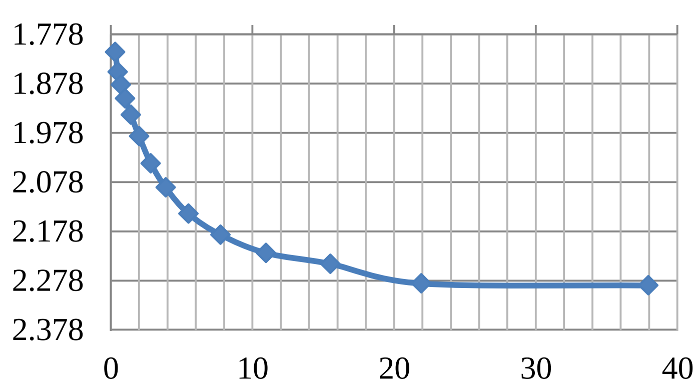

TableA1-4: Calculation of consolidation coefficient versus effective pressure by using square root method for TP-5-2

Pressure (KPa)	Do	Deformation dial reading at 90% consolidation	Deformation Dial reading Representing 100% Primary Consolidation	Deformation dial reading at 50% consolidation	Time for Root 90% consolidation	Time for 90% consolidation	Thickness of specimen at 50% consolidation	Half-thickness of specimen at 50% consolidation	Coefficient of consolidation Cv (m^2/year)
50	0.246	0.300	0.306	0.276	3.87	15.0	19.724	9.862	*2.89*
100	0.486	0.550	0.557	0.522	3.87	15.0	19.478	9.739	*2.82*
200	0.832	0.931	0.942	0.887	5.48	30.0	19.113	9.557	*1.36*
400	1.286	1.468	1.488	1.387	7.17	51.4	18.613	9.306	*0.75*
800	1.880	2.169	2.201	2.041	6.9	47.6	17.959	8.980	*0.75*
400	2.232	2.060	2.041	2.136	6.62	43.8	17.864	8.932	*0.81*
200	2.130	2.090	2.086	2.108	5.48	30.0	17.892	8.946	*1.19*
100	1.998	1.921	1.912	1.955	14	196.0	18.045	9.022	*0.19*
50	1.868	1.820	1.815	1.841	10.956	120.0	18.159	9.079	*0.31*

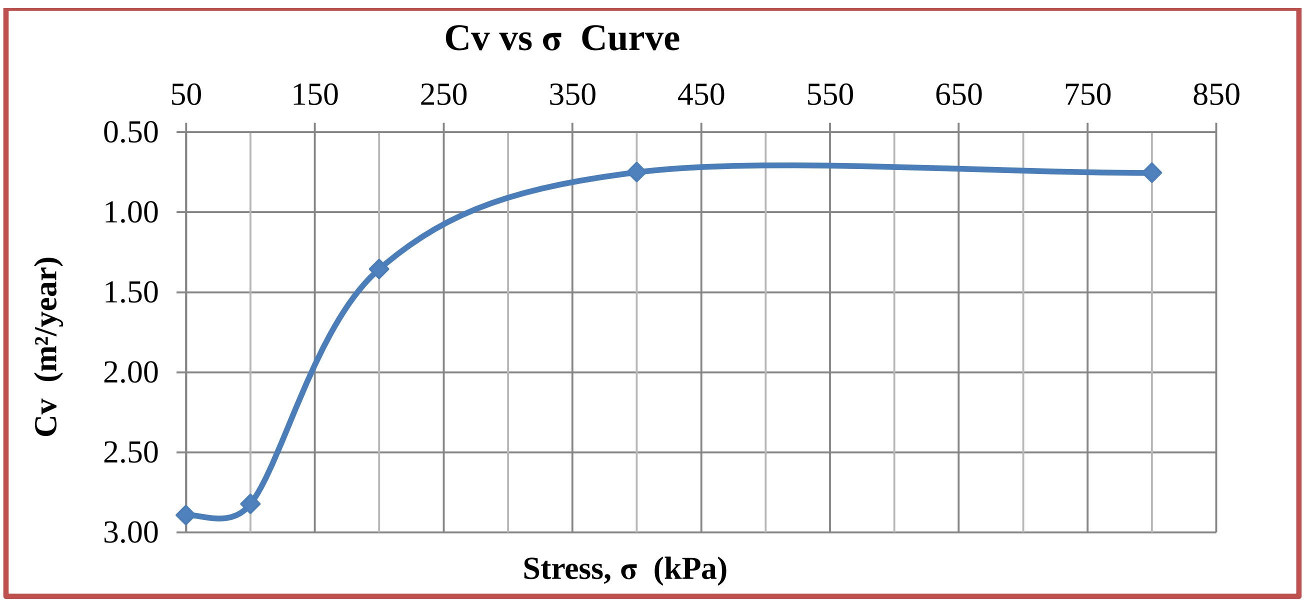

FigureA1-4: Consolidation coefficient versus effective pressure by using square root method for TP-5-2

Square time versus dial reading for different loading for TP-7-1

Load increment	50 kPa	100 kPa
√Time	Deformation	Deformation
0.00	0.038	0.446
0.32	0.040	0.448
0.50	0.061	0.524
0.71	0.118	0.548
1.00	0.162	0.56
1.41	0.164	0.574
2.00	0.232	0.582
2.83	0.286	0.594
3.87	0.318	0.608
5.48	0.348	0.628
7.75	0.370	0.654
10.95	0.386	0.682
15.49	0.414	0.72
21.91	0.438	0.758
37.95	0.446	0.772

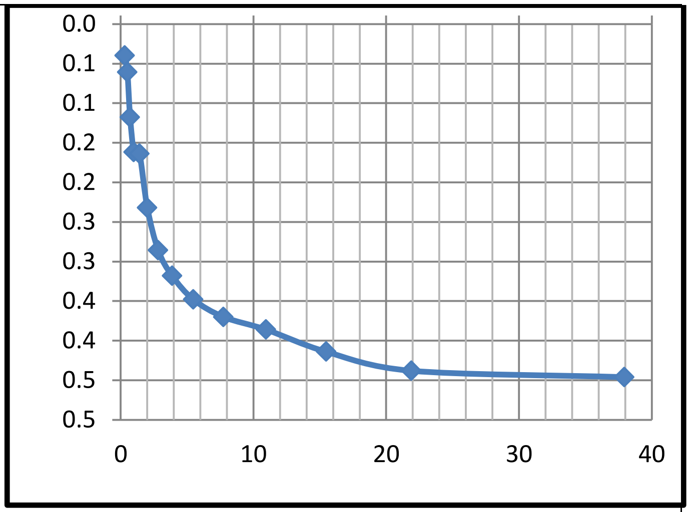

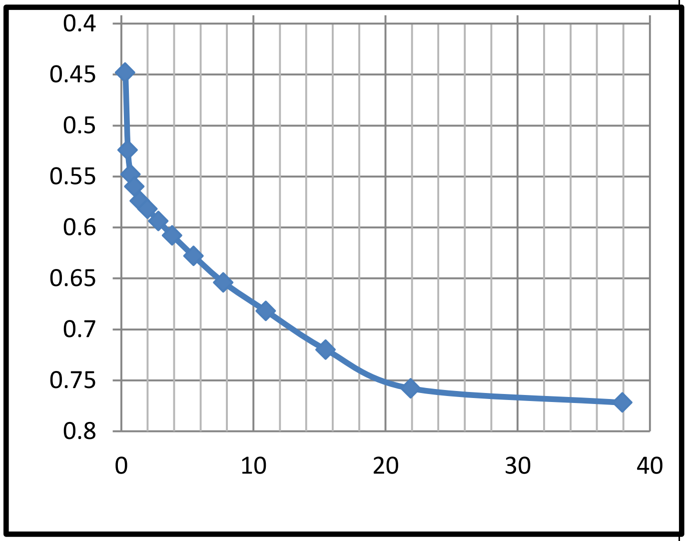

Load increment	200 kPa	400 kPa	800 kPa
√Time	Deformation	Deformation	Deformation
0.00	0.772	1.35	2.208
0.32	0.78	1.398	2.264
0.50	0.788	1.462	2.418
0.71	0.806	1.478	2.43
1.00	0.82	1.496	2.448
1.41	0.84	1.52	2.47
2.00	0.866	1.552	2.52
2.83	0.888	1.596	2.544
3.87	0.942	1.652	2.598
5.48	1.004	1.724	2.676
7.75	1.082	1.822	2.79
10.95	1.166	1.936	2.882
15.49	1.26	2.062	2.974
21.91	1.348	2.196	3.048
37.95	1.35	2.208	3.074

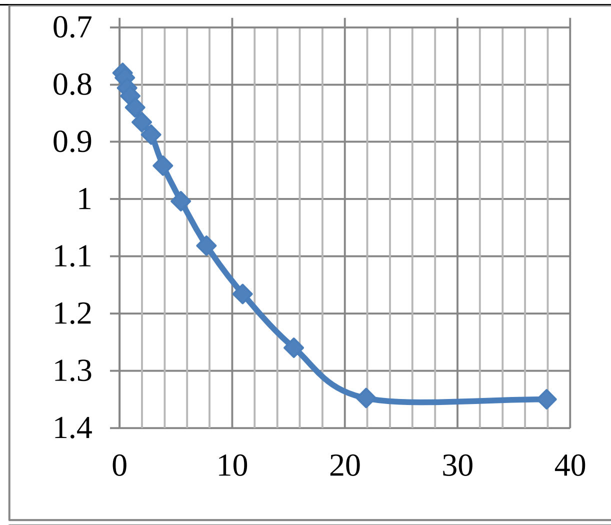

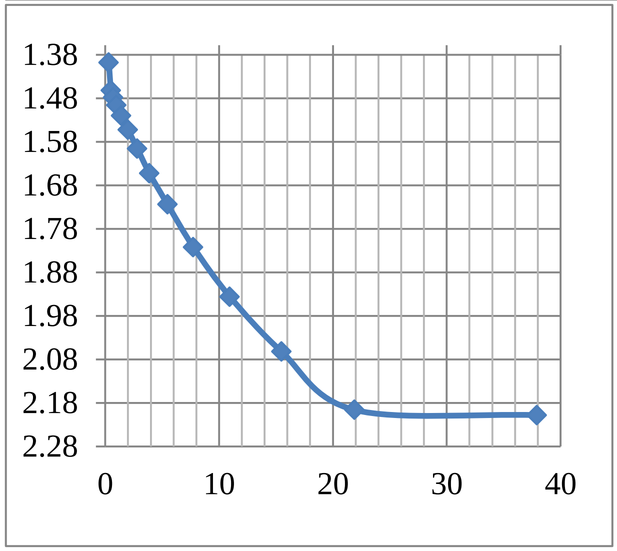

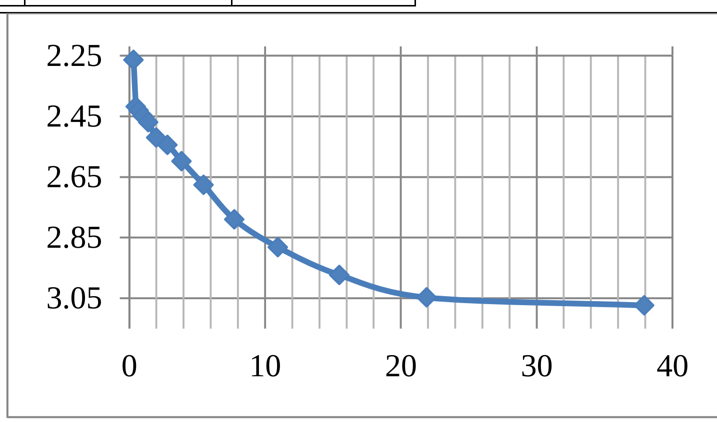

TableA1-5: Calculation of consolidation coefficient versus effective pressure by using square root method for TP-7-1

Pressure (KPa)	Do	Deformation dial reading at 90% consolidation	Deformation Dial reading Representing 100% Primary Consolidation	Deformation dial reading at 50% consolidation	Time for Root 90% consolidation	Time for 90% consolidation	Thickness of specimen at 50% consolidation	Half-thickness of specimen at 50% consolidation	Coefficient of consolidation Cv (m^2/year)
50	0.118	0.348	0.374	0.246	5.48	30.0	19.754	9.877	*1.45*
100	0.560	0.720	0.738	0.649	10.956	120.0	19.351	9.676	*0.35*
200	0.806	1.166	1.206	1.006	10.956	120.0	18.994	9.497	*0.33*
400	1.462	2.062	2.129	1.795	15.49	239.9	18.205	9.102	*0.15*
800	2.418	2.974	3.036	2.727	15.49	239.9	17.273	8.637	*0.14*
400	3.030	2.872	2.854	2.942	21.91	480.0	17.058	8.529	*0.07*
200	2.822	2.639	2.619	2.720	24	576.0	17.280	8.640	*0.06*
100	2.564	2.372	2.351	2.457	30	900.0	17.543	8.771	*0.04*
50	1.984	1.966	1.964	1.974	2.83	8.0	18.026	9.013	*4.52*

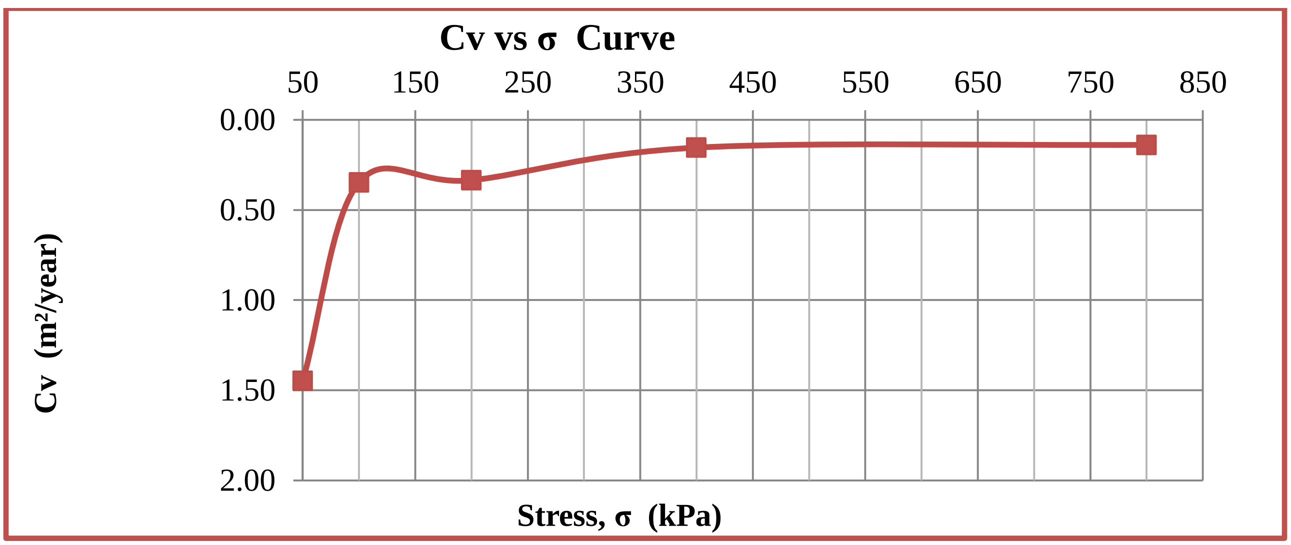

Figure A1-5: Consolidation coefficient versus effective pressure by using square root method for TP-7-1

Square time versus dial reading for different loading for TP-9-2

Load increment	50 kPa	100 kPa
√Time	Deformation	Deformation
0.00	0.114	0.432
0.32	0.332	0.64
0.50	0.342	0.644
0.71	0.358	0.654
1.00	0.365	0.664
1.41	0.371	0.674
2.00	0.375	0.683
2.83	0.382	0.69
3.87	0.385	0.696
5.48	0.388	0.702
7.75	0.401	0.708
10.95	0.414	0.71
15.49	0.422	0.734
21.91	0.428	0.738
37.95	0.432	0.744

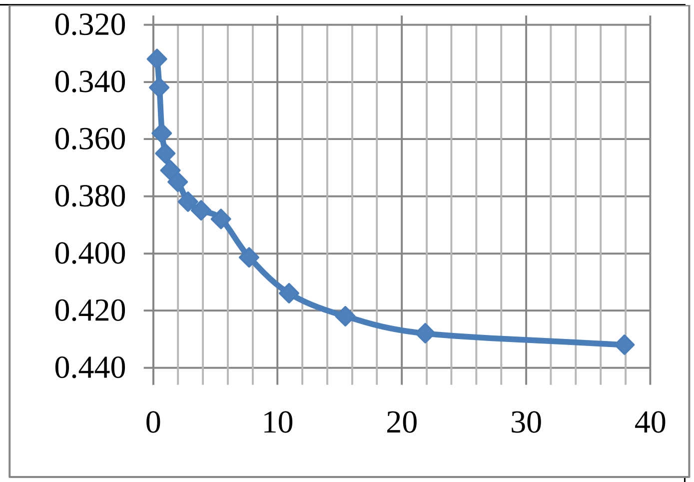

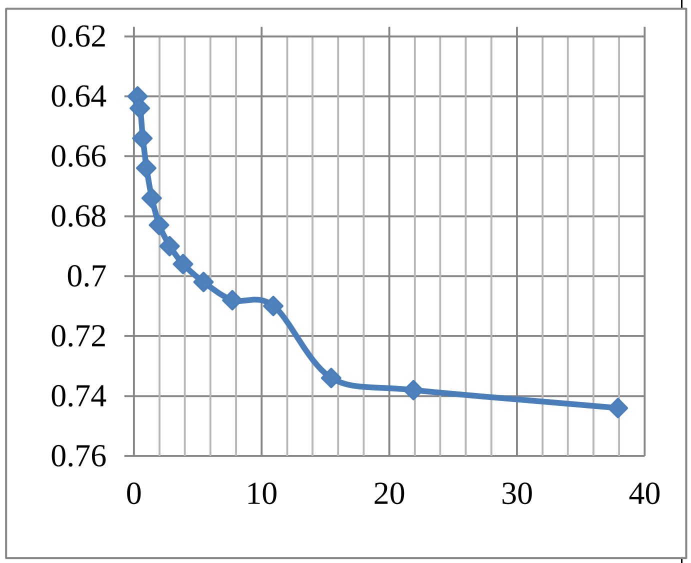

Load increment	200 kPa	400 kPa	800 kPa
√Time	Deformation	Deformation	Deformation
0.00	0.744	1.084	1.498
0.32	0.934	1.28	1.906
0.50	0.942	1.3	1.922
0.71	0.956	1.324	1.928
1.00	0.962	1.344	1.945
1.41	0.974	1.354	2.011
2.00	0.984	1.361	2.044
2.83	1.004	1.378	2.068
3.87	1.021	1.41	2.131
5.48	1.027	1.415	2.142
7.75	1.032	1.428	2.16
10.95	1.034	1.458	2.24
15.49	1.052	1.478	2.26
21.91	1.076	1.492	2.276
37.95	1.084	1.498	2.282

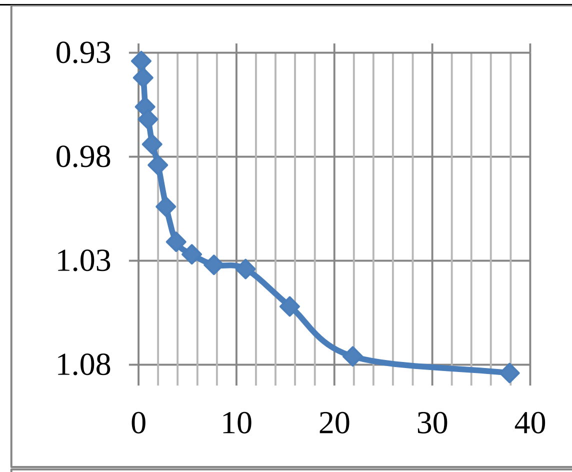

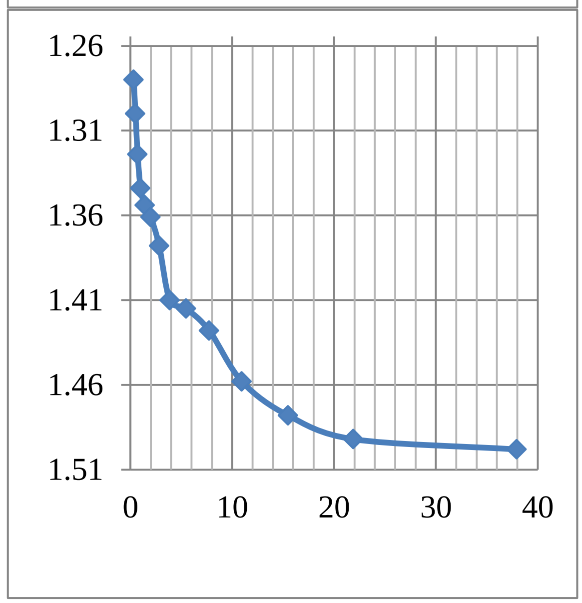

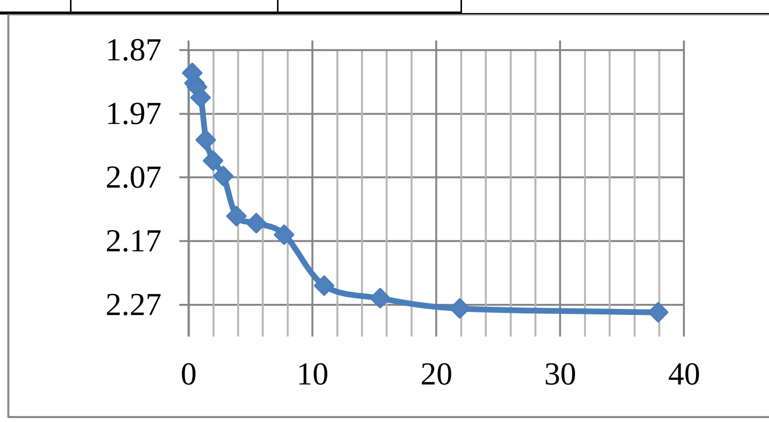

Table A1-6: Calculation of consolidation coefficient versus effective pressure by using square root method for TP-9-1

Pressure (KPa)	Do	Deformation dial reading at 90% consolidation	Deformation Dial reading Representing 100% Primary Consolidation	Deformation dial reading at 50% consolidation	Time for Root 90% consolidation	Time for 90% consolidation	Thickness of specimen at 50% consolidation	Half-thickness of specimen at 50% consolidation	Coefficient of consolidation Cv (m^2/year)
50	0.358	0.385	0.388	0.373	3.87	15.0	19.627	9.814	*2.87*
100	0.654	0.700	0.705	0.680	4.94	24.4	19.320	9.660	*1.70*
200	0.956	1.027	1.035	0.995	5.48	30.0	19.005	9.502	*1.34*
400	1.324	1.414	1.424	1.374	5.2	27.0	18.626	9.313	*1.43*
800	1.922	2.142	2.166	2.044	5.48	30.0	17.956	8.978	*1.20*
400	2.264	2.201	2.194	2.229	3.45	11.9	17.771	8.886	*2.96*
200	2.134	2.114	2.112	2.123	5.48	30.0	17.877	8.939	*1.19*
100	2.072	2.045	2.042	2.057	4.27	18.2	17.943	8.972	*1.97*
50	1.984	1.966	1.964	1.974	2.83	8.0	18.026	9.013	*4.52*

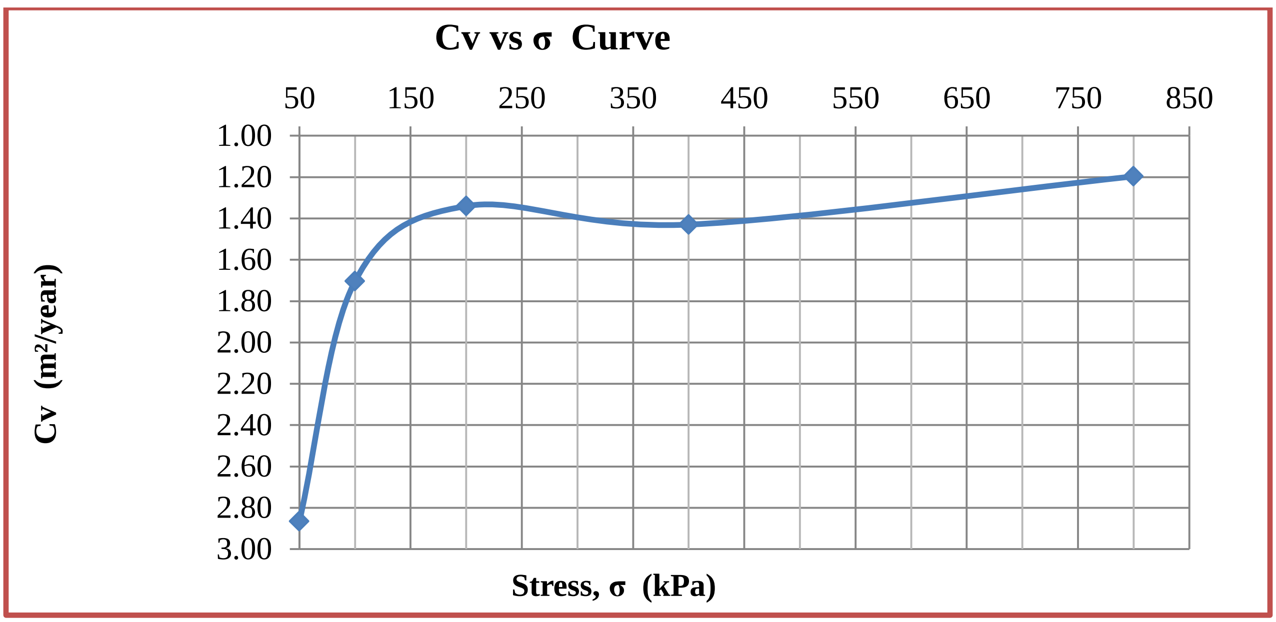

Figure A1-6: Consolidation coefficient versus effective pressure by using square root method for TP-9-2

A-2 Coefficient of compression (Cc) values and e versus log p Curves

Table A2-1: Coefficient of compression (Cc) for Matric village, sample TP-1-1 and TP-1-2

Pressure, σ (kPa)	Final deformation, mm	Final specimen Height, mm	Void ratio (e)	TP-1-1
50	0.357	19.635	1.189	Cc = 0.287
100	0.442	19.509	1.162	
200	0.932	18.872	1.062	
400	2.604	17.244	0.948	
800	3.045	16.809	0.902	
Pressure, σ (kPa)	Final deformation, mm	Final specimen Height, mm	Void ratio (e)	TP-1-2
50	0.314	19.556	1.304	Cc = 0.274
100	0.59	19.335	1.243	
200	0.738	19.191	1.195	
400	0.91	18.769	1.098	
800	1.536	18.082	0.995	

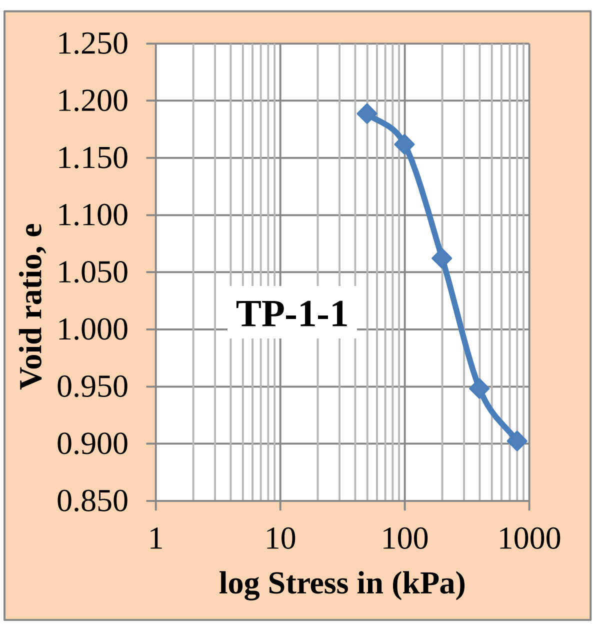

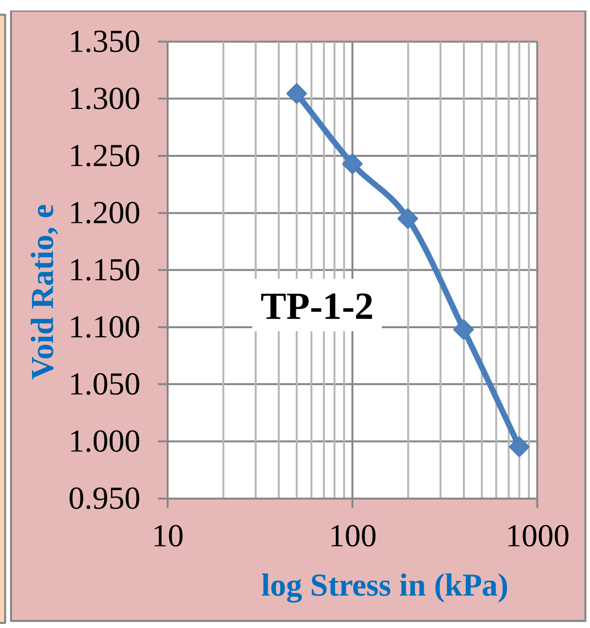

Figure A2-1: e-log p Curve for Matric village, sample TP-1-1 and TP-1-2

Table A2-2: Coefficient of compression (Cc) for Bacho Bore, sample TP-2-1 and TP-2-2

Pressure, σ (kPa)	Final deformation, mm	Final specimen Height, mm	Void ratio (e)	TP-2-1
50	0.734	19.047	1.179	Cc = 0.232
100	1.174	18.744	1.152	
200	1.338	18.596	1.121	
400	1.484	18.280	1.035	
800	2.190	17.774	0.942	
Pressure, σ (kPa)	Final deformation, mm	Final specimen Height, mm	Void ratio (e)	TP-2-2
50	0.250	19.591	1.270	Cc = 0.227
100	0.572	19.344	1.247	
200	0.738	19.187	1.224	
400	0.888	18.780	1.134	
800	1.550	18.110	1.042	

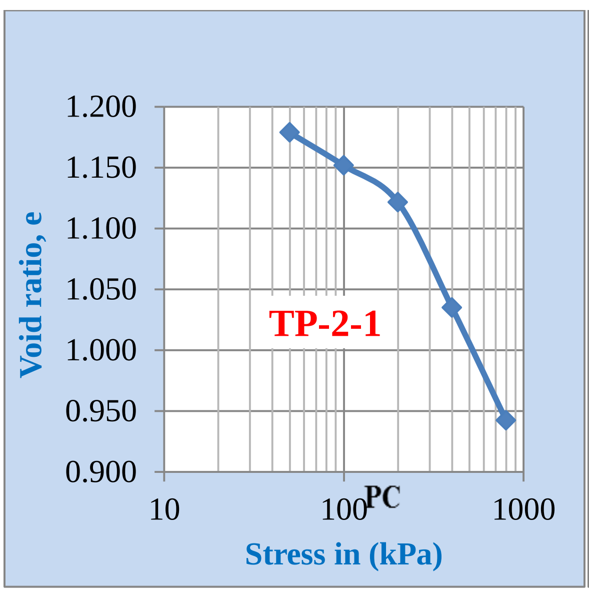

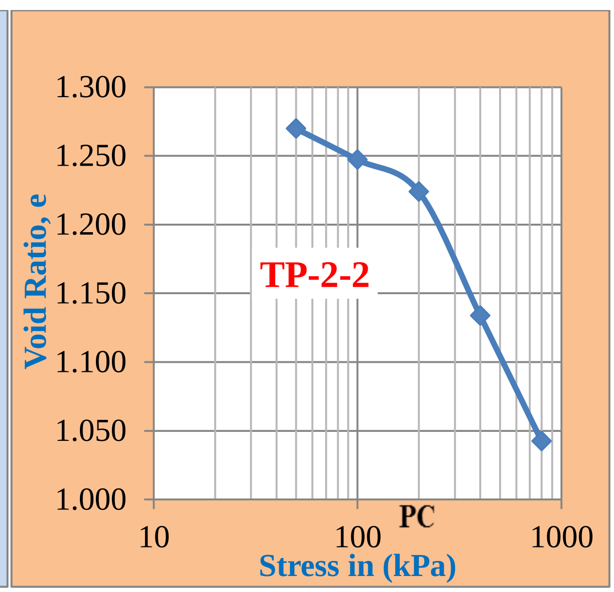

Figure A2-2: e-log p Curve for Bacho Bore, sample TP-2-1 and TP-2-2

Table A2-3: Coefficient of compression (Cc) for Awetu village, sample TP-3-1 and TP-3-2

Pressure, σ (kPa)	Final deformation, mm	Final specimen Height, mm	Void ratio (e)	TP-3-1
50	0.508	19.368	1.156	Cc = 0.248
100	0.904	19.023	1.090	
200	1.269	18.659	1.049	
400	1.648	18.109	0.945	
800	2.367	17.409	0.866	
Pressure, σ (kPa)	Final deformation, mm	Final specimen Height, mm	Void ratio (e)	TP-3-2
50	0.488	19.383	1.118	Cc = 0.244
100	0.756	19.073	1.058	
200	1.257	18.673	1.023	
400	1.614	18.131	0.918	
800	2.367	17.418	0.838	

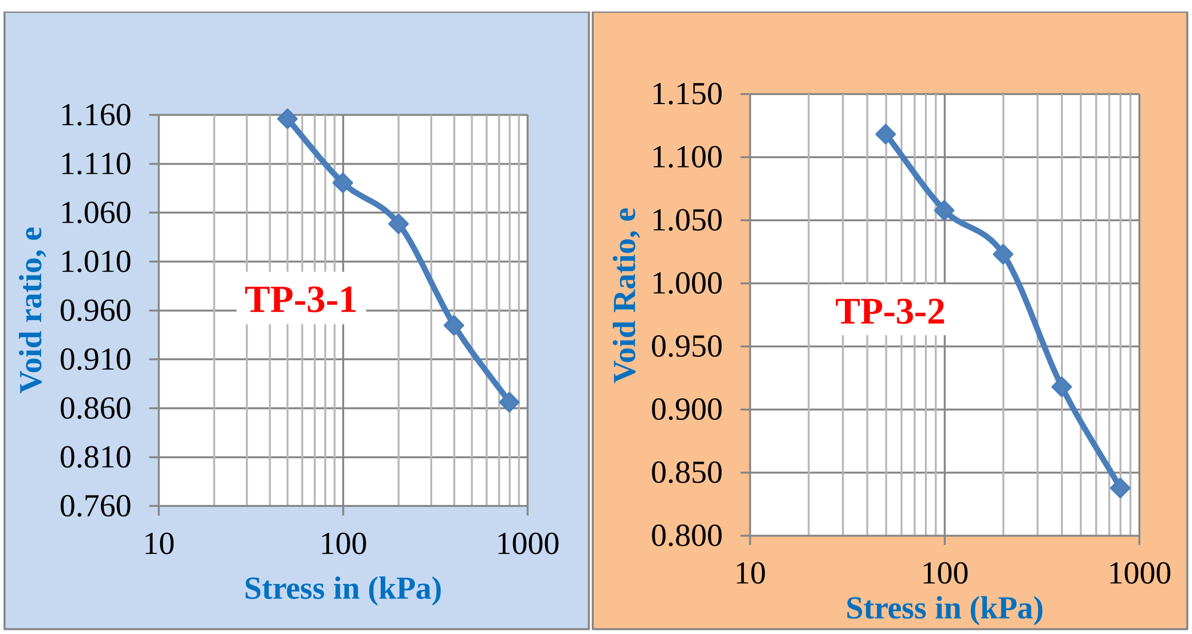

Figure A2-3: e-log p Curve for Awetu village, sample TP-3-1 and TP-3-2

Table A2-4: Coefficient of compression (Cc) for Bossa Kitto, sample TP-4-1 and TP-4-2

Pressure, σ (kPa)	Final deformation, mm	Final specimen Height, mm	Void ratio (e)	TP-4-1
50	0.304	19.669	1.250	Cc = 0.286
100	0.460	19.475	1.201	
200	0.742	19.173	1.130	
400	1.022	18.911	1.043	
800	1.396	18.462	0.943	
Pressure, σ (kPa)	Final deformation, mm	Final specimen Height, mm	Void ratio (e)	TP-4-2
50	0.237	19.705	1.281	Cc = 0.310
100	0.492	19.470	1.232	
200	0.727	19.218	1.167	
400	1.026	18.916	1.081	
800	1.407	18.462	0.951	

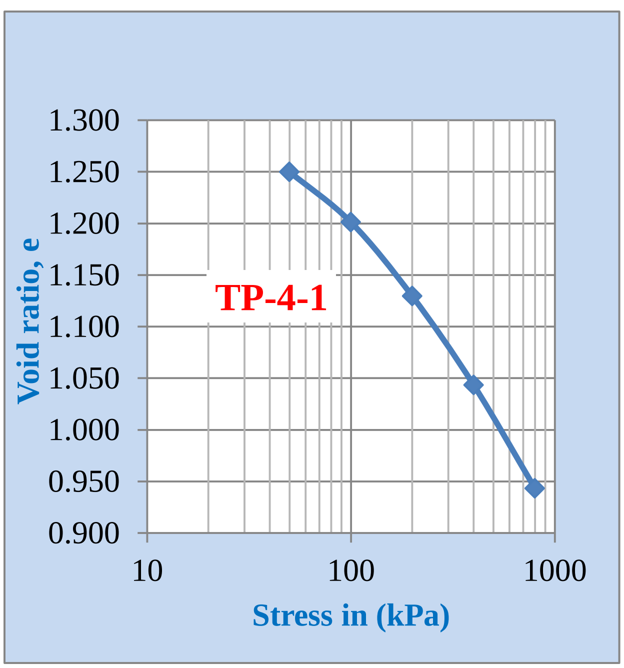

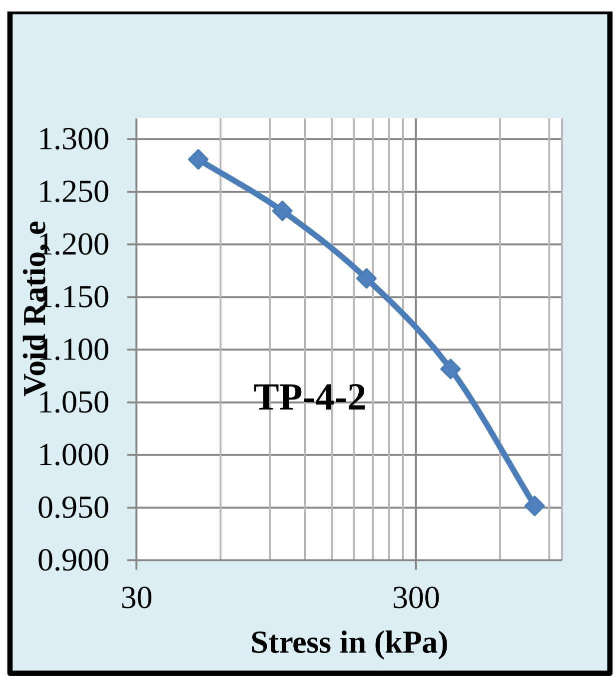

Figure A2-4: e-log p Curve for Bossa Kitto, sample TP-4-1 and TP-4-2

Table A2-5: Coefficient of compression (Cc) for Hermata Merkato, sample TP-5-1 and TP-5-2

Pressure, σ (kPa)	Final deformation, mm	Final specimen Height, mm	Void ratio (e)	TP-5-1
50	0.280	19.666	1.366	
100	0.444	19.485	1.322	Cc = 0.264
200	0.690	19.186	1.239	
400	1.068	18.773	1.155	
800	1.412	18.303	1.084	
Pressure, σ (kPa)	Final deformation, mm	Final specimen Height, mm	Void ratio (e)	TP-5-2
50	0.238	19.713	1.326	
100	0.473	19.462	1.281	Cc = 0.243
200	0.813	19.097	1.214	
400	1.249	18.599	1.148	
800	1.831	17.943	1.062	

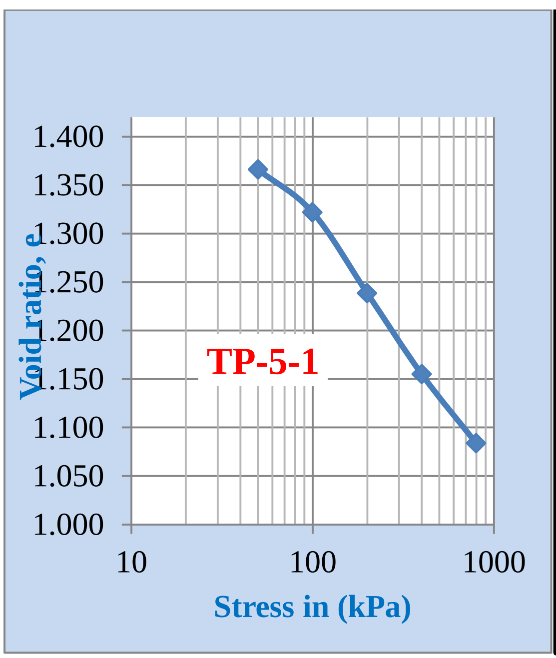

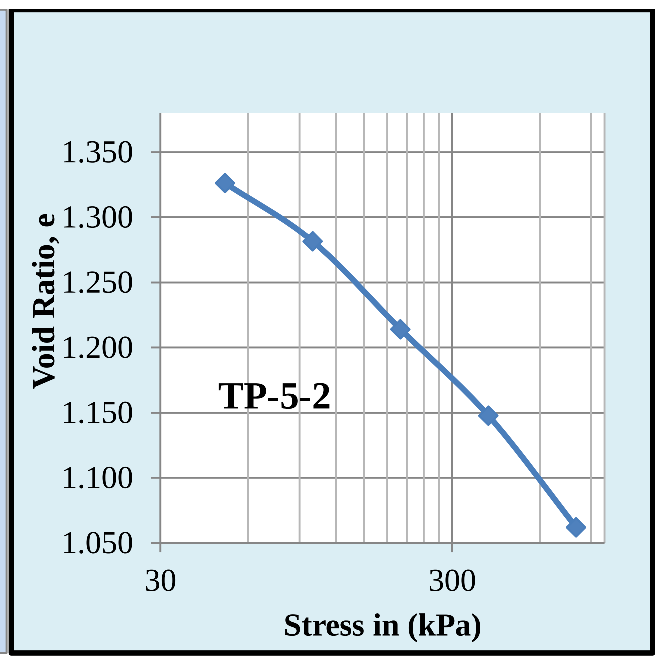

Figure A2-5: e-log p Curve for Hermata Merkato, sample TP-5-1 and TP-5-2

Table A2-6: Coefficient of compression (Cc) for BA KG Model School, sample TP-6-1 and TP-6-2

Pressure, σ (kPa)	Final deformation, mm	Final specimen Height, mm	Void ratio (e)	TP-6-1
50	0.412	19.543	1.271	Cc = 0.252
100	0.739	19.209	1.196	
200	0.853	19.123	1.132	
400	1.233	18.658	1.036	
800	1.660	18.201	0.968	
Pressure, σ (kPa)	Final deformation, mm	Final specimen Height, mm	Void ratio (e)	TP-6-2
50	0.400	19.544	1.255	Cc = 0.241
100	0.526	19.405	1.191	
200	0.840	19.124	1.127	
400	1.284	18.628	1.033	
800	1.604	18.226	0.973	

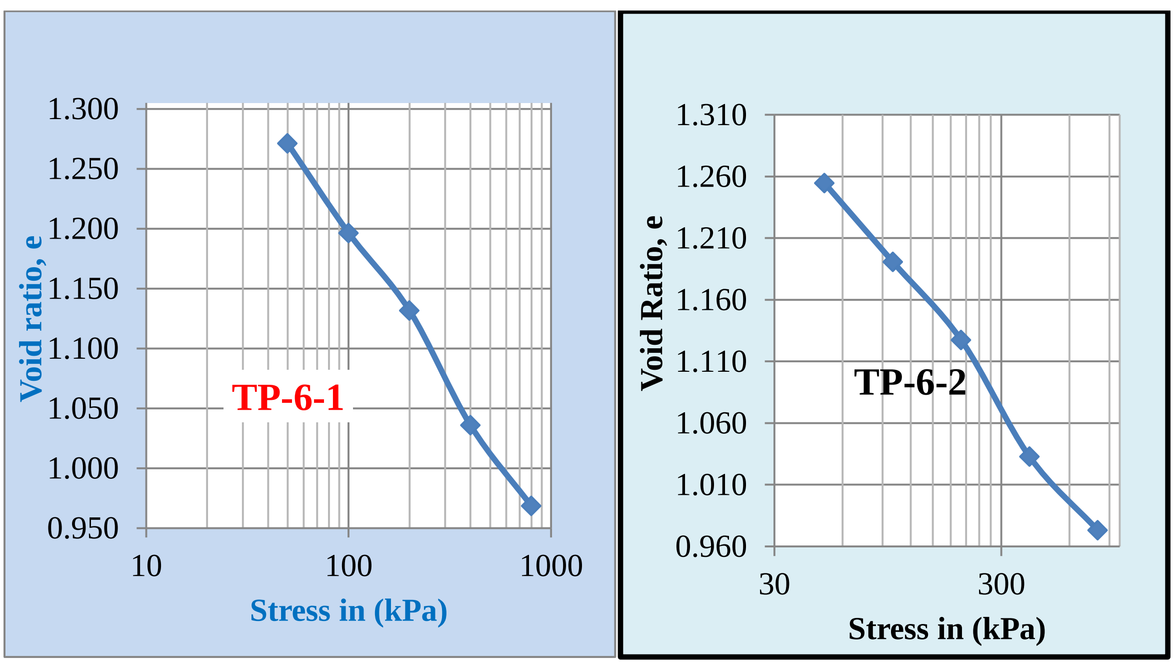

Figure A2-6: e-log p Curve for BA KG Model School, sample TP-6-1 and TP-6-2

Table A2-7: Coefficient of compression (Cc) for JiT/stadium, sample TP-7-1 and TP-7-2

Pressure, σ (kPa)	Final deformation, mm	Final specimen Height, mm	Void ratio (e)	TP-7-1
50	0.092	19.735	1.594	Cc = 0.256
100	0.538	19.352	1.580	
200	0.774	18.939	1.517	
400	1.440	18.182	1.445	
800	2.376	17.288	1.349	
Pressure, σ (kPa)	Final deformation, mm	Final specimen Height, mm	Void ratio (e)	TP-7-2
50	0.102	19.735	1.643	Cc = 0.305
100	0.542	19.352	1.594	
200	0.684	18.939	1.543	
400	1.245	18.182	1.423	
800	2.421	17.288	1.318	

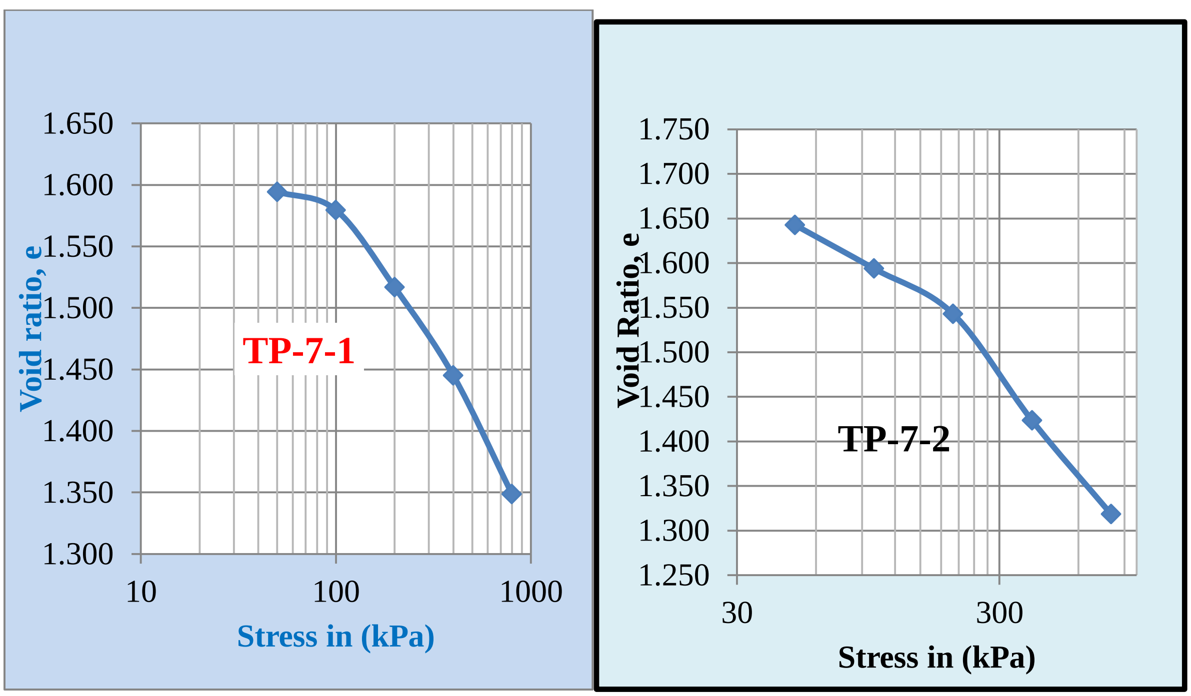

Figure A2-7: e-log p Curve for JiT/stadium, sample TP-7-1 and TP-7-2

Table A2-8: Coefficient of compression (Cc) for JiT/dorm, sample TP-8-1 and TP-8-2

Pressure, σ (kPa)	Final deformation, mm	Final specimen Height, mm	Void ratio (e)	TP-8-1
50	0.018	19.965	1.431	
100	0.044	19.914	1.428	Cc = 0.296
200	0.286	19.612	1.402	
400	0.840	18.965	1.305	
800	1.420	18.265	1.161	
Pressure, σ (kPa)	Final deformation, mm	Final specimen Height, mm	Void ratio (e)	TP-8-2
50	0.055	19.757	1.283	
100	0.445	19.406	1.235	Cc = 0.294
200	0.940	18.988	1.172	
400	1.327	18.588	1.105	
800	1.846	17.939	0.969	

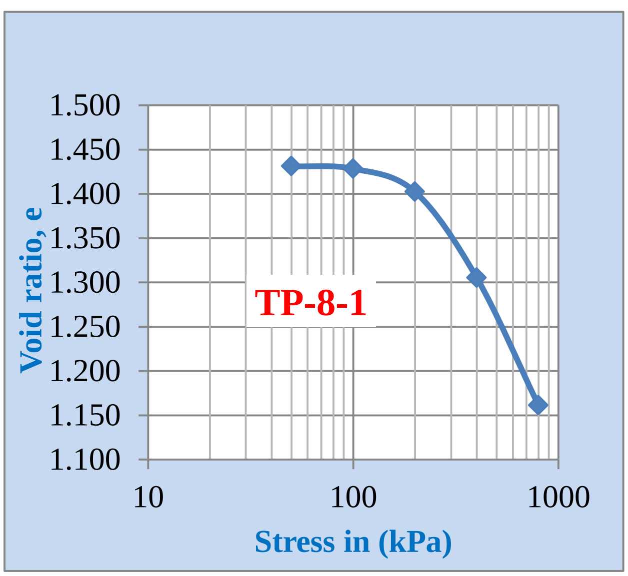

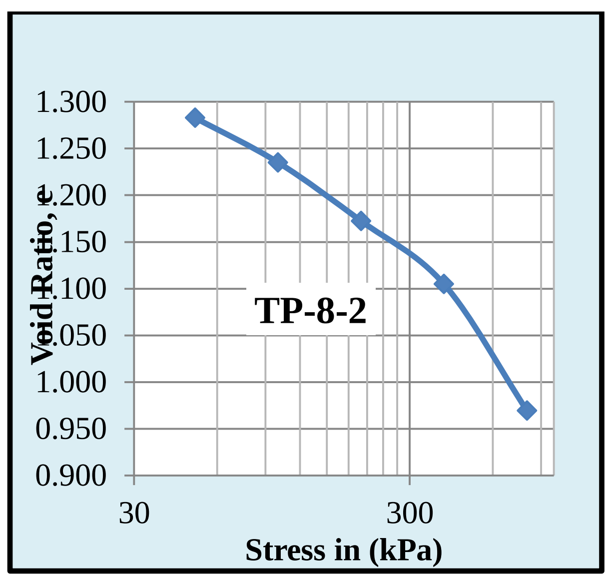

Figure A2-8: e-log p Curve for JiT/dorm, sample TP-8-1 and TP-8-2

Table A2-9: Coefficient of compression (Cc) for Kochi village, sample TP-9-1 and TP-9-2

Pressure, σ (kPa)	Final deformation, mm	Final specimen Height, mm	Void ratio (e)	TP-9-1
50	0.355	19.607	1.304	
100	0.622	19.320	1.244	Cc = 0.260
200	0.945	18.991	1.177	
400	1.292	18.611	1.104	
800	1.836	17.956	1.009	
Pressure, σ (kPa)	Final deformation, mm	Final specimen Height, mm	Void ratio (e)	TP-9-2
50	0.355	19.607	1.236	
100	0.645	19.306	1.193	Cc = 0.290
200	0.940	18.988	1.127	
400	1.327	18.588	1.064	
800	1.846	17.939	0.931	

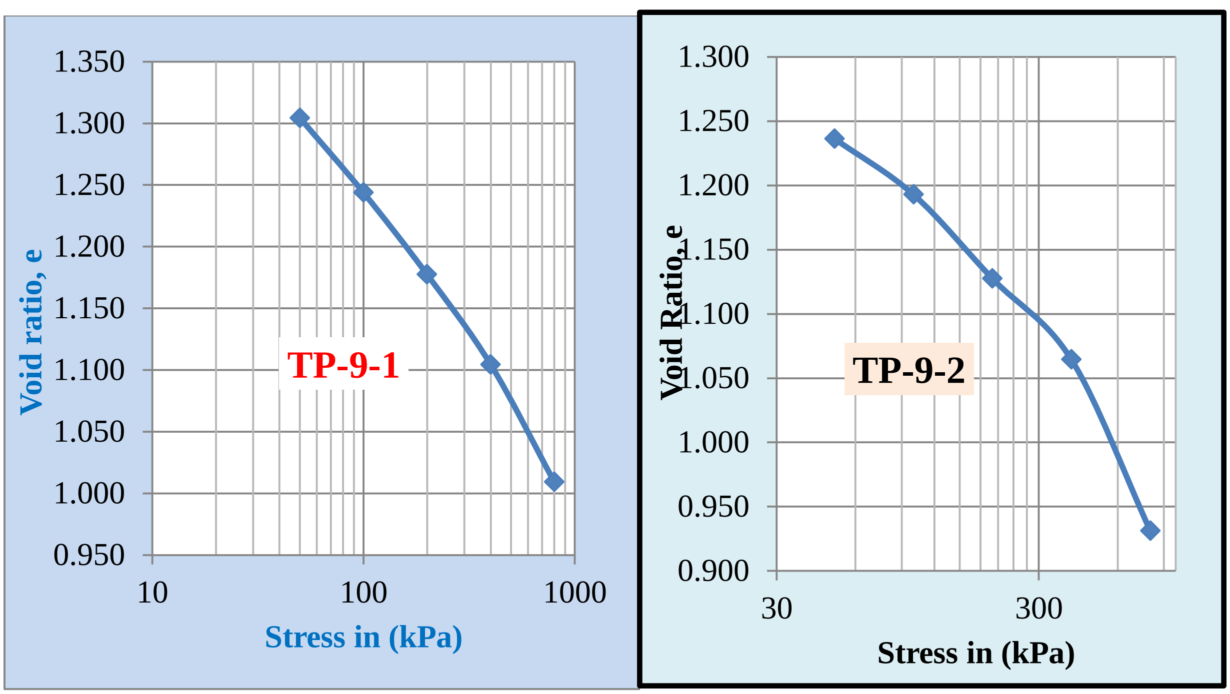

Figure A2-9: e-log p Curve for Kochi village, sample TP-9-1 and TP-9-2

Table A2-10: Coefficient of compression (Cc) for Arround CBE, sample TP-10-1 and TP-10-2

Pressure, σ (kPa)	Final deformation, mm	Final specimen Height, mm	Void ratio (e)	TP-10-1
50	0.310	19.527	1.248	
100	0.696	19.207	1.217	Cc = 0.264
200	0.950	18.950	1.189	
400	1.274	18.363	1.091	
800	1.674	17.763	0.978	
Pressure, σ (kPa)	Final deformation, mm	Final specimen Height, mm	Void ratio (e)	TP-10-2
50	0.310	19.527	1.329	
100	0.696	19.207	1.273	Cc = 0.324
200	0.950	18.950	1.209	
400	1.274	18.363	1.097	
800	1.674	17.763	0.980	

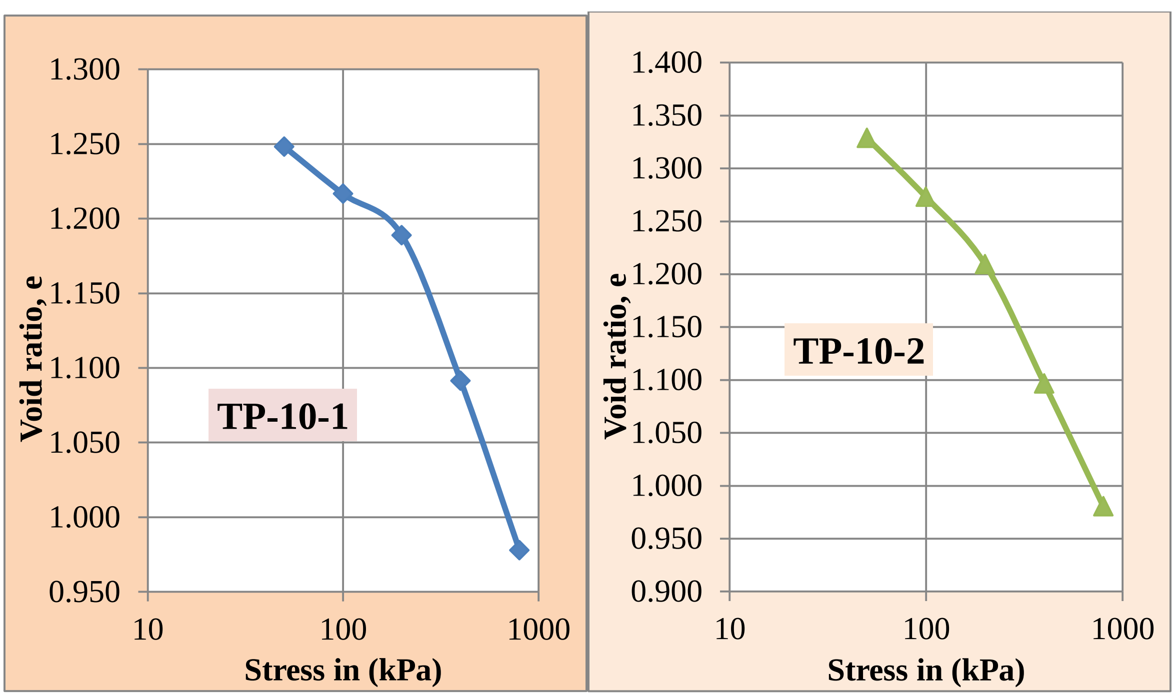

Figure A2-10: e-log p Curve for Arround CBE, sample TP-10-1 and TP-10-2

Table A2-11: Coefficient of compression (Cc) for Sato Samaro, sample TP-11-1 and TP-12-2

Pressure, σ (kPa)	Final deformation, mm	Final specimen Height, mm	Void ratio (e)	TP-11-1
50	0.262	19.710	1.125	
100	0.410	19.519	1.100	Cc = 0.267
200	0.828	19.071	1.038	
400	1.434	18.387	0.957	
800	2.220	17.530	0.859	
Pressure, σ (kPa)	Final deformation, mm	Final specimen Height, mm	Void ratio (e)	TP-11-2
50	0.264	19.736	1.123	
100	0.416	19.581	1.103	Cc = 0.272
200	0.830	19.174	1.050	
400	1.392	18.606	0.997	
800	2.240	17.480	0.858	

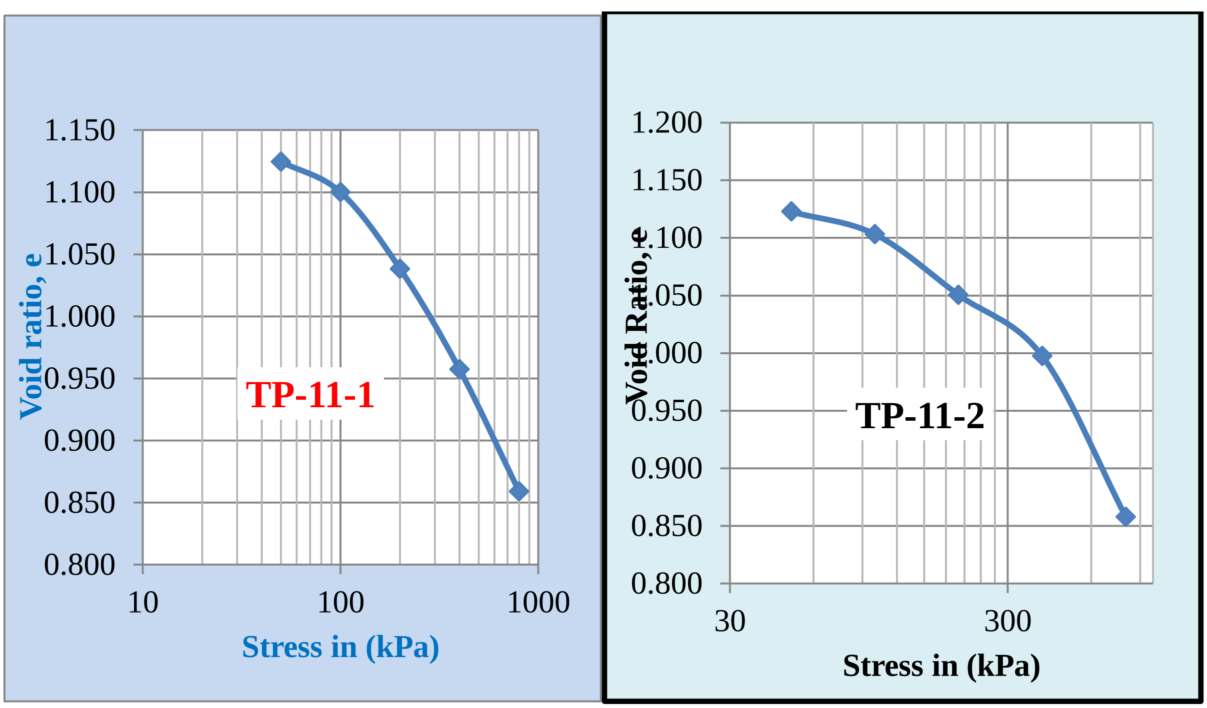

Figure A2-11: e-log p Curve for Sato Samaro, sample TP-11-1 and TP-11-2

Table A2-12: Coefficient of compression (Cc) for Ginjo Guduru, sample TP-12-1 and TP-12-2

Pressure, σ (kPa)	Final deformation, mm	Final specimen Height, mm	Void ratio (e)	TP-12-1
50	0.018	19.97	1.263	Cc = 0.321
100	0.052	19.91	1.251	
200	0.286	19.61	1.201	
400	0.818	18.97	1.072	
800	1.492	18.22	0.962	
Pressure, σ (kPa)	Final deformation, mm	Final specimen Height, mm	Void ratio (e)	TP-12-2
50	0.102	19.683	1.304	Cc = 0.330
100	0.600	19.366	1.238	
200	0.678	19.285	1.162	
400	0.804	19.044	1.068	
800	1.126	18.427	0.940	

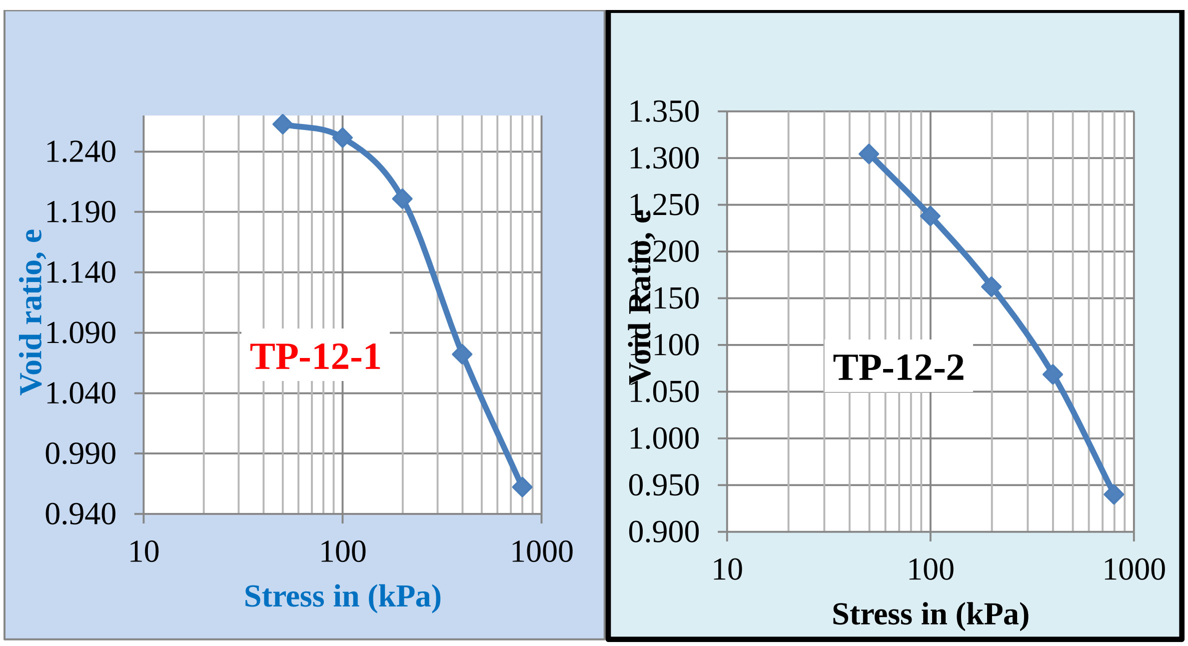

Figure A2-12: e-log p Curve for Ginjo Guduru, sample TP-12-1 and TP-12-2

B. Natural moisture contents sample calculation

Table B1 Moisture Contents test results for TP-1 at D = 1.5m and D = 2.5m

TP-1	TP-1 @1.5m			TP-1 @2.5m		
Trial	1	2	3	1	2	3
MC	29.6	17.6	18	37.6	17.7	49.6
MCWS	164.1	84	108.5	161	91.7	161.5
MCDS	122.4	64	81	120.9	68.7	124.7
MW	41.7	20	27.5	40.1	23	36.8
MDS	92.8	46.4	63	83.3	51	75.1
NMC, w (%)	44.94	43.10	43.65	48.14	45.10	49.00
Av. w (%)	43.90			47.41		

Table B2 Moisture Contents test results for TP-2 at D = 2.5m and D = 3m

TP-2	TP-2 @2.5m			TP-2 @ 3m		
Trial	1	2	3	1	2	3
MC	17.8	17.3	17.5	35.6	25.2	37.2
MCWS	160.4	150.4	143.1	146.9	153.1	153
MCDS	107.2	102.6	98.3	113.1	113.7	116.8
MW	53.2	47.8	44.8	33.8	39.4	36.2
MDS	89.4	85.3	80.8	77.5	88.5	79.6
NMC, w (%)	59.51	56.04	55.45	43.61	44.52	45.48
Av. w (%)	57.00			44.54		

Table B3 Moisture Contents test results for TP-3 at D = 1.5m and D = 2.5m

TP-3	TP-3 @1.5m			TP-3@2.5m		
Trial	1	2	3	1	2	3
MC	26.6	17.4	10.3	25.24	17.99	18.48
MCWS	76.8	77.9	82	106.19	83.29	91.98
MCDS	62.2	59.7	58.8	80.07	62.28	68.34
MW	14.6	18.2	23.2	26.12	21.01	23.64
MDS	35.6	42.3	48.5	54.83	44.29	49.86
NMC, w (%)	41.01	43.03	47.84	47.64	47.44	47.41
Av. w (%)	43.96			47.50		

Table B4 Moisture Contents test results for TP-4 at D = 1.5m and D = 2.5m

TP-4	TP-4 @1.5m			TP-4@2.5m		
Trial	1	2	3	1	2	3
MC	17.3	17.4	17.3	25.24	17.99	18.48
MCWS	112.6	112.3	112.6	106.19	83.29	91.98
MCDS	81.8	81.9	82	80.07	62.28	68.34
MW	30.8	30.4	30.6	26.12	21.01	23.64
MDS	64.5	64.5	64.7	54.8 3	44.29	49.86
NMC, w (%)	47.75	47.13	47.30	47.64	47.44	47.41
Av. w (%)	47.39			47.50		

C. Specific gravity calculation sample

Table C-1 Specific Gravity Test Result for TP1 at D = 1.5m and D = 2.5m

TP-1	TP 1@1.5m			TP 1@2.5m		
Pycno. No.	#3	#7	#8	#9	#1	B
K (@Tx˚C)	0.9996	0.9996	0.9996	0.9996	0.9996	0.9996
Ws	25.01	25.01	25.01	25.01	25.01	25.01
Ti ˚C	21	21	21	21	21	21
Tx˚C	25	25	25	25	25	25
DTx	0.997	0.997	0.997	0.997	0.997	0.997
DTi	0.998	0.998	0.998	0.998	0.998	0.998
DTx/DTi	0.999	0.999	0.999	0.999	0.999	0.999
Wp	26.84	26.84	26.32	26.93	22.45	26.56
Wpws	136.46	137.14	137.67	136.14	133.83	136.72
Wpw (@Ti˚C)	120.63	121.2	122	120.5	118.13	120.91
Wpw(@Tx˚C)	120.63	121.32	121.9	120.4	118.05	120.96
Gs	2.72	2.72	2.71	2.7	2.69	2.7
Av. Gs	**2.72**			**2.7**		

Table C-2 Specific Gravity Test Result for TP-2 at D = 2.5m and D = 3m

TP-2	TP-2@2.5m			TP -2 @ 3m		
Pycno. No.	#9	#B	#1	#7	#8	#11
K (@Tx˚C)	0.9996	0.9996	0.9996	0.9996	0.9996	0.9996
Ws	25.3	25.3	25.1	25.2	25.4	25.2
Ti ˚C	20	20	20	20	20	20
Tx˚C	22	22	22	22	22	22
DTx	0.998	0.998	0.998	0.998	0.998	0.998
DTi	0.9982343	0.99823	0.99823	0.99823	0.99823	0.99823
DTx/DTi	0.99977	0.99977	0.99957	0.99977	0.99977	0.99957
Wp	26.93	26.23	22.44	26.93	26.23	22.44
Wpws	136.8	137.4	133.3	136.8	137.7	133.6
Wpw(@Ti˚C)	121.6	122.6	118.1	121.6	122.8	118.1
Wpw(@Tx˚C)	121.15	121.75	117.76	121.28	122.08	118.1
Gs	2.62	2.62	2.62	2.60	2.60	2.60
Av. Gs	**2.62**			**2.60**		

D. Atterberg limit test results sample calculation

Table D-1 Liquid Limit and Plastic Limit Test Results for TP-1 at D =1.5 m and D = 2.5 m

TP-1	TP-1 @ 1.5m					TP-1 @ 2.5m				
	Liquid Limit			Plastic limit		Liquid Limit			Plastic limit	
Determination No.	1	2	3	1	2	1	2	3	1	2
Number of blows	35	23	16			26	21	18		
Mass of can + Moist Soil, g	30.27	19.92	17.3	12.5	10.3	33	32.4	14.6	25.18	36.82
Mass of can + dry soil, g	24.2	14	12.2	10.80	9.2	27.2	26.6	10.5	23.1	34.8
Mass of can, g	16.2	6.7	6.2	6.20	6.2	19.5	19.7	5.9	17.50	29.4
Mass of water	6.27	5.92	5.1	1.72	1.1	6.1	5.9	4.1	2.1	2
Mass of dry soil, g	8	7.3	6	4.6	3	7.4	6.8	4.6	5.6	5.4
Moisture content, w (%)	78.38	81.1	85	36.6	36.7	75.32.	84.06	89.13	37.14	37.41
LL	81.3			36.6		77.4			37.3	
PI	44.7					40.0				

Figure D-1 Water Content Vs No of Blows for TP-1 at D = 1.5 m and D = 2.5 m

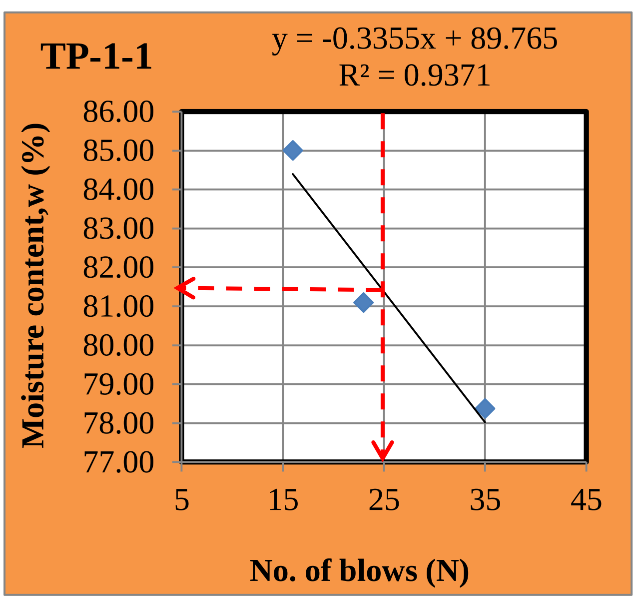

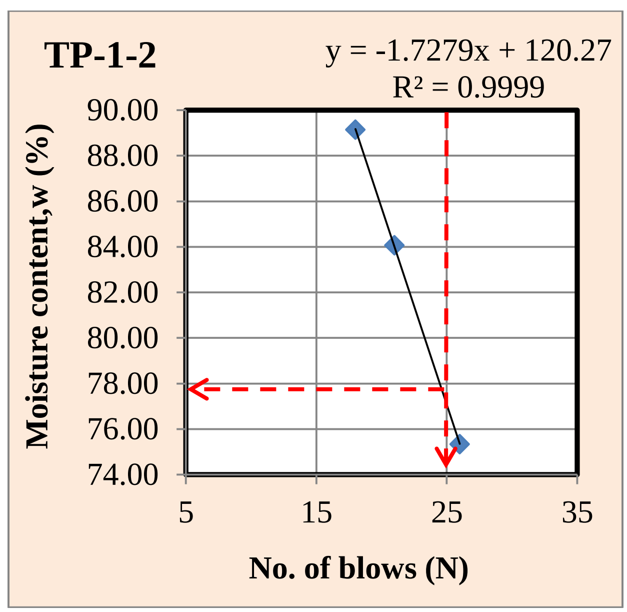

Table D-2 Liquid limit and plastic limit test results for TP-2 at D = 2.5m and D= 3m

TP-2	TP-2 @ 2.5m					TP-2@ 3 m				
	Liquid Limit			Plastic limit		Liquid Limit			Plastic limit	
Determination No.	1	2	3	1	2	1	2	3	1	2
Number of blows	33	23	17			31	21	18		
Mass of can + Moist Soil, g	38.6	39.65	34.7	12.67	12.45	39.6	40.8	35.5	15.00	13.14
Mass of can + dry soil, g	31.2	31.5	28	11.20	10.96	31.81	32.13	28.3	13.24	11.64
Mass of can, g	17.32	17.89	18.04	6.16	5.59	17.32	17.9	18.04	6.16	5.59
Mass of water	7.4	8.15	6.7	1.47	1.49	7.79	8.67	7.2	1.76	1.5
Mass of dry soil, g	13.88	13.61	9.96	5.041	5.37	14.49	14.23	10.26	7.081	6.05
Moisture content, w (%)	53.31	59.88	67.27	29.16	27.75	53.76	60.93	70.18	24.86	24.79
LL	59.6			28.5		59.8			24.8	
PI	31.1					35				

Figure D-2 Water Content Vs No of Blows for TP-2 at D = 2.5 m and D = 3 m

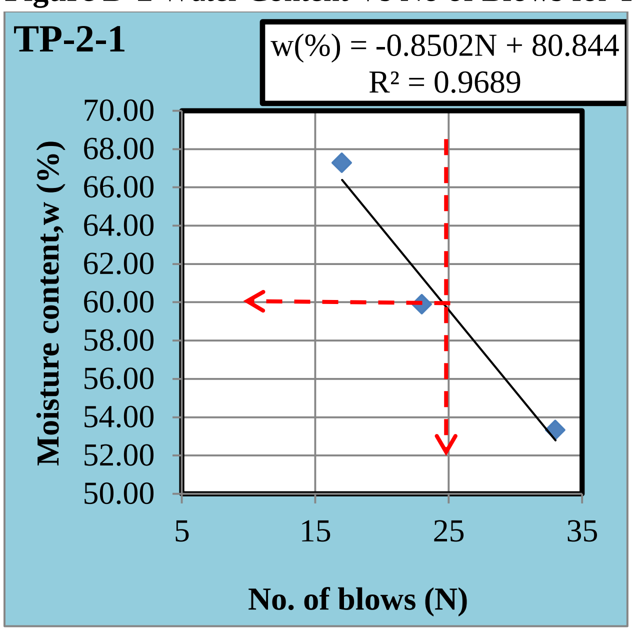

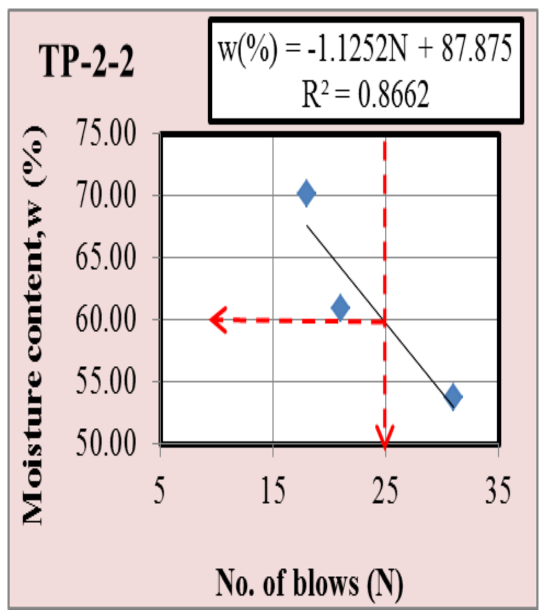

Figure D-3 Liquid limit test results with water content vs no. of blows for TP-3

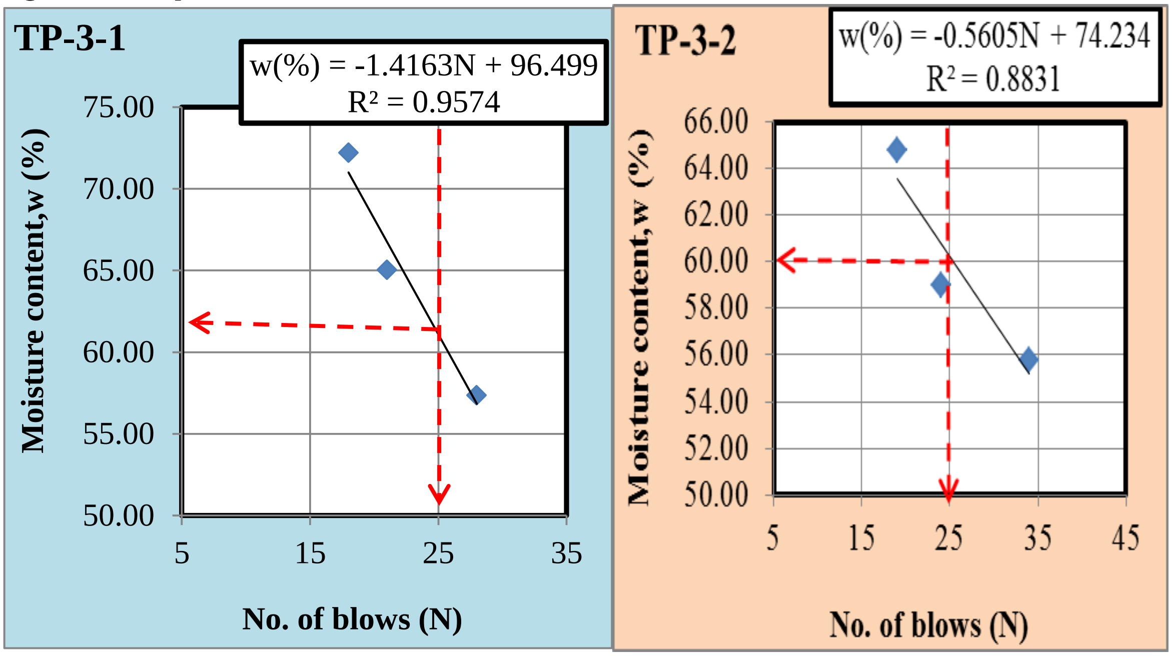

Figure D-4 Liquid limit test results with water content vs no. of blows for TP-4

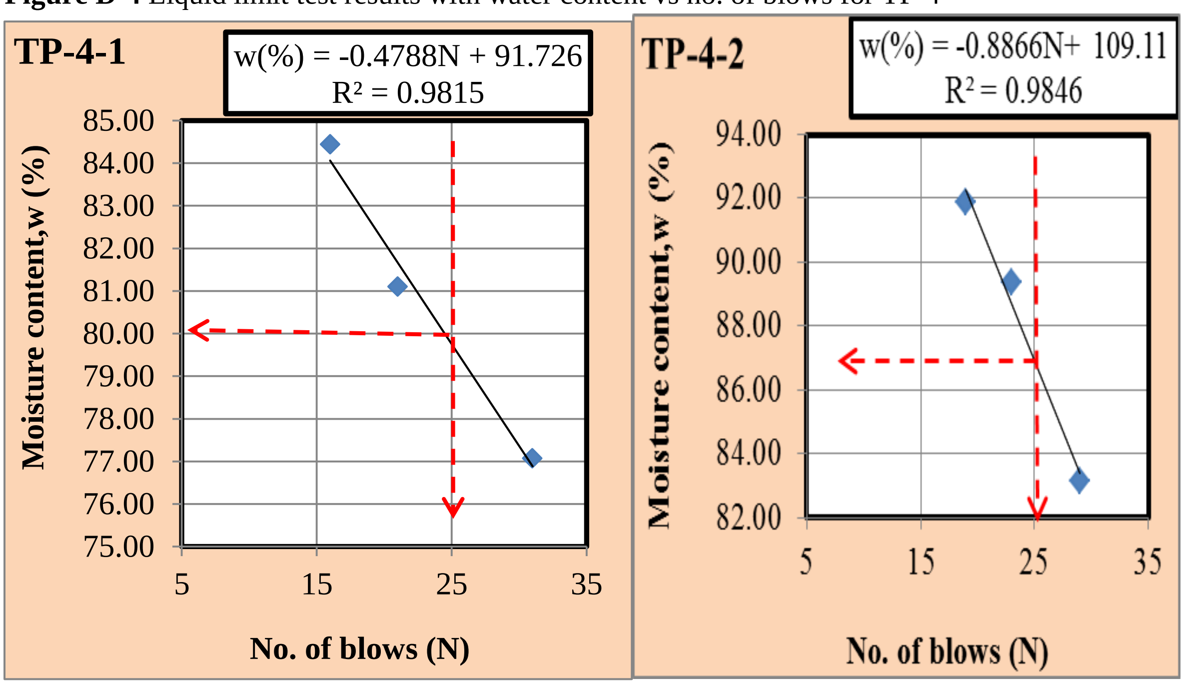

Figure D-5 Liquid limit test results with water content vs no. of blows for TP-5

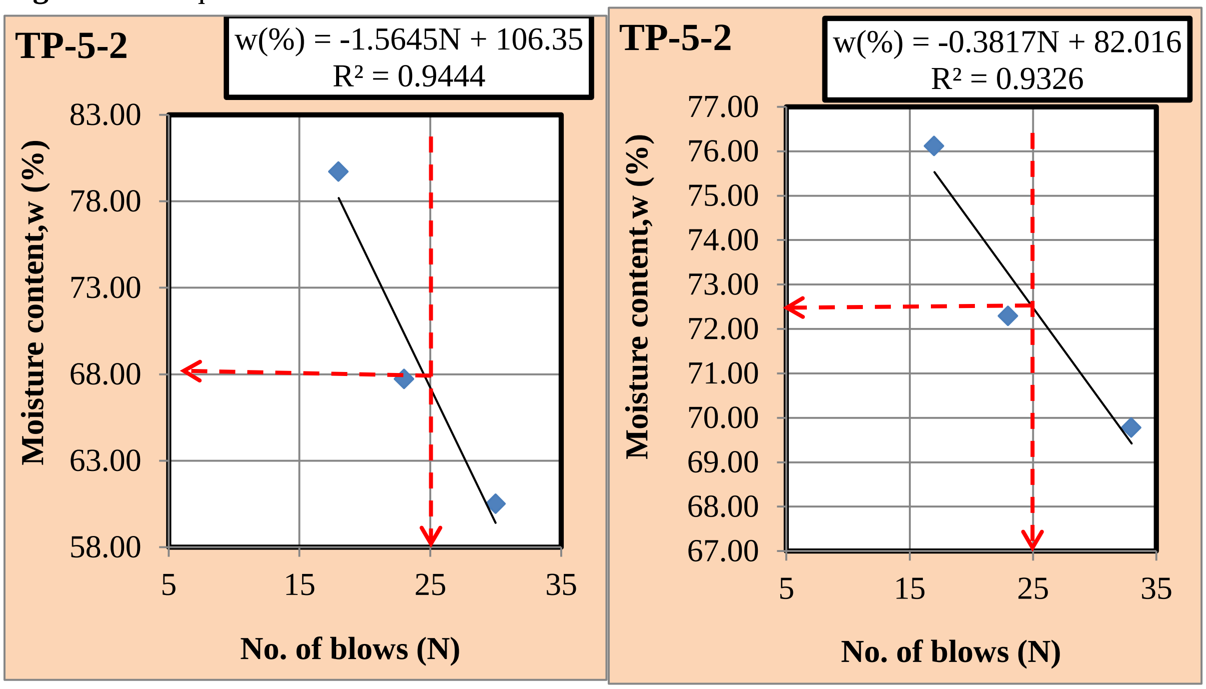

Figure D-6 Liquid limit test results with water content vs no. of blows for TP-6

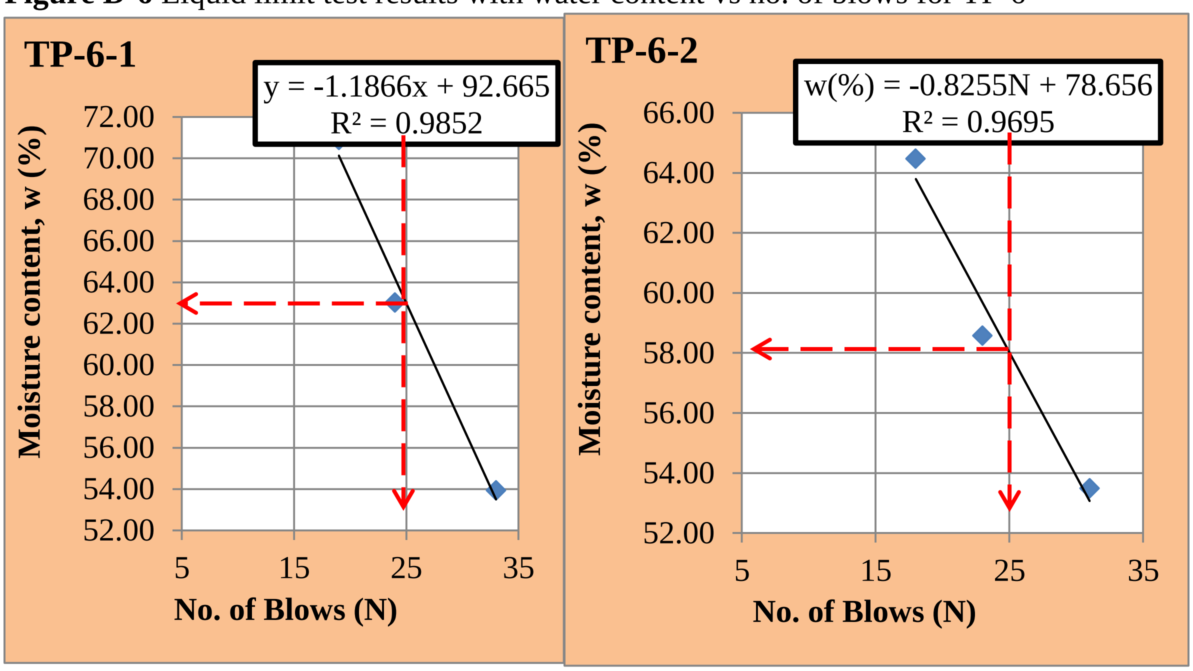

Figure D-7 Liquid limit test results with water content vs no. of blows for TP-7

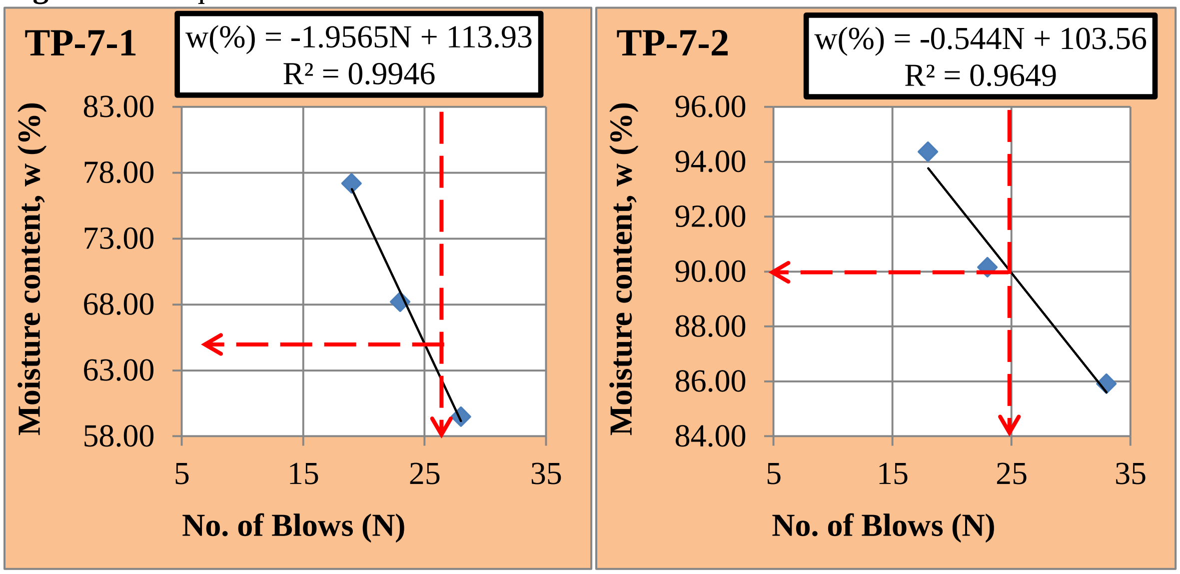

Figure D-8 Liquid limit test results with water content vs no. of blows for TP-8

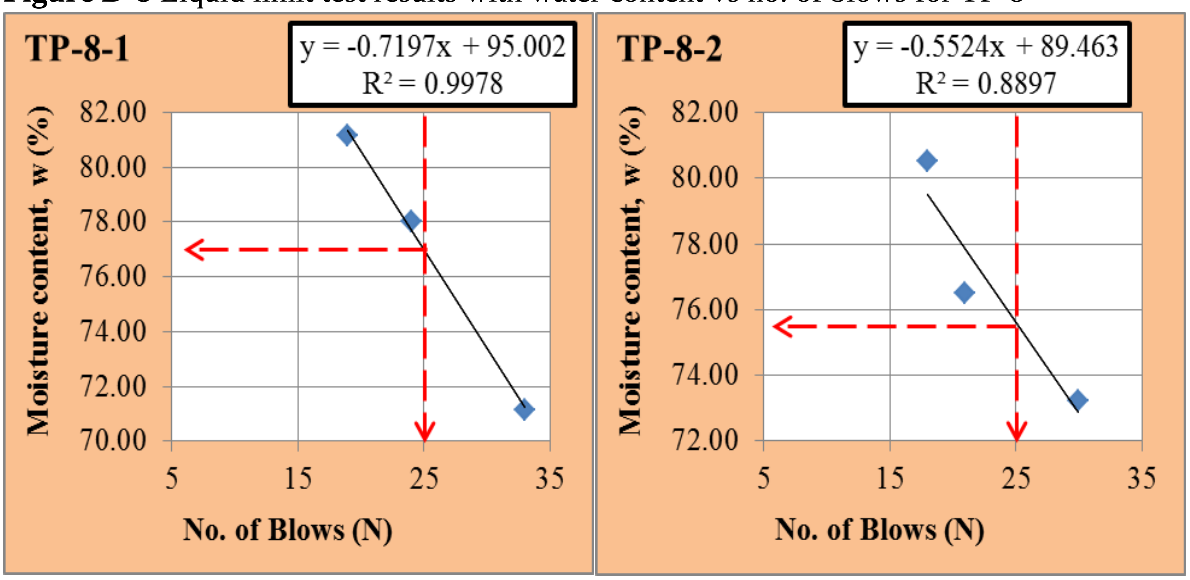

Figure D-9 Liquid limit test results with water content vs no. of blows for TP-9

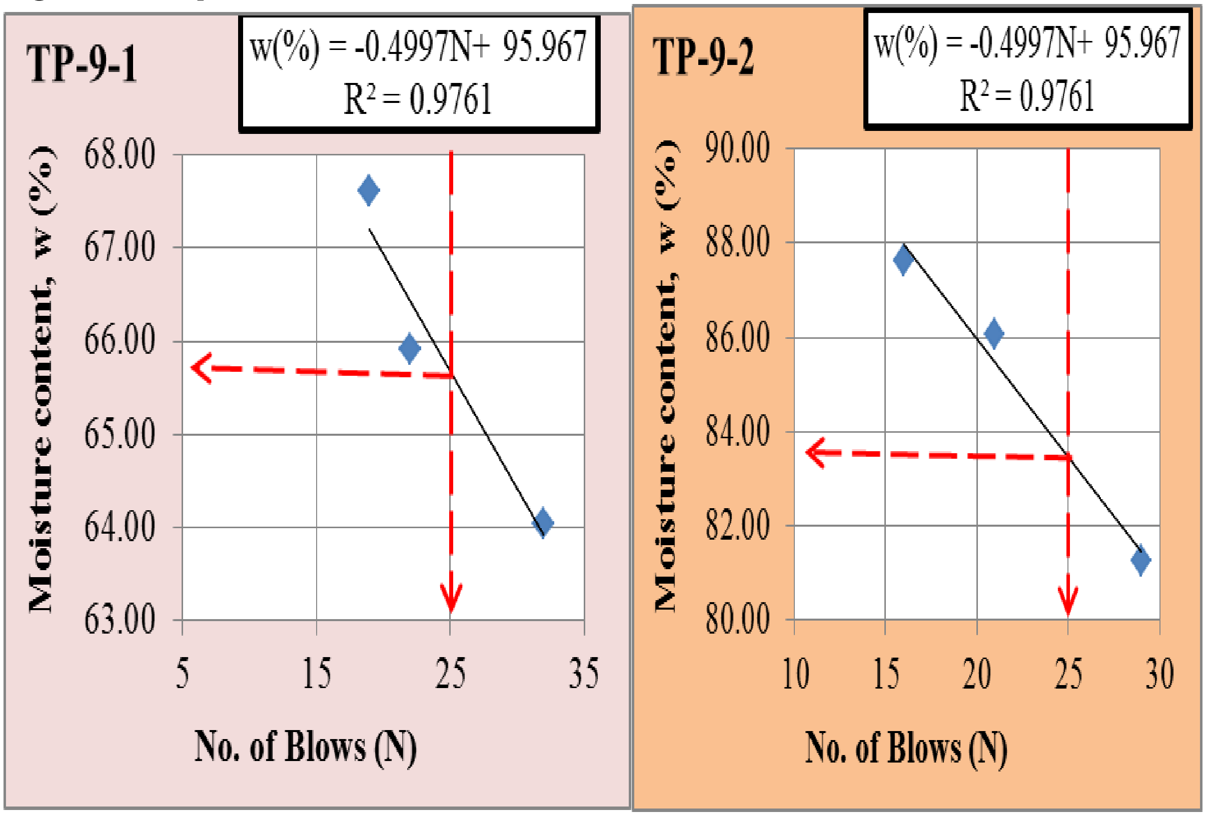

Figure D-10 Liquid limit test results with water content vs no. of blows for TP-10

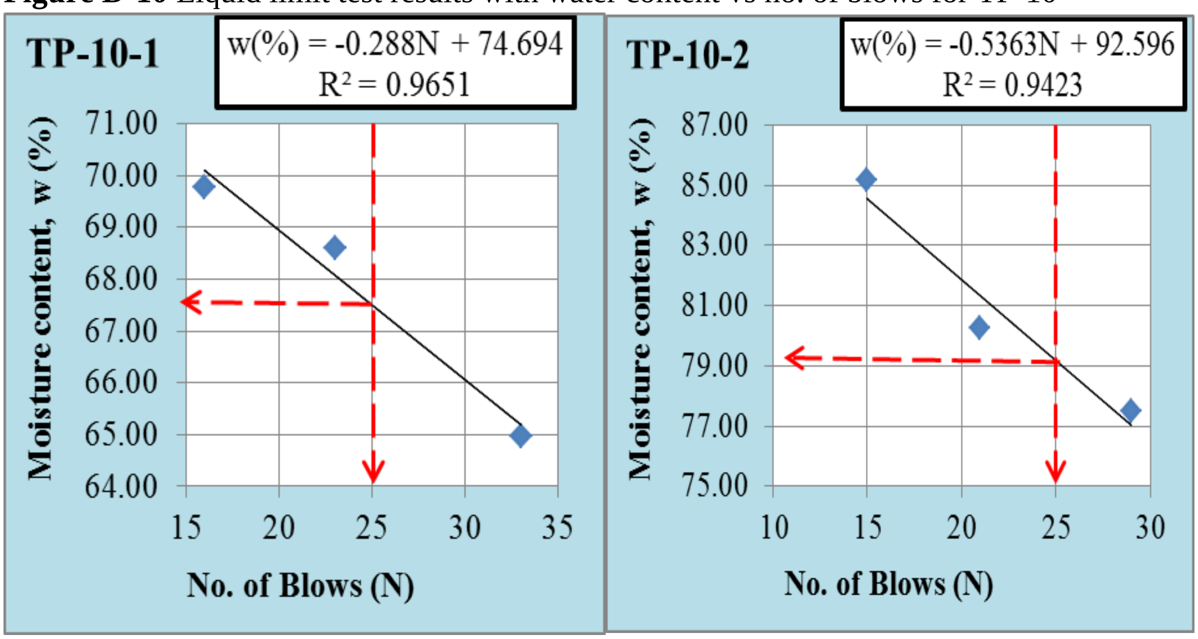

Figure D-11 Liquid limit test results with water content vs no. of blows for TP-11

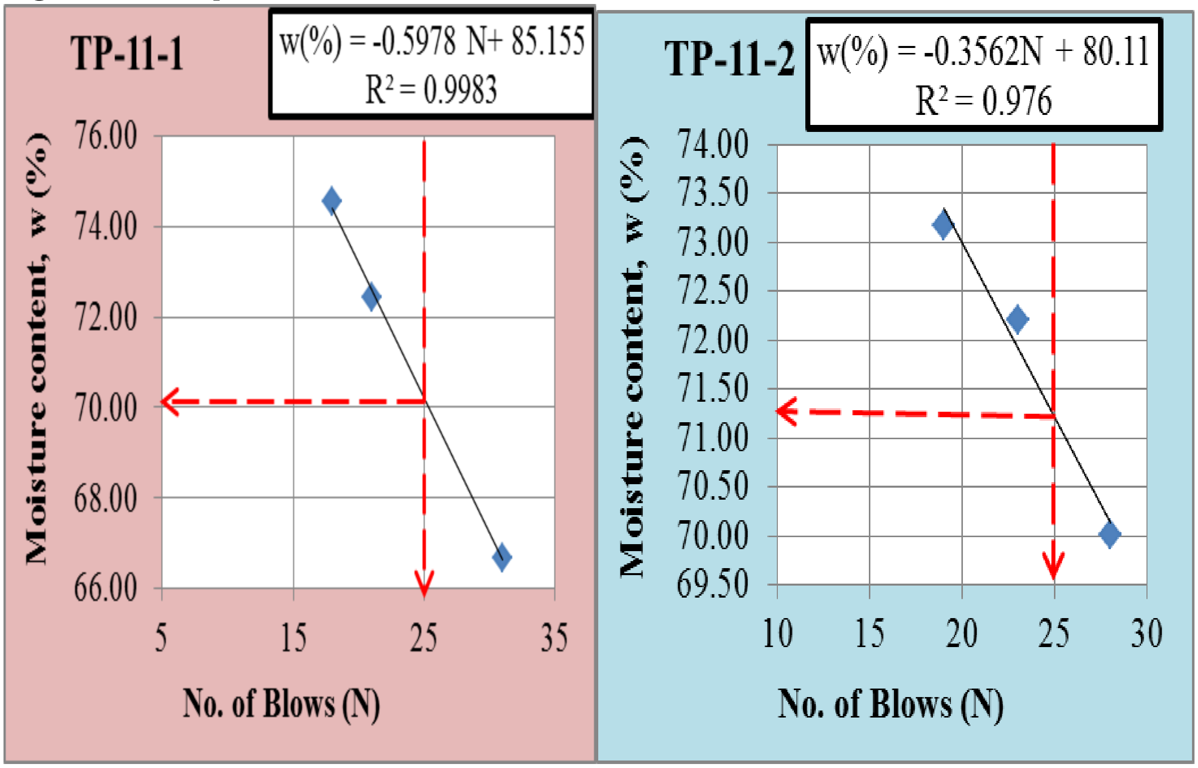

Figure D-12 Liquid limit test results with water content vs no. of blows for TP-12

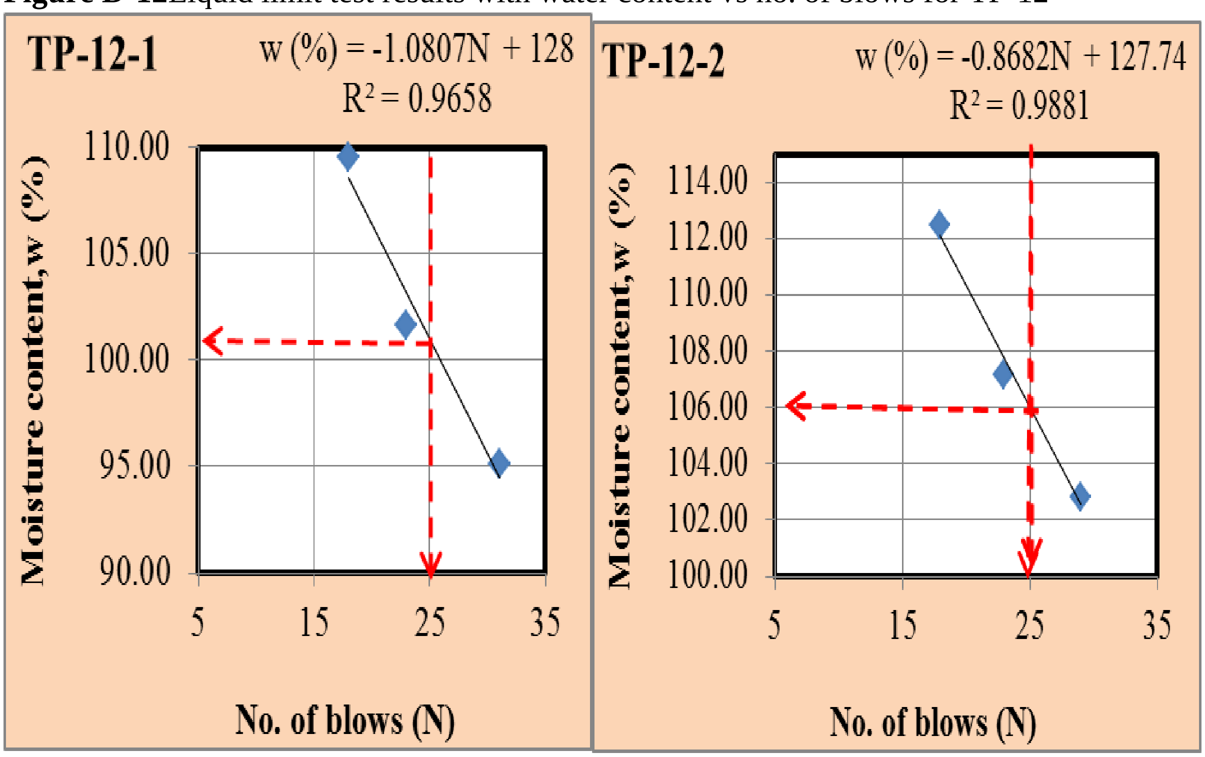

E. Grain Size Analysis Test Results with sample calculation

Table E: Grain size analysis test results

Test Pits code	Depth (m)	Percentage amount of particle size (%)		
		Gravel	sand	% of finer than 0.075 mm
TP-1	1.5	0.00	0.87	99.13
	2.5	0.00	0.85	99.15
TP-2	2.5	0.41	2.96	96.63
	3	0.13	2.14	97.73
TP-3	1.5	0.02	2.03	97.95
	2.5	0.17	6.15	93.68
TP-4	1.5	0.00	0.67	99.33
	2.5	0.00	0.91	99.09
TP-5	1.5	0.15	12.89	86.96
	2.5	0.13	10.36	89.51
TP-6	1.5	0.00	0.77	89.23
	2.5	0.00	1.05	98.95
TP-7	1.5	0.00	1.5	98.5
	2.5	0.06	1.30	98.64
TP-8	1.5	0.02	2.03	97.95
	2.5	0.06	1.32	98.62
TP-9	1.5	0.25	7.18	92.57
	3	0.15	7.61	92.24
TP-10	1.5	0.12	2.95	96.93
	3	0.25	5.73	94.02

Table E-1 Sieve analysis TP-1-1 at D = 1.5m

Sieve Opening, (mm)	Mass of Retained, g	Percentage of Retained soil (%)	Percentage Cum. Retained (%)	Percent Passing (%)
9.5	0	0	0	100
4.75	0	0	0	100
2	0.3	0.03	0.03	99.97
0.85	0.2	0.02	0.05	99.95
0.425	0.6	0.06	0.11	99.89
0.3	0.8	0.08	0.19	99.81
0.15	4.5	0.45	0.64	99.36
0.075	2.3	0.23	0.87	99.13
Pass	991	99.13	100	0

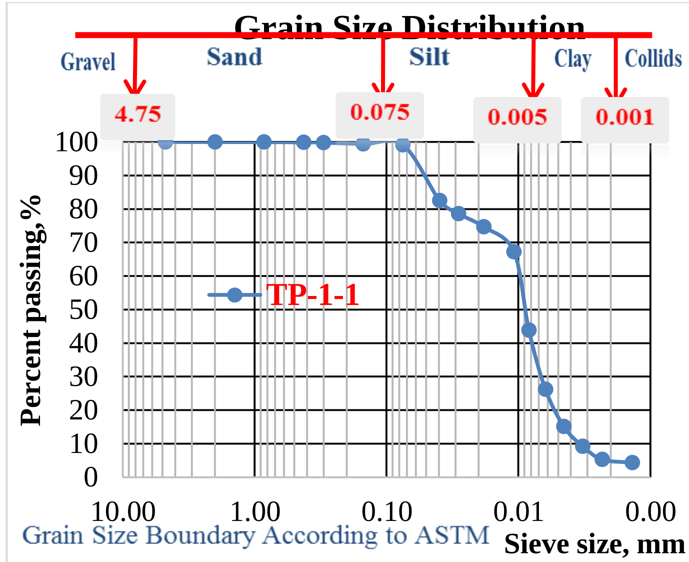

Table E-2 Hydrometer analysis Specific Gravity 2.72

TP-1-1		Correction for Hydrometer Reading								
Time (min.)	Actual Hydrometer Reading	Temperature	T° correction	Corrected H. Reading, (Rc)	Correction factor (a)	Eff. Depth of Hydrometer	Values of K	Diameter of soil Particle (mm)	% finer, P	Adjusted % of finer
1	45	21	0.2	42.2	0.986	9.0	0.0132	0.0396	83.22	82.49
2	43	21	0.2	40.2	0.986	9.3	0.0132	0.0285	79.27	78.58
5	41	21	0.2	38.2	0.986	9.6	0.0132	0.0183	75.33	74.68
15	37	22	0.4	34.4	0.986	10.3	0.01305	0.0108	67.84	67.25
30	25	22	0.4	22.4	0.986	12.2	0.01305	0.0083	44.17	43.79
60	16	22	0.4	13.4	0.986	13.7	0.01305	0.0062	26.42	26.19
120	10	23	0.7	7.7	0.986	14.7	0.0129	0.0045	15.18	15.05
240	7	23	0.7	4.7	0.986	15.2	0.0129	0.0032	9.27	9.19
480	5	23	0.7	2.7	0.986	15.5	0.0129	0.0023	5.32	5.28
1440	5	21	0.2	2.2	0.986	15.5	0.0132	0.0014	4.34	4.30

Figure E-1 Grain size distribution graph for TP-1-2 at D =2.5 and TP-3 at D =2.5 and 3 m

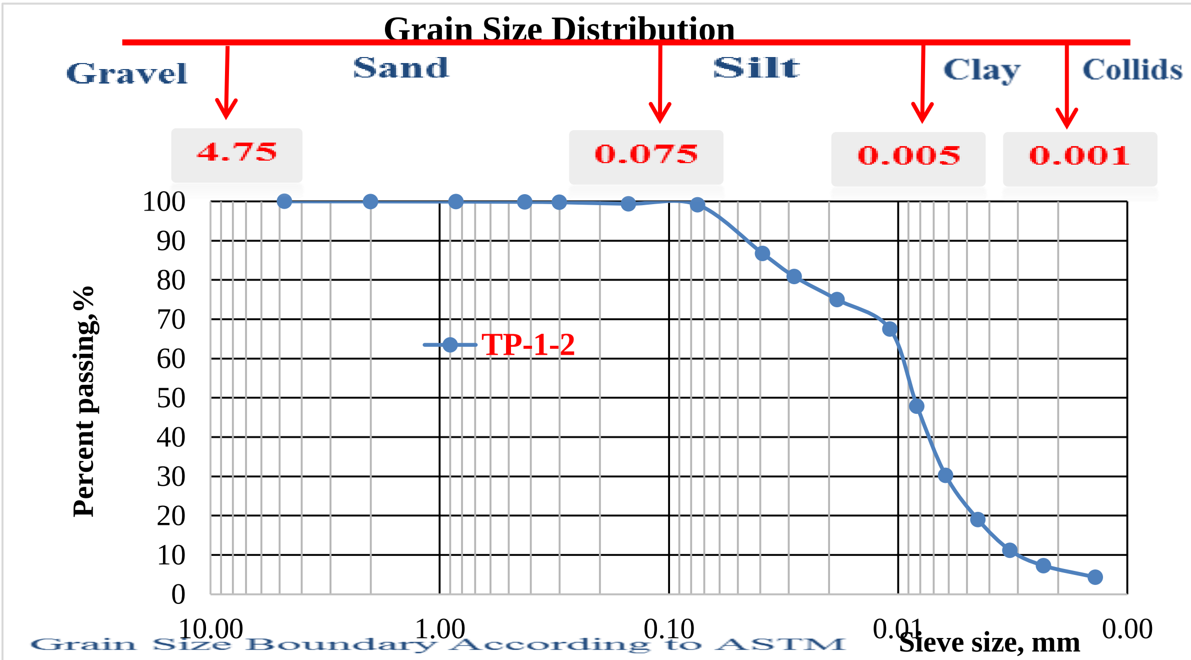

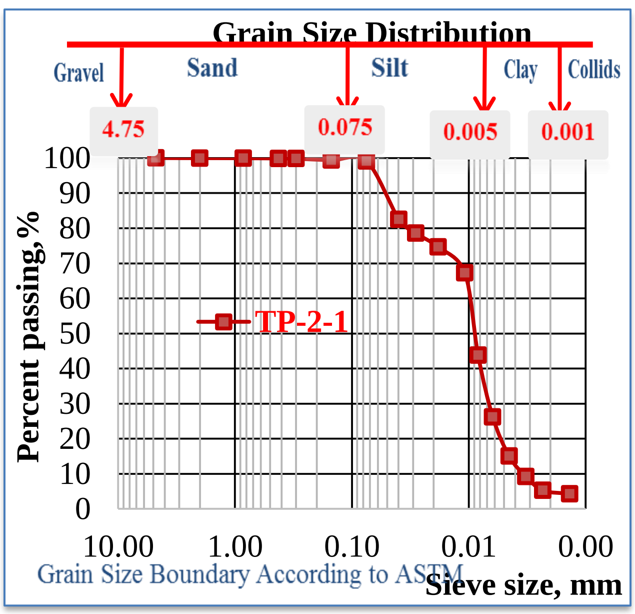

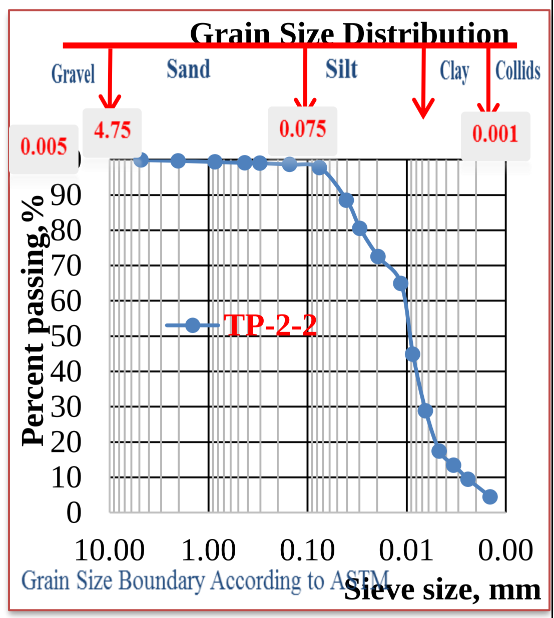

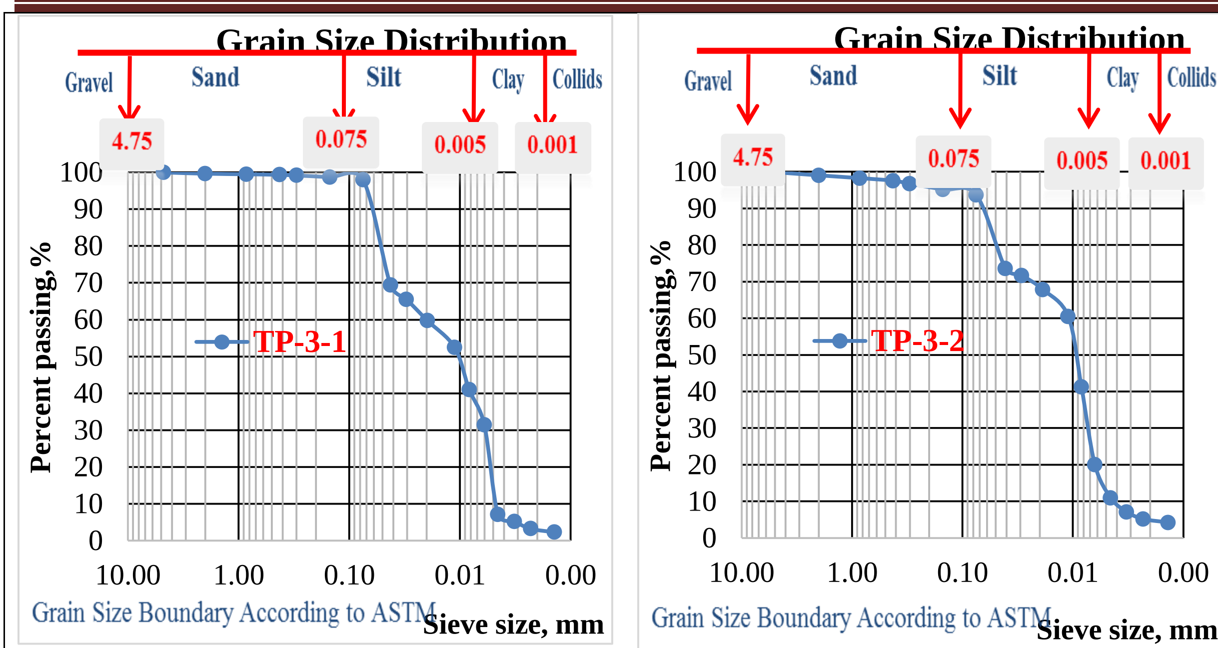

Figure E-2**:** Grain size distribution graph for TP-3 at D =1.5 and 2.5 m

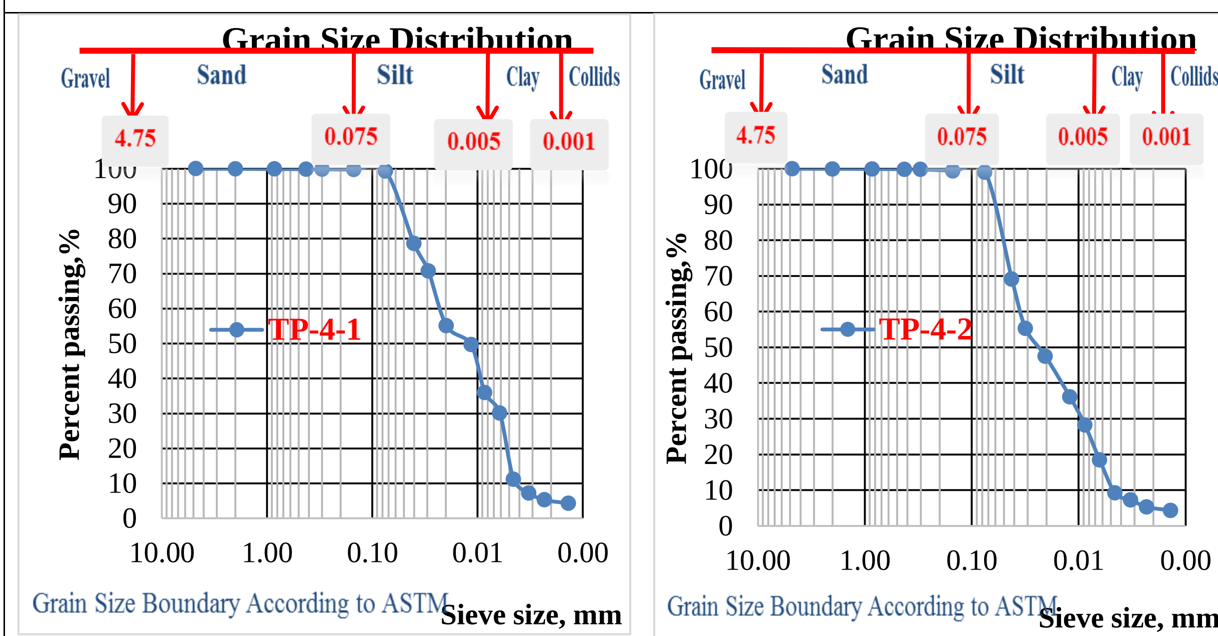

Figure E-3: Grain size distribution graph for TP-4 at D =1.5 and 2.5 m

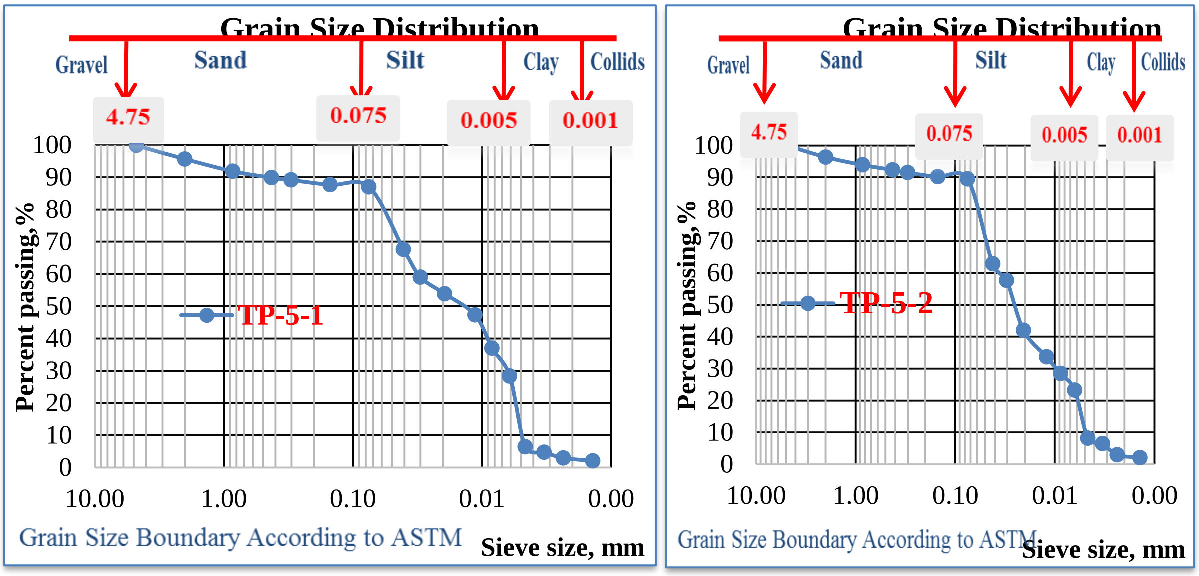

Figure E-4 Grain size distribution graph for TP-5at D =1.5 and 2.5

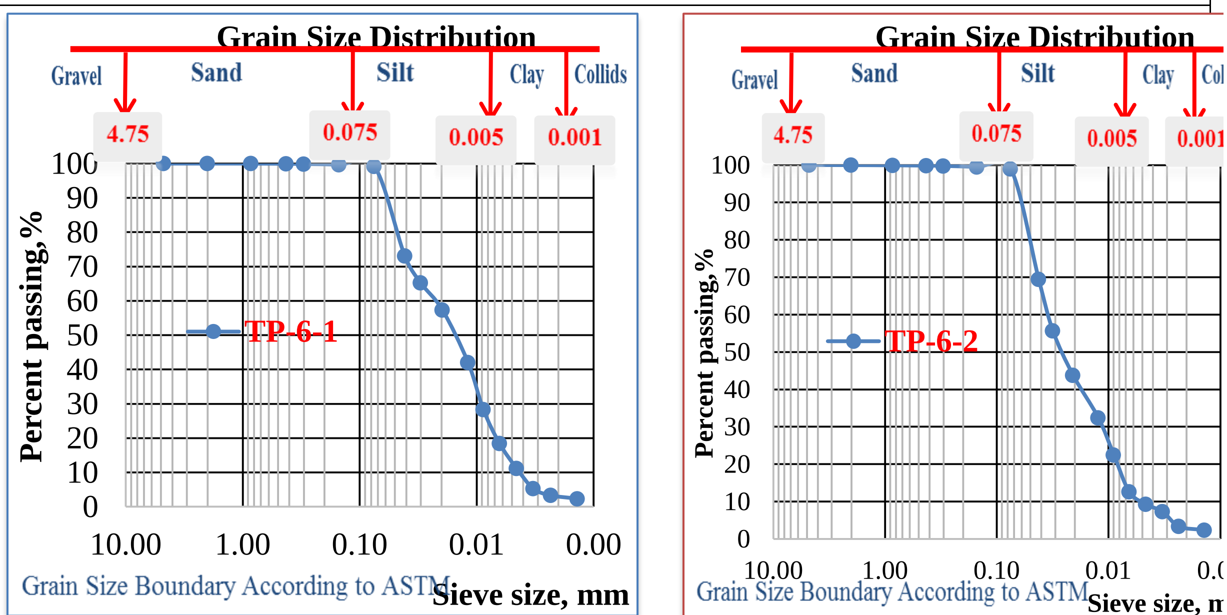

Figure **E-5:** Grain size distribution graph for TP-6 at D =1.5 and 2.5 m

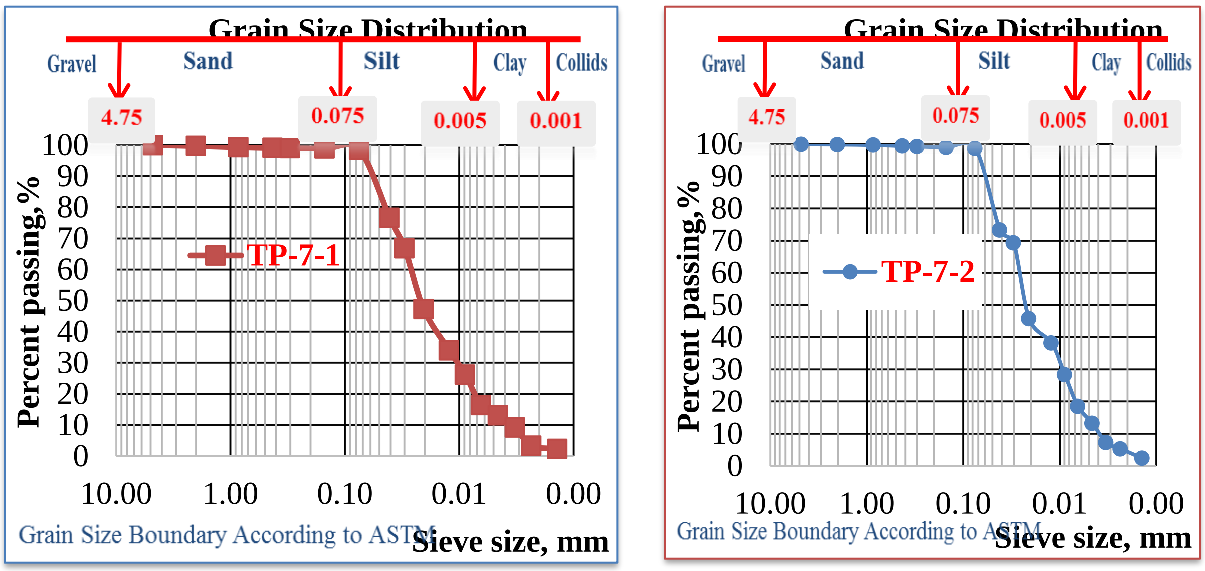

Figure **E-6:** Grain size distribution graph for TP-7 at D =1.5 and 2.5 m

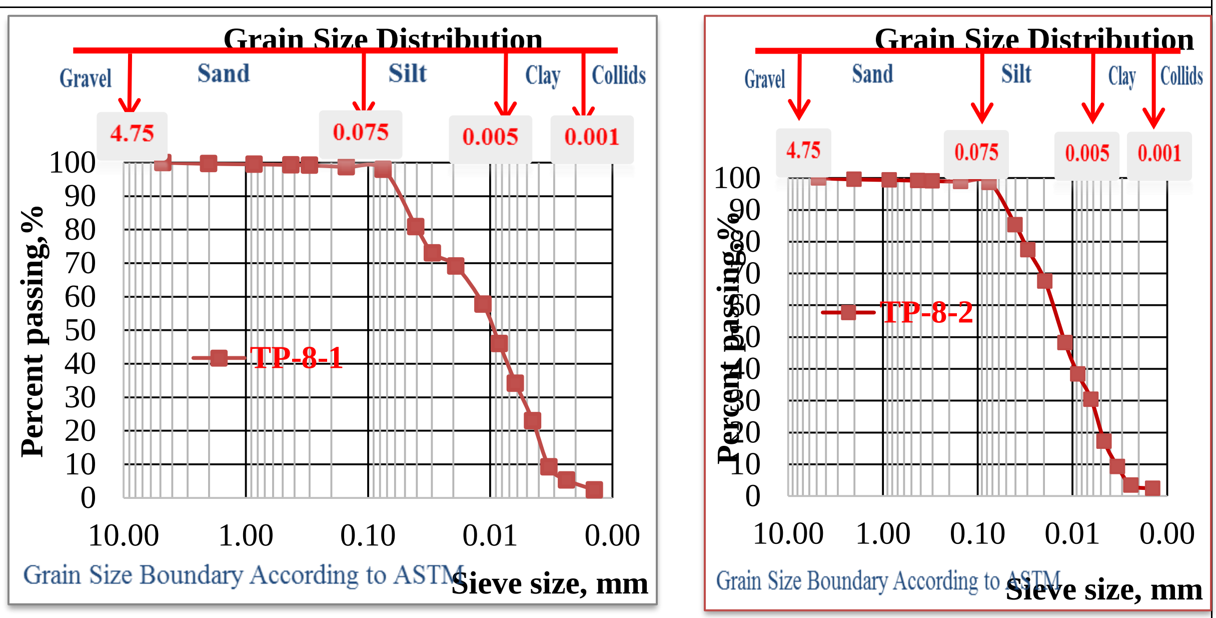

Figure E-7: Grain size distribution graph for TP-8 at D =1.5 and 2.5 m

APPENDIX -2

F. PHOTOS

Figure 1: An over view of test pits while soil sample extracted. (Photo captured by Bilisumma L.)

Figure 2: Disturbed sample preparation procedure

Figure 0: Undisturbed sample preparation (a) The sample has placed inside the metal ring and (b) calibrates specimen height

Figure 4: Determination of specific gravity by using pycnometer method (a) adding the soil sample with water into bottle density (b) insert the density bottle into discallator by connecting vacuum pump (photo captured by Deribu M.)

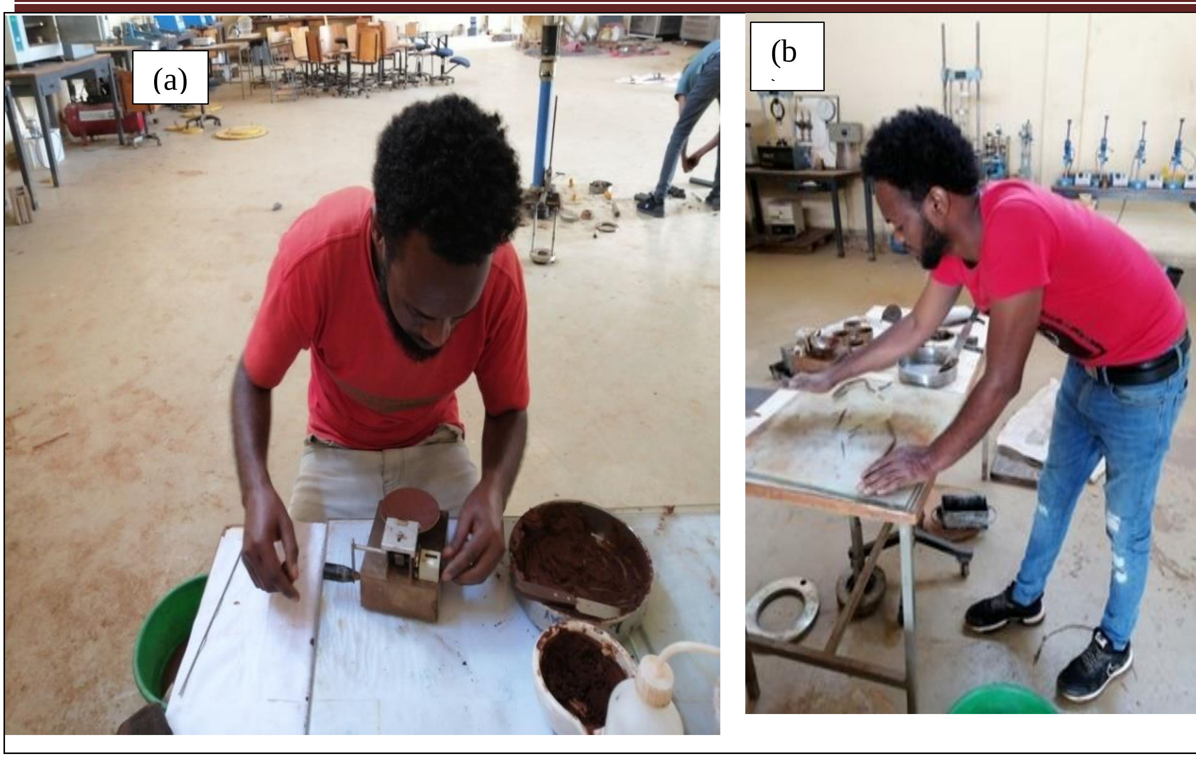

Figure 5: Determination Atterberg's limit tests (a) liquid limit using Casagrande apparatus (b) plastic limit using plastic method (photo captured by Adisalem G.)

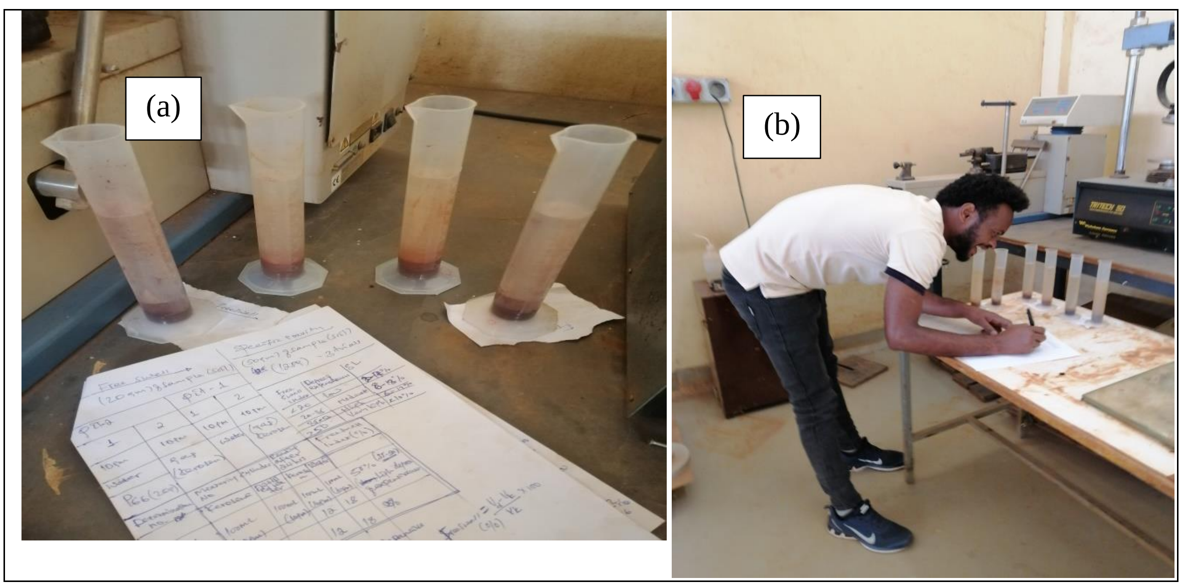

Figure 6: Free swell test Procedure and data recorded period (photo captured by Deribu.) (a) Soil sample preparation (b) recording the data

Figure 7: Determination hydrometer tests (photo captured by Adisalem G.) (a) sample preparation and add dispersing agent (b) mixing the soil sample with dispersing agent by using string (c) insert the thermometer into glass jar and d) recording the data

Figure 8 Loading and unloading stages when increment weights added and removed (a) Loading stage (b) unloading stage

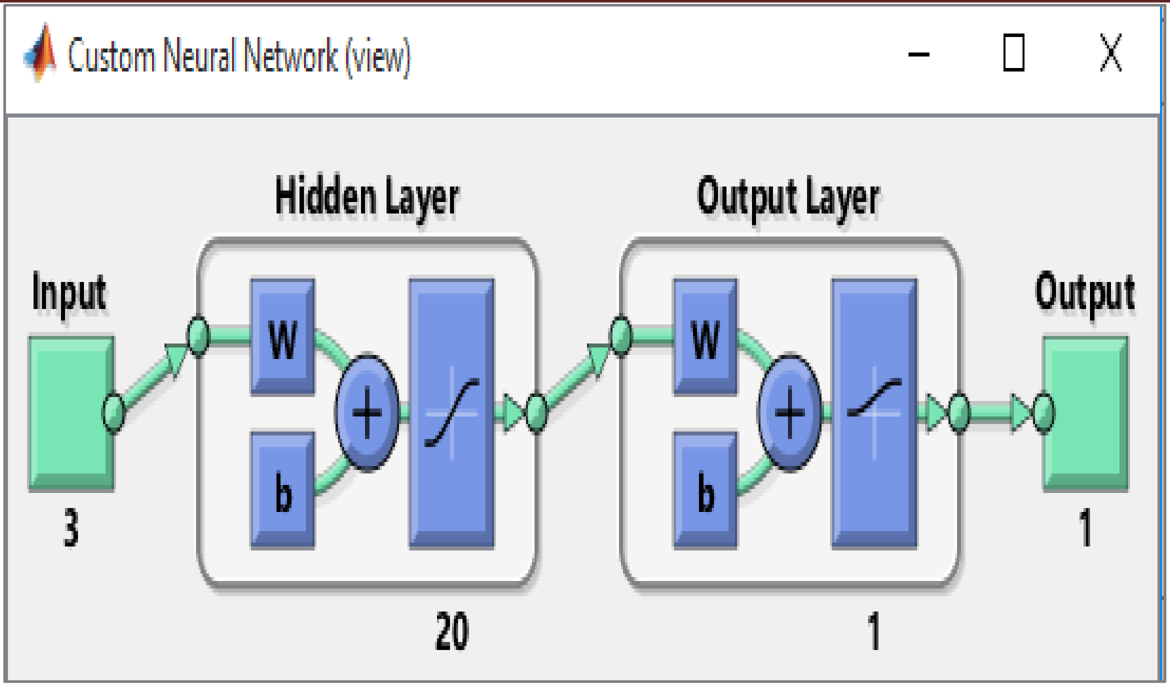

Figure 9: Mechanisms of ANN

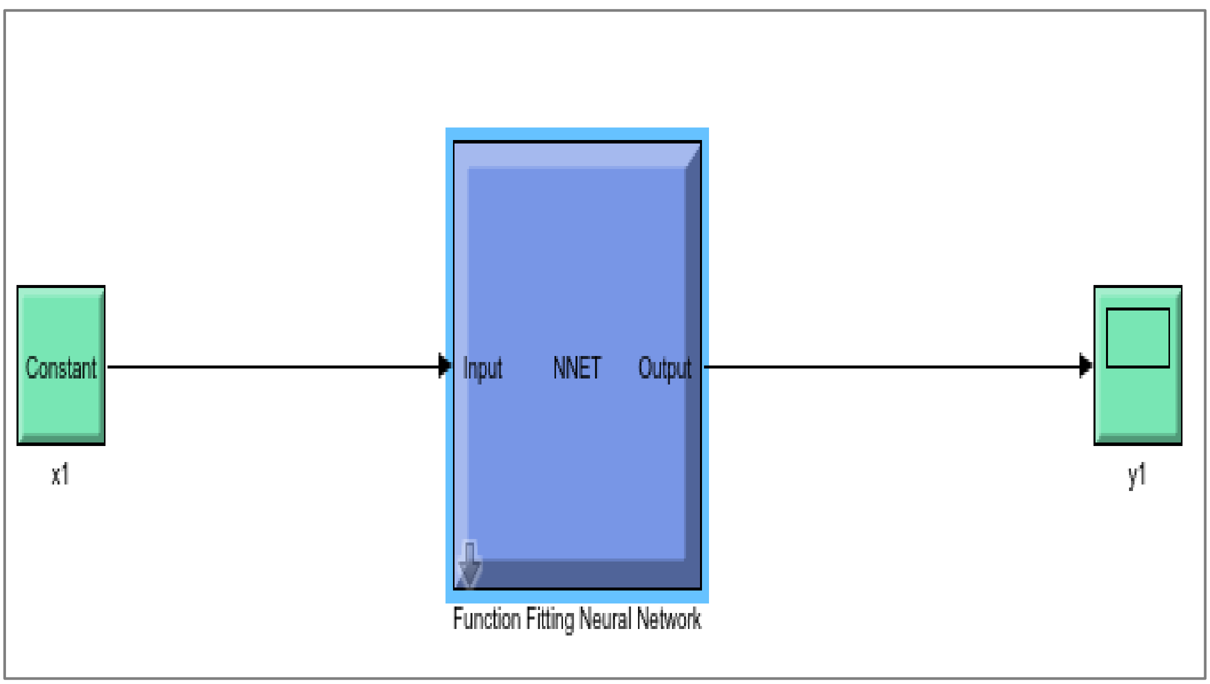

Figure 10: Simulation Diagram in ANN